Πανεπιστημιο Της Περουτζα

Τμήμα Χημείας, Βιολογίας & Βιοτεχνολογίας

ΠΜΣ Τοξικολογία

Συσσώρευση **Hg** (Υδραργύρου) και άλλων χημικών στοιχείων σε επιλεγμένους ιστούς ενός 'επεμβατικού' είδους καραβίδας, **Procambarus clarkii,** από τη λίμνη Αλβιάνο

Επιβλέπων Καθηγητής:
David Michele Cappelletti

Διπλωματική εργασία της φοιτήτριας:
Χρυσοβαλάντου Μίχου

Ακαδημαϊκό έτος 2020/ 2021

Institutional Repository - Library & Information Centre - University of Thessaly
19/04/2024 03:53:45 EEST - 18.222.197.243

UNIVERSITÀ DEGLI STUDI DI PERUGIA

Department of Chemistry, Biology and Biotechnology

MSc in Toxicology

Accumulation of Hg and Other Trace Elements in Selected Tissues of an Invasive Crayfish Species, Procambarus clarkii, from Alviano Lake

Supervisor:
Prof. David Michele CAPPELLETTI

Master's thesis by:
Chrysovalantou MICHOU

Academic year 2020/21

Institutional Repository - Library & Information Centre - University of Thessaly
19/04/2024 03:53:45 EEST - 18.222.197.243

Institutional Repository - Library & Information Centre - University of Thessaly
19/04/2024 03:53:45 EEST - 18.222.197.243

Abstract

Metal pollution is a global problem which represents a growing threat to the environment. Because of bioaccumulation and negative effects of heavy metals, their bioavailability needs to be monitored. Many studies showed accumulation of metals in crayfish tissues as dose- and time-dependent without significant differences in tissue concentration levels comparing males and females. The aim of this project was to estimate the levels of bioaccumulation in crayfish samples of Alviano, by ICP-MS-QQQ (triple quadrupole Iductively Coupled Plasma-Mass Spectometer), and the use of molecular markers (SOD, CAT,GPx, GST) to identify gene differences in the specimen. The present work details the analysis of Hg and other 29 elements concentrations in hepatopancreas and abdominal muscle tissues of 45 crayfish (Procrambarus clarkii) specimens collected from Alviano Lake, with the potential source of Hg located in Mountain Amiata, while a significant transport of mercury is documented in the streams draining the district. By far the largest output occurs to the southeast in the Paglia River catchment; this river is tributary of Tiber River, from which Alviano Lake derives. The elements Zn (15.8 mg/ kg) and Cd (0.01 mg/ kg) were the most and the least accumulated elements in the abdominal muscle tissue, while the elements Zn (18.97 mg/ kg) and Hg (0.03 mg/ kg) were the most and the least accumulated elements in hepatopancreas.

Institutional Repository - Library & Information Centre - University of Thessaly
19/04/2024 03:53:45 EEST - 18.222.197.243

Institutional Repository - Library & Information Centre - University of Thessaly
19/04/2024 03:53:45 EEST - 18.222.197.243

Contents

Institutional Repository - Library & Information Centre - University of Thessaly
19/04/2024 03:53:45 EEST - 18.222.197.243

Institutional Repository - Library & Information Centre - University of Thessaly
19/04/2024 03:53:45 EEST - 18.222.197.243

List of Figures

Institutional Repository - Library & Information Centre - University of Thessaly
19/04/2024 03:53:45 EEST - 18.222.197.243

Institutional Repository - Library & Information Centre - University of Thessaly
19/04/2024 03:53:45 EEST - 18.222.197.243

Institutional Repository - Library & Information Centre - University of Thessaly
19/04/2024 03:53:45 EEST - 18.222.197.243

Institutional Repository - Library & Information Centre - University of Thessaly
19/04/2024 03:53:45 EEST - 18.222.197.243

Institutional Repository - Library & Information Centre - University of Thessaly
19/04/2024 03:53:45 EEST - 18.222.197.243

Institutional Repository - Library & Information Centre - University of Thessaly
19/04/2024 03:53:45 EEST - 18.222.197.243

Institutional Repository - Library & Information Centre - University of Thessaly
19/04/2024 03:53:45 EEST - 18.222.197.243

Institutional Repository - Library & Information Centre - University of Thessaly
19/04/2024 03:53:45 EEST - 18.222.197.243

List of Tables

Institutional Repository - Library & Information Centre - University of Thessaly
19/04/2024 03:53:45 EEST - 18.222.197.243

Institutional Repository - Library & Information Centre - University of Thessaly
19/04/2024 03:53:45 EEST - 18.222.197.243

Chapter 1

Introduction

1.1 General Properties of Mercury

The chemical symbol for mercury, Hg, is derived from the Greek word, hydrargyrum, which means silver water. Elemental mercury is found in the Earth's crust in only a limited number of regions in the world. Mercury is more abundant in mineral form, with cinnabar (HgS) being the most prevalent. Several of the less abundant minerals include calomel, Livingstonite, and Tiemannite. Mercury is found primarily in deposits formed by hydrothermal systems, which are more common at converging tectonic margins. It also tends to be enriched in some basic metallic minerals and presented with other chalcophilic (having a sulfur affinity) elements.The elemental form of mercury (Hg^0) has had a great number of uses historically, including barometers, thermometers, electrical switches, fluorescent light bulbs, and ballast for submarines. Elemental mercury has a unique combination of properties that seem to make it ideal for these applications. Hg0 is the only abundant metal that is liquid at room temperature. It has a melting point of –39°C and a boiling temperature of 357°C. It also has a rather high vapor pressure despite having a density 13 times greater than water and slightly greater than lead. This anomalous behavior is caused by weak inter-atomic bonding, which is due to the nucleus having a tight hold on its valence electrons. Hg0 is also relatively insoluble in water (49 μg/L or 4.4 ppt at 20°C which is 4 to 6 orders of magnitude smaller than the solubility of the predominant Hg compounds) and will readily avoid liquids. So, it is often described as preferring to be in the gas phase. Mercury can also be found in two ionic forms, oxidation states +1 and +2, which are more prevalent in water than in the atmosphere [1].

A number of the mercury compounds that occur in the environment have not been directly identified. Rather, several different fractions of mercury have been defined based on how they are collected (e.g., on a filter) and how elemental mercury can be released from them (e.g., heating the filter to 800°C). These distinctions, called "operationally defined fractions," are then used in place of specific compounds. The properties of the different fractions (e.g., solubility, volatility, etc.) are used in modeling the fate of mercury.

Mercury enters the waterways via deposition of particles or ionic compounds from the atmosphere, runoff and erosion from the land surface, leaching from landfills, geothermal inputs, combustion and industrial discharges. Once in the water environ-

Institutional Repository - Library & Information Centre - University of Thessaly
19/04/2024 03:53:45 EEST - 18.222.197.243

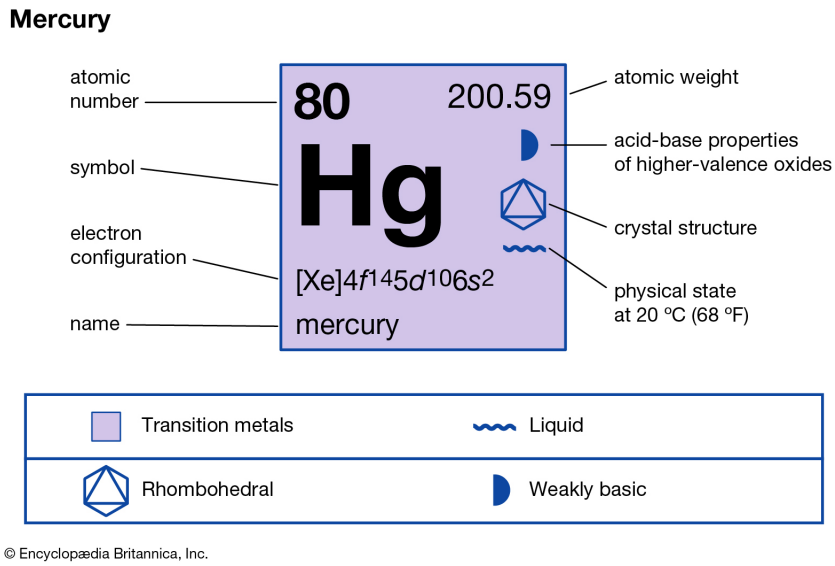

Figure 1.1: Basic properties of Mercury (Encyclopedia Britannica, Inc.).

ment, mercury undergoes similar oxidation-reduction, sorption-desorption processes on to mineral surfaces and organic matter, and methylation-demethylation reactions as occur in the land environment.

In a similar manner to the land environment, elemental mercury can be evaporated back to the atmosphere directly from water (this process is also called evasion) or it can be oxidized to form Mercury(II). This ionic form of mercury can then be either reduced back to elemental mercury and again evaporate to the atmosphere, or it can form methylmercury. Mercury(II) can also form complexes with organic matter or be sorbed onto suspended particulate matter within the water environment. Mercury(II) complexes are thought to be the dominant form in which mercury is found in natural waters. Mercury(II) complexes can be transported over very long distances [2].

The methylation reactions in the aquatic environment are of particular concern due to the bioaccumulation of methylmercury in aquatic species. As a result, top-level predators acquire greater body burdens of mercury than the fish they consume. Bioaccumulation and biomagnification within the food chain can lead to top-level predators (fish-eating fish, birds and humans) having bioaccumulation factors of the order of 10 million [3]. In other words, concentrations within the bodies of these predators can be 10 million times higher than the environments in which they live.

Both oxidized mercury(II) and methylmercury can be deposited into the underlying sediments, where similar processes and transformations occur as those described for the land environment. Sediments at the bottom of water bodies can act as mercury sinks from which mercury can be distributed back into circulation for many years after initial deposition [4].

1.1.1 Chemical Species of Mercury

Hg^0 is elemental mercury. Hg0 has an anomalously high vapor pressure for a heavy metal. It is slightly water-soluble (50 μg/L at 20°C) and has a high Henry's law coefficient (729 at 20°C). In the natural environment, it can exist in the gaseous or

Institutional Repository - Library & Information Centre - University of Thessaly
19/04/2024 03:53:45 EEST - 18.222.197.243

Table 1.1: Physical and chemical forms of mercury: Some recent and present pathways of human exposure

	Inorganic mercury	
Hg vapor	Mercurous	Mercuric
Hg^0	Hg-Hg^2+	Hg2+
Occupational	Laxatives	Skin creams
Dental amalgam	Teething powders	
	Organic mercury*	
Short chain alkyl		Other organics
$CH_3(CH_2)_n$-Hg^2		(R-C-Hg^+])
Mehtylmercury in fish		Phenyl Hg antiseptic
Ethylmercury in preservatives		Mercurial diureties

*Some organic mercury compounds involve two carbon atoms attached to mercury, such as dimethylmercury (CH_3-Hg-CH_3)

liquid state. Gaseous element mercury (GEM), is the dominant form in the atmosphere. Most natural waters are nearly saturated, or are supersaturated with respect to atmospheric Hg^0.

Hg(II) or divalent mercury. Inorganic and organic divalent mercury compounds exist in gaseous, dissolved, and solid states. Their toxicity, solubility, vapor pressure, and reactivity vary greatly. Hg(II) is much more prevalent in waters than in the atmosphere. Methylated mercury compounds (below) are of particular interest because of their role in the biologic cycling of Hg and accordingly make up >95% of the mercury in fish [5].

DMHg is dimethylmercury, $(CH_3)_2Hg$. DMHg is significantly more toxic than Hg^0 on a milligrams per kilogram of body weight ingestion basis (due to more efficient absorption in the gut). It is believed to be present in the atmosphere in only negligible concentrations, but it is thought to be ubiquitous in the deeper ocean.

MMHg is monomethylmercury, CH_3Hg^+. MMHg is significantly more toxic than Hg^0 on a milligrams per kilogram of body weight ingestion basis (due to more efficient absorption in the gut) and readily bioaccumulates up the food chain. MMHg has not been reliably detected in the open oceans apart from the Equatorial Pacific Ocean [6].

1.1.2 Operational defined forms of Mercury

DGHg is dissolved gaseous Hg. It is a fraction of mercury measured in water that is defined by its ability to be volatilized only by purging with a clean, inert gas. It includes DMHg [6].

HgR is reactive Hg dissolved in water. It is defined based on its ability to be volatilized after reduction with $SnCl_2$, and purging with a clean, inert gas [6]. Hg(II) has also been used as an operationally defined fraction of dissolved Hg. It is determined by subtracting mercury that is readily volatilized (DGHg) from reactive Hg (HgR). It has been used as a measure of bio-available mercury, but is known to not be universally appropriate [6].

Hg-Col is colloidal mercury. It is mercury associated with colloidal matter that can be trapped on an ultrafine membrane after filtration of larger particulate matter. Col-

Institutional Repository - Library & Information Centre - University of Thessaly
19/04/2024 03:53:45 EEST - 18.222.197.243

loidal mercury is generally considered to be larger than 1000 Da (molecular weight) but smaller than 0.1–0.5 μm.

RGM or reactive gaseous mercury, refers to Hg that can be captured on a KCl surface. RGM is believed to consist primarily of gaseous Hg(II) compounds. It is regarded as the fraction of airborne Hg that is readily deposited to the surface via wet or dry deposition. The exact chemical form of RGM is not known, but likely candidates include Hg^O, $HgCl_2$, and $HgBr_2$. In many reports, RGM and gaseous Hg(II) are used interchangeably, but it is important to recognize that RGM is an operation definition whereas Hg(II) is a chemical definition.

PHg, or particulate-bound mercury, refers to mercury that is extracted from particles, either airborne or waterborne. The observed PHg concentration can be dependent on the size of particles that are collected; for example, most airborne PHg measurements include only particles < 2.5 μm (aerodynamic diameter), so mercury on larger particles would be excluded from the reported concentration.

The amount of mercury extracted from the particles can be dependent on the technique used. Waterborne particulate mercury is generally determined by filtration, addition of BrCl, reduction with $SnCl_2$, and purging with a clean, inert gas. Measuring airborne PHg also requires capturing particles on a filter. The filters can be analyzed in the aqueous phase using the previously described technique. Or, the mercury on particles can be thermally reduced/desorbed, and quantified as GEM [7].

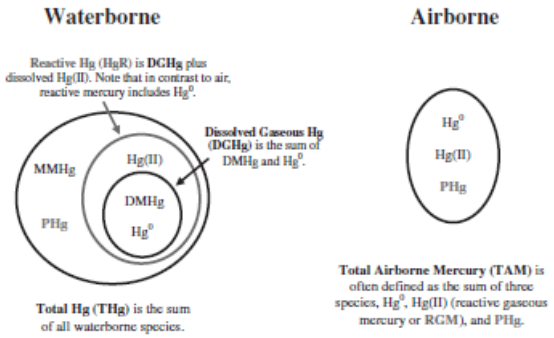

Figure 1.2: A simplified diagram of the major chemical forms of mercury found in water and air. (Mercury in the Environment, Michael S. Bank, University of California Press)

Any form of mercury in the environment may evolve into a more toxic species (methyl mercury) under biogeochemical transformation processes. Due to these processes and the high mobility of mercury species, a good understanding of how mercury species transform and accurate monitoring are essential for assessing the risk of mercury in the environment. The impact of mercury depends strongly on its chemical species; understanding mercury transformations and the impact of its various chemical forms are vital to preventing harmful effects on humans and the environment. Nevertheless, physicochemical characteristics of mercury are either useful or necessary for many industrial and agricultural applications, and mercury may be scattered over large area, depending on the source.

Institutional Repository - Library & Information Centre - University of Thessaly
19/04/2024 03:53:45 EEST - 18.222.197.243

1.2 Production and Uses of Mercury

Mercury is a natural component of the earth, with an average abundance of approximately 0.05 mg/kg in the earth's crust, with significant local variations. Mercury ores that are mined generally contain about one percent mercury, although the strata mined in Spain typically contain up to 12-14 percent mercury. While about 25 principal mercury minerals are known, virtually the only deposits that have been harvested for the extraction of mercury are cinnabar. Mercury is also present at very low levels throughout the biosphere. Its absorption by plants may account for the presence of mercury within fossil fuels like coal, oil, and gas, since these fuels are conventionally thought to be formed from geologic transformation of organic residues.

The mercury available on the world market is supplied from a number of different sources, including (not listed in order of importance):

Mine production of primary mercury (meaning extracted from ores within the earth's crust):

1. Either as the main product of the mining activity, or as by-product of mining or refining of other metals (such as zinc, gold, silver) or minerals;
2. Recovered primary mercury from refining of natural gas (actually a by-product, when marketed, however, is not marketed in all countries);
3. Reprocessing or secondary mining of historic mine tailings containing mercury;
4. Recycled mercury recovered from spent products and waste from industrial production processes. Large amounts ("reservoirs") of mercury are "stored" in society within products still in use and "on the users' shelves";
5. Mercury from government reserve stocks, or inventories;
6. Private stocks (such as mercury in use in chlor-alkali and other industries), some of which may later be returned to the market.

The mining and other mineral extraction of primary mercury constitute the human mobilisation of mercury for intentional use in products and processes. Recycled mercury and mercury from stocks can be regarded as an anthropogenic re-mobilisation of mercury previously extracted from the Earth.

Despite a decline in global mercury consumption (global demand is less than half of 1980 levels), supply from competing sources and low prices, production of mercury from mining is still occurring in a number of countries. Spain, China, Kyrgyzstan and Algeria have dominated this activity in recent years, and several of the mines are state-owned. The table below gives information on recorded global primary production of mercury since 1981. There are also reports of small-scale, artisanal mining of mercury in China, Russia (Siberia), Outer Mongolia, Peru, and Mexico. It is likely that this production serves robust local demand for mercury, often for artisanal mining of gold – whether legal or illegal. Such mercury production would require both accessible mercury ores and low-cost labor in order for it to occur despite low-priced mercury available in the global commodity market.

In connection with its use, mercury has been found in Egyptian tombs dating back to 1500 B.C., and it has been used for centuries in medicines. While mercury is no longer sold as a dermal or oral antiseptic, an organic form continues to be used as

Institutional Repository - Library & Information Centre - University of Thessaly
19/04/2024 03:53:45 EEST - 18.222.197.243

a vaccine preservative. The ancient Greeks and Romans used mercury in cosmetics and it was also one of the primary cures for syphilis in Europe before modern times. During the medieval period, alchemists thought mercury could be hardened to produce gold. In some cultures, spiritualists associate mercury with mystic qualities and it continues to be used to "bless" homes, cars and apartments. Although its toxic effects are well understood, mercury continues to be used in a wide variety of products and manufacturing processes because it is very useful.

Elemental mercury is used in thermometers, blood pressure devices, and thermostats because its ability to expand and contract uniformly makes it useful for measuring changes in temperature and pressure. Although many liquids could be used in pressure measuring devices, mercury is used because its high density requires less space. It is also a good conductor of electricity, so it is a useful component of electrical switches.

Mercury is also used in dental fillings, paints, soaps, batteries, and fluorescent lighting. Mercury will dissolve numerous metals to form amalgams and is used to extract gold dust from rocks by dissolving the gold and then boiling off the mercury. The amalgam used in dental fillings contains tin and silver alloyed with mercury. Because it works as a biocide, mercury has been used as a fungicide in paint, though this kind of paint is no longer sold.

1.2.1 Sources of Mercury in Water

1.2.1.1 Atmospheric Wet and Dry Deposition

The largest and most important source of mercury in water is wet and dry deposition from the atmosphere. This includes both a natural and anthropogenic component. Globally, about 1% of the total oceanic burden is deposited and emitted each year. Most of the mercury deposited to oceans in precipitation is either bound to particles or is dissolved in an ionic state, Hg(II). Over the oceans, the overwhelming portion that is dry deposited is RGM, which has been produced near the water surface from photochemically driven oxidation by halogens. A portion (10%) of the RGM that is deposited to the ocean is reduced to elemental mercury in the surface waters, either directly by sunlight, or through biologic activity (Fitzgerald et al., 2007). This tends to make the surface waters supersaturated with respect to dissolved elemental mercury. Therefore, (gaseous) elemental mercury is generally evading from the ocean surface. Lakes and wetlands are more variable in their interaction with GEM.

Mercury that is bound to particles and bound to soluble organic complexes can also be incorporated into the hydrologic cycle as a part of runoff after rain or fl ooding events and through the movement of subsurface pore water. Subsurface geothermal and hydrothermal vents are also sources of mercury in the ocean, although the magnitude of these inputs is believed to be negligible as compared with the total oceanic burden. Subsurface vents may, nonetheless, be important in enhancing the concentrations in ambient waters and sediments near the vent site. Some mercury is also thought to enter (or perhaps reenter) the hydrologic cycle from diagenetic reactions, which are physical, chemical, or biologic changes that occur as sediment (settled particulate matter that contains mercury) is deposited, compressed, and transformed to rock.

Institutional Repository - Library & Information Centre - University of Thessaly
19/04/2024 03:53:45 EEST - 18.222.197.243

1.2.1.2 Industrial Point Sources

Industrial waste is an important source of Hg to some watersheds. The most prominent example of anthropogenic input of mercury to aquatic system occurred in Minimata, Japan, in the early 1950s. Throughout this period, the Chisso Corporation dumped more than 20 tons of mercury that had been used as a catalyst in the production of acetaldehyde, into Minamata Bay. The mercury contaminated the sediments, water, and ecosystem and ultimately the fish, which were a staple of the local diet. In the following years, more than 100 people died and more than 1000 were permanently disabled from the resulting methylmercury poisoning, which consequently bears the name, Minimata Disease.

It is also important to note that, by definition, the increased deposition (of RGM and particulate-bound Hg) to oceans and lakes throughout the globe as compared with preindustrial times is ultimately attributable to anthropogenic activities. Though the input occurs after transport through the atmosphere, it is nonetheless of anthropogenic origin.

1.2.1.3 Mining Runoff

An additional important source of mercury to aquatic systems is runoff or leaching resulting from mining activities. Large-scale mercury mines often produce large quantities of tailings or leave mining passages open after operations cease (e.g., Sulfur Bank Mercury Mine, California; Almadén, Spain; Idrija, Slovenia. Early gold and silver mining also produced large quantities of Hg-enriched tailings because Hg was added to crushed ore in order to amalgamate and extract the gold and silver. The wastes, along with the open mine passages, allow rain and groundwater to leach and mobilize mercury. Even smaller-scale mining activities, in particular artisanal mining practiced in China, Indonesia, South America, and Africa produce significant amounts of waste matter that is enriched in mercury. This is often dumped into streams or lakes, or otherwise allowed to leach in an uncontrolled manner.

1.2.1.4 Methylated Species

Perhaps the most crucial process in the global cycling of mercury, at least from the standpoint of toxicity, is the concentration and accumulation of MMHg or DMHg up the food chain (called “bio-accumulation”). Most of the DMHg and MMHg that is bio-accumulated is produced in situ in natural waters or near the sediment–water interface. The production of MMHg and DMHg from dissolved Hg(II) (methylation) occurs primarily in sulfate-reducing bacteria in anoxic environments and has been hypothesized to be a cellular detoxification mechanism. A limited number of other methylation mechanisms have been proposed, but bacteria appear to be the largest producers in lakes and wetlands. Little DMHg and MMHg is found in the surface waters of the open ocean. Higher concentrations of DMHg can be found below the mixed layer of the open ocean and peripheral seas, while MMHg has been unambiguously detected only in coastal zones, peripheral seas, and the Equatorial Pacific Ocean [6].

Institutional Repository - Library & Information Centre - University of Thessaly
19/04/2024 03:53:45 EEST - 18.222.197.243

1.3 Mercury in Nature

1.3.1 Mercury Cycle

The cycling of Hg in the environment is influenced by both natural and anthropogenic activities. The atmospheric transport is of particular importance for the dispersion of Hg in the global environment either released by natural or anthropogenic processes. Particularly, gaseous elemental Hg (Hg(0)) is efficiently transported over long distances with air masses and moves between the continents, thereby reaching even isolated regions. It is suggested that more than 90% of the Hg in surface waters results from atmospheric deposition. Consistently, several data on Hg contents in lake sediments, peat cores, and ice cores point out that the average global Hg deposition has increased by about a factor of 3 since preindustrial times (»1850), with more pronounced increases in regions influenced by regional sources.

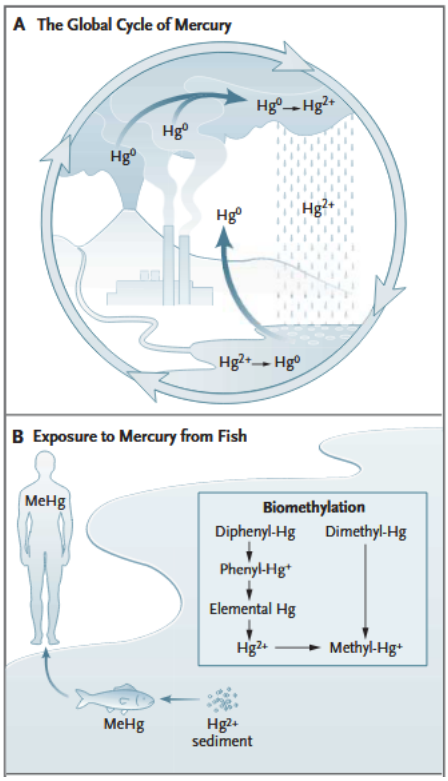

Figure 1.3: In nature, mercury vapor (Hg^0), a stable monatomic gas, evaporates from the earth's surface (both soil and water) and is emitted by volcanoes (Panel A). Anthropogenic sources include emissions from coal-burning power stations and municipal incinerators. After approximately one year, mercury vapor is converted to a soluble form (Hg^2+) and returned to the earth in rainwater. It may be converted back to the vapor form both in soil and in water by microorganisms and reemitted into the atmosphere. Thus, mercury may recirculate for long periods. Mercury attached to aquatic sediments is subject to microbial conversion to methyl mercury (MeHg), where up-on it enters the aquatic food chain. It reaches its highest concentrations in long-lived predatory fish, such as sharks. Panel B indicates the routes of transformation to methyl mercury as originally suggested by Jernelov.

The impact of mercury depends strongly on its chemical species; understanding mer-

Institutional Repository - Library & Information Centre - University of Thessaly
19/04/2024 03:53:45 EEST - 18.222.197.243

cury transformations and the impact of its various chemical forms are vital to preventing harmful effects on humans and the environment. Nevertheless, the physicochemical characteristics of mercury are either useful or necessary for many industrial and agricultural applications, and mercury may be scattered over large area, depending on the source.

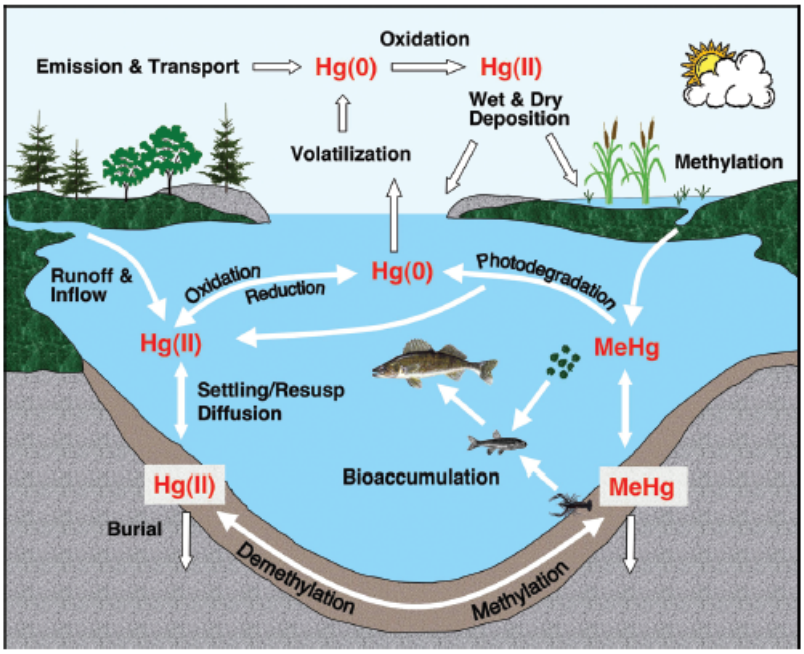

Figure 1.4: Mercury cycling in a lake and its watershed. Hg(0), mercury in its elemental form; Hg(II), divalent mercury; MeHg, methylmercury; Resusp, resuspension

Mercury in the environment is constantly cycled and recycled through a biogeochemical cycle 1.3. The cycle has six major steps:

1. Degassing of mercury from rock, soils, and surface waters, or emissions from volcanoes and from human activities.
2. Movement in gaseous form through the atmosphere.
3. Deposition of mercury on land and surface waters.
4. Conversion of the element into insoluble mercury sulfide.
5. Precipitation or bioconversion into more volatile or soluble forms such as methylmercury.
6. Reentry into the atmosphere or bioaccumulation in food chains.

The modern, industrial cycle of mercury differs from the preindustrial cycle 1.6 because of the extraction and mobilization of Hg from deep reservoirs. Deep reservoirs are defined as reservoirs that are physically below the surface ocean and land surface which contain a large mass of mercury relative to the mass that cycles through the land, air, and water, on an annual basis). Anthropogenic activities have greatly increased the mobilization of Hg (e.g., coal combustion and mining) from deep reservoirs. This enhanced Hg extraction is thought to have increased the total atmospheric burden of Hg by about a factor of 3, which has resulted in a nearly threefold increase

Institutional Repository - Library & Information Centre - University of Thessaly
19/04/2024 03:53:45 EEST - 18.222.197.243

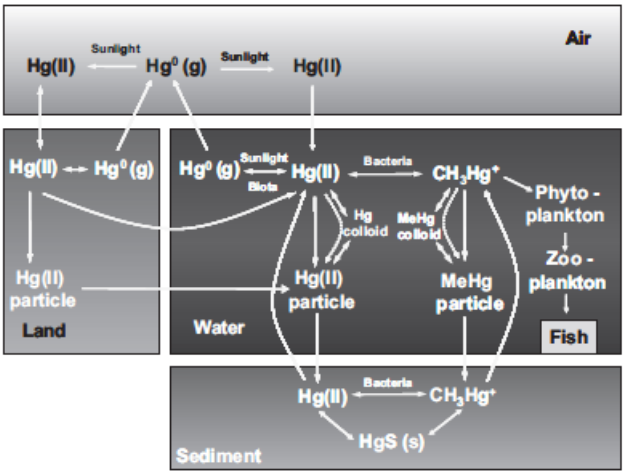

Figure 1.5: A biogeochemical cycle of mercury in the environment, illustrating the common forms of mercury often quantified.

in deposition to the land and ocean. But, it should be noted that the observational record of Hg in the atmosphere is relatively short, so no clear pattern of change has been found. Increased concentrations in the surface ocean and land surface have accordingly increased emissions back to the atmosphere. Thus, the total amount of mercury cycling through the land surface, surface oceans, and atmosphere, has increased significantly. The burden of total mercury in the deep oceans has also increased, but by a much smaller factor. The smaller increase in deep ocean concentrations is largely a result of the much greater reservoir of Hg and slower mixing and turnover times. This produces a lag in uptake on the order of decades to centuries in the surface waters and deep ocean, respectively.

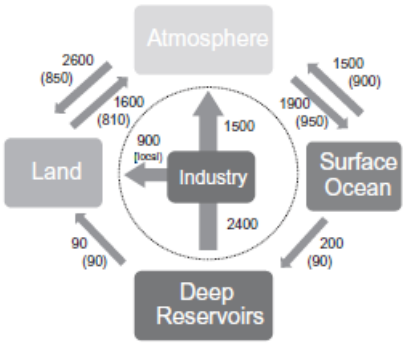

Figure 1.6: Simplified global geochemical mercury cycle. All values are tons per year. Preindustrial values are given in parentheses below the modern values. The inner, dashed circle indicates the perturbation of industrial activities that significantly increased the extraction of mercury from deep reservoirs. This results in significantly greater local deposition and also increased input to the global atmospheric pool, which increases global deposition. Upward arrows from the land and ocean are net evasion and downward arrows are wet and dry deposition.

The primary anthropogenic sources are: fossil fuel combustion and smelting activities. Both these natural and human activities release elemental mercury vapor (Hg^0)

Institutional Repository - Library & Information Centre - University of Thessaly
19/04/2024 03:53:45 EEST - 18.222.197.243

into the atmosphere. Once in the atmosphere, the mercury vapor can circulate for up to a year, and hence become widely dispersed. The elemental mercury vapor can then undergo a photochemical oxidation to become inorganic mercury that can combine with water vapors and travel back to the Earth's surface as rain. This 'mercury-water' is deposited in soils and bodies of water. Once in soil, the mercury accumulates until a physical event causes it to be released again. In water, inorganic mercury can be converted into insoluble mercury sulfide which settles out of the water and into the sediment, or it can be converted by bacteria that process sulfate into methylmercury. The conversion of inorganic mercury to methylmercury is important for two reasons:

The conversion of inorganic mercury to methylmercury is important for two reasons:

1. Methylmercury is much more toxic than inorganic mercury.
2. Organisms require a long time to eliminate methylmercury, which leads to bioaccumulation.

Now the methylmercury-processing bacteria may be consumed by the next higher organism up the food chain, or the bacteria may release the methylmercury into the water where it can adsorb (stick) to plankton, which can also be consumed by the next higher organism up the food chain. This pattern continues as small fish/organisms get eaten by progressively bigger and bigger fish until the fish are finally eaten by humans or other animals. Alternatively, both elemental mercury and organic (methyl) mercury can vaporize and re-enter the atmosphere and cycle through the environment.

1.3.1.1 Transformation/Methylation Processes

An early advance in the understanding of Hg cycling in terrestrial/freshwater ecosystems was the recognition of MeHg as the form responsible for most bio-accumulation of Hg. The abundance of MeHg is controlled by two counteracting microbiologic processes: Hg methylation and MeHg demethylation. The pattern of net methylation in the landscape (i.e. the balance of these processes in space and time) determines the risk of biota to Hg bioaccumulation. Here we address terrestrial methylation, including wetlands. Until recently, Hg methylation was viewed primarily as an aquatic process affecting primarily the aquatic food web. However, aquatic MeHg finds its way into terrestrial food webs, and high MeHg has been documented in songbirds nourished from purely terrestrial food webs, making it clear that terrestrial Hg methylation cannot be ignored. The importance of terrestrial relative to aquatic methylation can be expected to vary with their relative areas on the landscape (e.g., the ratio of catchment to lake surface area), as well as the relative strength of the methylation sources (such as wetlands). There is great variability in MeHg concentrations in soil water and groundwater. They are generally low (up to a few tenths of a nanogram per liter) where there are low DOC concentrations and/or oxic conditions. However, in waters with more than a few milligrams per liter of DOC, MeHg concentrations are often higher, with concentrations of one to several nanograms per liter possible, but with considerable variations. These patterns, which reflect the local balance between methylation and demethylation, vary in space but are less well characterized in time.

Although elevated inputs of ionic Hg (Hg^2+) to ecosystems are generally thought to result in high concentrations in fish, there are many factors that mediate the ultimate fate and trophic transfer of Hg in the environment. Elevated MeHg bio-accumulation

Institutional Repository - Library & Information Centre - University of Thessaly
19/04/2024 03:53:45 EEST - 18.222.197.243

in fish and piscivorous birds and mammals results from a complex sequence of biotic and abiotic mechanisms that control the transport and availability of Hg^2+, MeHg production, bio-accumulation, or biomagnification. These mechanisms occur at critical points in the transfer of Hg in the environment which include: (1) Hg supply and inputs to the ecosystem (e.g., deposition to the landscape); (2) transport to aquatic ecosystems (e.g., from terrestrial watersheds); (3) transformation in wetlands and sediments to MeHg; and finally, (4) bio-accumulation and trophic transfer in aquatic food webs. Moreover, the effect of each of these processes can be enhanced or diminished depending on environmental conditions.

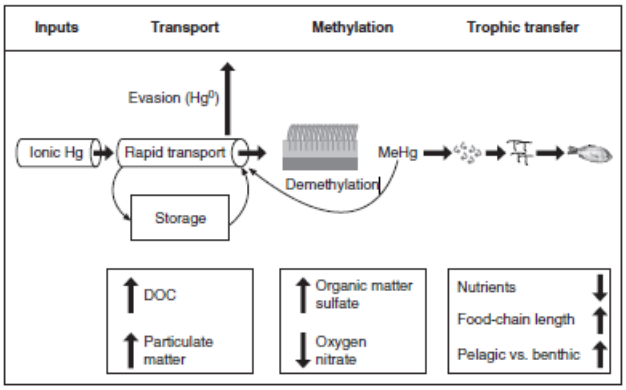

Figure 1.7: Conceptual model of important transformation and transfer points in the Hg cycle.

1.3.1.2 Bio-Availability and Transformation

An important factor controlling concentrations of Hg to fish and other biota is net methylation. Methylation is the process by which microbes convert Hg^2+ to MeHg. This process is important because MeHg is the form that readily bioaccumulates in the terrestrial and aquatic food chain resulting in potential exposure to wildlife and humans. Although methylation can be mediated by a variety of microbes, the most important of these is sulfate-reducing bacteria. Sulfate-reducing bacteria flourish in reducing environments, such as wetlands and lake and river sediments. As a result, zones of high methylation activity occur only at restricted locations on the landscape. Conditions that promote the methylation of Hg2+ are low oxygen, high inputs of labile organic carbon, and a supply of sulfate and Hg^2+. Inputs of oxygen or nitrate inhibit sulfate reduction and therefore methylation of Hg^2+. In the presence of elevated concentrations of sulfide, methylation of Hg2+ is also restricted because the sulfide binds Hg^2+, making it unavailable for methylation and because of the formation of charged Hg-sulfide complexes, which cannot be readily assimilated by sulfate-reducing bacteria. MeHg can be demethylated by oxidative or reductive processes, resulting in the formation of either Hg^2+ or GEM. Therefore, the net production of MeHg is the result of two processes: methylation and demethylation.

1.3.1.3 Bio-Accumulation and Trophic Transfer

The final process in the sequence is bio-accumulation (uptake from food and water) and trophic transfer of $Hg_2{}^+$ and MeHg. MeHg and $Hg_2{}^+$ are bioconcentrated (from water) and assimilated by phytoplankton. MeHg in phytoplankton is assimi-

Institutional Repository - Library & Information Centre - University of Thessaly
19/04/2024 03:53:45 EEST - 18.222.197.243

lated more efficiently by zooplankton than $Hg_2{}^+$, resulting in an enrichment in MeHg content. Phytoplankton in the water column exhibit the largest bioconcentration step in aquatic food webs resulting in log bio-accumulation factors of 5–6. A bio-accumulation factor is the ratio of the concentration of a contaminant (e.g., MeHg) in the organism to the value in water. A number of mechanisms influence the bio-accumulation of MeHg in phytoplankton, including bio-availability of MeHg to algal uptake and phytoplankton growth. Phytoplankton bio-accumulate both Hg2+ and MeHg from water but partition the MeHg to the cytoplasm, leaving $Hg_2{}^+$ bound to the cell wall. Zooplankton appear to assimilate the MeHg inside algal cells and egest the $Hg_2{}^+$ with the cell walls. Fish also obtain MeHg from ingestion of food and take up far less directly from water. Enrichment of MeHg continues up the food chain to top consumers, who are found to have virtually all their Hg occurring as MeHg. Several factors influence this trophic transfer of MeHg in aquatic ecosystems. Elevated inputs of growth-limiting nutrients (e.g., P, N) increase biomass, resulting in a decrease in the Hg concentration of individual organisms; this phenomenon is called biodilution. Higher growth rates in individuals also result in lower mass-specific concentrations in their tissues because of growth dilution. Growth dilution has been hypothesized as the mechanism explaining lower MeHg concentrations in fish and shellfish from the more productive lakes. Differences in food-web structure and type affect the fate of MeHg as well. Several studies have found chain length to be positively related to MeHg concentrations in top-trophic level fish, suggesting that the increased number of trophic levels results in greater biomagnification of MeHg. Finally the Hg concentration of fish is greater for those species feeding from a pelagic food chain rather than a benthic food chain. Some studies have shown that bioaccumulation of MeHg also occurs along the terrestrial food chain.

1.3.2 Freshwater Systems

Much of the research that has been conducted on aquatic mercury cycling has occurred in freshwater ecosystems. Mercury contamination of freshwater systems is widespread, while ecosystems are also affected by point sources of mercury owing to local contamination issues.

In areas away from point sources, atmospheric mercury reaches freshwater ecosystems by direct deposition to lake surfaces and through runoff from watersheds. Wet and dry deposition to watersheds and lake surfaces, as in terrestrial systems, is predominantly as Hg(II). Hg(II) can reduce to Hg(0), which may then volatilize to the atmosphere. A small portion of Hg(II) is converted to the more toxic form of methylmercury (MeHg). Methylation of mercury is a biologically mediated process known to be facilitated by some strains of sulfate- and ironreducing bacteria ([10], [11], [12]). Wetlands and lake sediments are important environments where methylation occurs. The spatial extent of these areas in particular ecosystems influences net methylation. Methylmercury can bioconcentrate in living organisms and then further biomagnify up the food chain, as predators eat prey contaminated with methylmercury and further concentrate it in their tissues. This process of bioaccumulation means that methylmercury concentrations in predatory fish can be elevated relative to water by a factor of $\geq$106.

In aquatic sediments, microbes convert a small fraction of inorganic mercury (Hg(II)) to MeHg over time. Sulfur, organic carbon, sediment structure, and composition

Institutional Repository - Library & Information Centre - University of Thessaly
19/04/2024 03:53:45 EEST - 18.222.197.243

affect methylmercury production by changing the amount of bioavailable inorganic mercury and by stimulating microbial activity. In coastal sediments, sulfate-reducing bacteria are thought to be the principal agents responsible for MeHg production. These microbes thrive at the geochemical interface between oxic and anoxic conditions. A number of environmental factors are known to affect the rate of MeHg formation by influencing the supply of bioavailable Hg(II) and/or the activity of methylating microbes. In addition to Hg(II) concentrations, effective proxy indicators for MeHg production and accumulation identified by previous research include sulfide concentrations, total organic carbon, and redox potential. Methylmercury production has also been measured in the water column in lakes and in anoxic coastal waters.Ecosystems respond to changes in deposition on varying timescales, depending on ecosystem type and the influence of watersheds.

1.4 Enviromental and Health Concerns of Mercury

The primary motivations for researching mercury in the environment are related to its toxicity. The majority of the human population lives within 100 km of the ocean,and the benefits from marine ecosystems are greater than those from all other ecosystems combined. Those benefits include the consumption of seafood, which has many health benefits. Accordingly, the study of mercury biogeochemistry and environmental toxicology in marine systems is of great importance for both human and environmental health.

While mercury has long been recognized as a potent toxin, full appreciation of the threat of mercury contamination from environmental exposures has occurred only within the latter half of the past century. The environmental mercury problem was first documented in the 1950s in Minamata Bay, Japan, where many individuals suffered severe mercury poisoning from their consumption of seafood with elevated levels of methylmercury (5–35 μg $g^{-}1$). That contamination was traced to wastewater discharges of monomethylmercury to the bay from a chemical plant producing acetaldehyde and vinyl chloride. Since then, other cases of mercury poisoning have been chronicled, including in native populations of Arctic and sub-Arctic regions who consume relatively high amounts of fish, marine mammals, and marine birds. More recently, the focus has shifted to the potential sublethal or long-term toxicity of mercury to individuals consuming relatively large amounts of marine fish, and in a few cases marine mammals.

The greatest concern for human health related to environmental mercury pollution is the consumption of fish by the most susceptible populations, specifically pregnant women and children. Thus, while fish represent an important protein source for large segments of the population, and the consumption of fish has many health benefits, it is also the pathway responsible for most human exposure to mercury.

The growing awareness of mercury's sublethal toxicity in humans has increased concerns about mercury's adverse effects on other organisms. Ecosystems can be threatened by elevated environmental mercury levels, with higher trophic-level organisms considered most at risk. These include top predator fish, as well as piscivorous birds and mammals, which can have high body burdens of mercury (often described as "potentially toxic") because of the biomagnification of mercury in aquatic food chains. Some of the adverse effects associated with these elevated mercury concentrations

Institutional Repository - Library & Information Centre - University of Thessaly
19/04/2024 03:53:45 EEST - 18.222.197.243

are reduced reproductive success in fish and birds, altered behavioral traits or neurologic effects in marine mammals, and immunotoxic effects in birds and marine mammals.

1.4.1 Effects of Mercury in Aquatic Environment

Mercury concentrations systematically increase with increasing trophic level in freshwater, estuary, and marine food chains (Figure 7 and Table 8). Mercury levels in apex predators in the aquatic environment may be more than 1 million–fold higher than in surrounding waters. This enrichment underlies mercury's persistent and bioaccumulative nature as a toxicant, representing a serious environmental and human health concern. Table 10.5 summarizes data from various marine ecosystems, illustrating the general trend of increasing total mercury concentrations and increasing % MMHg with trophic level. Central to mercury's biomagnification is that only MMHg, not Hg(II), is biomagnified in marine food webs. The preferential bioaccumulation of MMHg, due to its relatively low elimination rate and relatively high assimilation efficiency, has been shown in kinetic models, laboratory studies, and field studies of mercury uptake by aquatic organisms. Those reports demonstrate that in most cases MMHg is the only form of mercury biomagnified and that MMHg constitutes a larger fraction of the overall body burden of mercury in aquatic organisms with increasing trophic level.

1.4.2 Effects of Mercury in Human Health

1.4.2.1 Potential Health Effects of Mercury

The toxicity of mercury depends on its chemical form, and thus symptoms and signs are rather different in exposure to elemental mercury, inorganic mercury compounds, or organic mercury compounds (notably alkylmercury compounds such as methylmercury and ethylmercury salts, and dimethylmercury). The sources of exposure are also markedly different for the different forms of mercury. For alkylmercury compounds, among which methylmercury is by far the most important, the major source of exposure is diet, especially fish and other seafood. For elemental mercury vapour, the most important source for the general population is dental amalgam, but exposure at work may in some situations exceed this by many times. For inorganic mercury compounds, diet is the most important source for the majority of people. However, for some segments of populations, use of skin-lightening creams and soaps that contain mercury, and use of mercury for cultural/ritualistic purposes or in traditional medicine, can also result in substantial exposures to inorganic or elemental mercury.

While it is fully recognised that mercury and its compounds are highly toxic substances for which potential impacts should be considered carefully, there is ongoing debate on how toxic these substances, especially methylmercury, are. New findings during the last decade indicate that toxic effects may be taking place at lower concentrations than previously thought, and potentially larger parts of the global population may be affected. As the mechanisms of subtle toxic effects – and proving whether such effects are taking place – are extremely complex issues, a complete understanding has so far not been reached on this very important question.

Of the organic mercury compounds, methylmercury occupies a special position in

Institutional Repository - Library & Information Centre - University of Thessaly
19/04/2024 03:53:45 EEST - 18.222.197.243

that large populations are exposed to it, and its toxicity is better characterized than that of other organic mercury compounds. Within the group of organic mercury compounds, alkylmercury compounds (especially ethylmercury and methylmercury) are thought to be rather similar as to toxicity (and also historical use as pesticides), while other organic mercury compounds, such as phenylmercury, resemble more inorganic mercury in their toxicity.

Methylmercury is a well-documented neurotoxicant, which may in particular cause adverse effects on the developing brain. Moreover, this compound readily passes both the placental barrier and the blood-brain barrier, therefore, exposures during pregnancy are of highest concern. Also, some studies suggest that even small increases in methylmercury exposures may cause adverse effects on the cardiovascular system, thereby leading to increased mortality. Given the importance of cardiovascular diseases worldwide, these findings, although yet to be confirmed, suggest that methylmercury exposures need close attention and additional follow-up. Moreover, methylmercury compounds are considered possibly carcinogenic to humans according to the International Agency for Research on Cancer (IARC, 1993), based on their overall evaluation.

Methylmercury can be formed in the environment by microbial metabolism (biotic processes), such as by certain bacteria, and by chemical processes that do not involve living organisms (abiotic processes). Although, it is generally believed that its formation in nature is predominantly due to biotic processes. Significant direct anthropogenic (or human generated) sources of methylmercury are currently not known, although historic sources have existed. Indirectly, however, anthropogenic releases contribute to the methylmercury levels found in nature because of the transformation of other forms. Examples of direct release of organic mercury compounds are the Minamata methylmercury-poisoning event that occurred in the 1950's where organic mercury by-products of industrial-scale acetaldehyde production were discharged in the local bay, and the Iraqi poisoning events where wheat treated with a seed dressing containing organic mercury compounds were used for bread. Also, new research has shown that methylmercury can be released directly from municipal waste landfills and sewage treatment plants, but the general significance of this source is still uncertain.

Once in the food chain mercury can bioaccumulate causing adverse effects to human health. The exact mechanism(s) by which mercury enters the food chain remains largely unknown, and probably varies among ecosystems. Figure 1 presents multiple routes through which humans are exposed to mercury.

Institutional Repository - Library & Information Centre - University of Thessaly
19/04/2024 03:53:45 EEST - 18.222.197.243

Chapter 2

Materials and Methods

In the present study, the red swamp crayfish, Procambarus clarkii of both sexes was collected from Lake Alviano. The sampling process was separated in two sections, site 1 and site 2, in e which

2.1 Study Area

Lake Alviano is an artificial basin, which was created by the construction of a dam on the Tiber river in 1963 for hydroelectric power production. The sampling site is affected by anthropic charge of the Tiber River with urban and industrial waste. The potential source of Hg is located in Mountain Amiata, while a significant transport of mercury is documented in the streams draining the district. By far the largest output occurs to the southeast in the Paglia River catchment; this river is tributary of Tiber River, from which Alviano Lake derives. Most transport is in particulate form, and mercury is temporarily stored in stream and overbank sediments, and can be significantly mobilized and redistributed by extreme events such as flash floods. This shallow reservoir has since turned into an interesting wetland, becoming a hotspot for thousands of migratory birds as well as an important nesting area. Alviano is situated below the confluence of the Paglia River with the Tiber, with an area of 3.49 km^2 and a maximum depth of 9 m.

Figure 2.1: Picture of Lake Alviano

The Alviano Lake is one of the widest WWF nature reservoirs and includes all the

Institutional Repository - Library & Information Centre - University of Thessaly
19/04/2024 03:53:45 EEST - 18.222.197.243

typical habitat of the fresh water wetlands. The Oasis of Alviano Lake was created in 1990, it contains most of the wetland habitats, many of which disappeared more than 100 years ago. This makes it a special place; in fact with its 900 hectares, it protects a unique biodiversity from hunting and property speculation, and is one of the widest WWF nature reserves and includes all the typical habitat of the fresh water wetlands: swamps, ponds, morass, water meadows, and a hygrophilous woodland, one of the largest in central Italy.

The nature reserve is part of the largerest Umbria regional park which also includes the Corbara Lake and the Forello gorges. It contains all the common freshwater habitats of wetlands: swamps, ponds, morass, water meadows, hygrophilous woodland, among the largest in the Appennines.

Alviano is most famous for its rich bird diversity: species include mallards, Eurasian teals, northern shovelers, wigeons, great cormorants, herons, Eurasian bitterns, little bitterns, Western marsh-harriers, ospreys, glossy ibises and spoonbills. There are also many species of passerine, particularly Eurasian siskins and thrushes the mammal population contains [13].

Furthermore, the area of the Tiber River basin south of its confluence with the Paglia River, and especially south of Lake Alviano, has considerable urban, agricultural, and industrial activities, which constitute additional potential Hg sources.

2.1.1 Sample Collection and Processing

Specimens of P. clarkii were sampled monthly, from July 2019 to September 2019, from Alviano Lake. The samples were captured within the day using tophi (large pots with circular section typical of the region) placed at a depth of about 1.5 meters and up to 1500 meters from the southeastern shore.

Figure 2.2: Tophi for crayfishes capture.

For the processing, P. clarkii specimens were purchased alive from fishermen's cooperatives in the two sites examined. The crayfishes were immediately transported to the Ecotoxicology laboratory of the Department of Chemistry, Biology and Biotechnology of the University of Perugia, where they were separated on the basis of sex. The presence of modified pereiopods (hooks), suitable for holding the female during mating, is exclusive to male specimens if sexually active. Subsequently, the specimens were placed in bags appropriately labeled with the date and place of sampling and placed in the freezer at -20°C until the tissues of interest (hepatopancreas or muscle) were taken for morphometric, chemical and biochemical analysis.

Institutional Repository - Library & Information Centre - University of Thessaly
19/04/2024 03:53:45 EEST - 18.222.197.243

2.2 Bioindicator : Red swamp crayfish (Procambarus clarkii)

Crayfish species have been used as a good bio-indicator species to determine the toxic metal contamination in the environment by many researchers. The red swamp crayfish (Procambarus clarkii), as a representative species of crustaceans, inhabits a wide range of aquatic environments, including those with heavy metals pollution. It is known for its hyperaccumulation potential and tolerance to various heavy metals. Several traits of its life history, e.g., polytrophism, rapid growth, high fecundity and disease resistance, make its invasion of the wild successful.

Figure 2.3: Procambarus clarkii in different color variations

It is widely used because of its following characteristics:

i can able to tolerate environmental stress better than other organisms;

ii have long life spans (2–5 years) and low fecundity with high juvenile survival;

iii ability to survive in physical contact with contaminated water and soil;

iv occupy higher tropical level in the food chain;

v huge in size to get samples from different tissue organs, which make them a suitable study specimen for environmental monitoring studies [14, 15, 16].

Generally, crayfish have been classified as herbivores, detritivores and omnivores, which magnify the metal levels by feeding the contaminated organisms from the lower trophic levels of the food chain. It feeds on detritus, algae, plant matter, aquatic invertebrates, amphibians and fish [17]. Therefore, the current study was aimed at assessing the effect of Hg toxicity on the aquatic environment by using crayfish, Procambarus clarkii, as a fundamental bioindicator in the freshwater system.

Institutional Repository - Library & Information Centre - University of Thessaly
19/04/2024 03:53:45 EEST - 18.222.197.243

2.3 Chemical Analysis

2.3.1 Optimization of the Digestion Method

The work in the laboratory is carried out according to the analysis of the samples by ICP-MS, which is used to determine the concentration of heavy metals present in the muscle and hepatopancreas of crabs taken from Lake Alviano.The sample preparation process has undergone, over time, an optimization of the method, as shown below:

1. Firstly, the thawed samples, were homogenized in small falcons while being kept in beakers with ice.

2. Following, the samples were prepared using a CEM Corporation MARS 6 microwave digestion system equipped with iWave technology. iWave is a novel technology advancement that utilizes Light Emitting Technology™ to accurately measure the temperature of the actual sample solution inside the vessel and does not require an internal probe. The samples were placed inside cylindrical PFA Teflon containers called vessels. The vessels were firsty weighed empty and subsequently they were reweighed containing the sample (which could be muscle or hepatopancreas). At this point, the calibration of the scale prior to the use is of big importance.

3. At this time, 5 ml of 67-69% HNO_3 Ultrapure NORMATOM is added in each sample. The vessels were capped hermetically and placed in the MARS 6 for digestion. The mixture is then heated in the microwave digestion system (MARS 6 ONE TOUCH CEM) as shown in Figure 2.3. The One Touch Technology automatically recognized the vessel type and counted the number of vessels. It then chosed the optimized conditions for the acid digestion.The maximum temperature achieved using this method is 180 °C. Animal tissue samples in general do not require extremely high temperatures to achieve complete digestion.

Figure 2.4: Microwave Digestion System MARS 6

Institutional Repository - Library & Information Centre - University of Thessaly
19/04/2024 03:53:45 EEST - 18.222.197.243

4. Prior to the analysis of the elements, the sample must undergo acid mineralization. This procedure serves to destroy the organic part present in the sample and to form soluble salts of the metal of interest. The technique was applied using a MARS 6 (Microwave Accelerated Reaction System) which is a microwave digestion system. Microwave acid digestion is a technique to dissolve metals, bound within a sample matrix, into liquid. This is achieved by exposing a sample to a strong acid, in a closed vessel and raising the temperature and pressure through microwave irradiation. Both the speed of thermal decomposition of the sample, and the solubility of heavy metals in solution are increased. Once these heavy metals are in solution, they can be quantified through elemental techniques. This instrument is proprietary technology that utilizes the emission of light from the sample (solution) to rapidly and accurately measure temperature. It reads the temperature of the solution itself, instead of reading the temperature of the vessel. This makes it the most accurate temperature sensor. The sensors are floor-mounted inside the cavity of the MARS 6 microwave digestion system. Every time a vessel rotates past a sensor, the temperature is accurately measured in real time. This allows the advanced MARS 6 software to automatically make power adjustments to ensure for a successful acid digestion.

5. At the end of the digestion process, the samples were diluted with ultrapure water to 25ml.

2.3.2 Analysis with ICP-MS-ggg

Inductively coupled plasma - mass spectrometry (ICP-MS) can be seen as one of the leading techniques in the field of elemental analysis, focusing on the determination of ultratrace levels of metals and metalloids in a large variety of sample types. It is a versatile, fast and extremely sensitive analytical technique, which allows to perform accurate multi-elementary analyzes. Some of the advantages of this technique are:

1. speed of analysis (35 elements can be determined in a sample within two minutes);

2. limits of detection for most elements in the parts per trillion range and for some parts per trillion (ppt) elements;

3. possibility of analyzing solid, liquid and gaseous samples;

4. ease of analysis of simple and complex matrices;

5. removal of uncertainty and ensurance of accuracy when using reaction gases;

6. consistent and reliable results, even when sample matrix and co-existing analytes change;

7. simplifcity in method development –same gas mode used for all samples;

8. enablement of accurate isotope analysis (no inter-isotope overlaps);

9. removal of direct isobaric overlaps.

Institutional Repository - Library & Information Centre - University of Thessaly
19/04/2024 03:53:45 EEST - 18.222.197.243

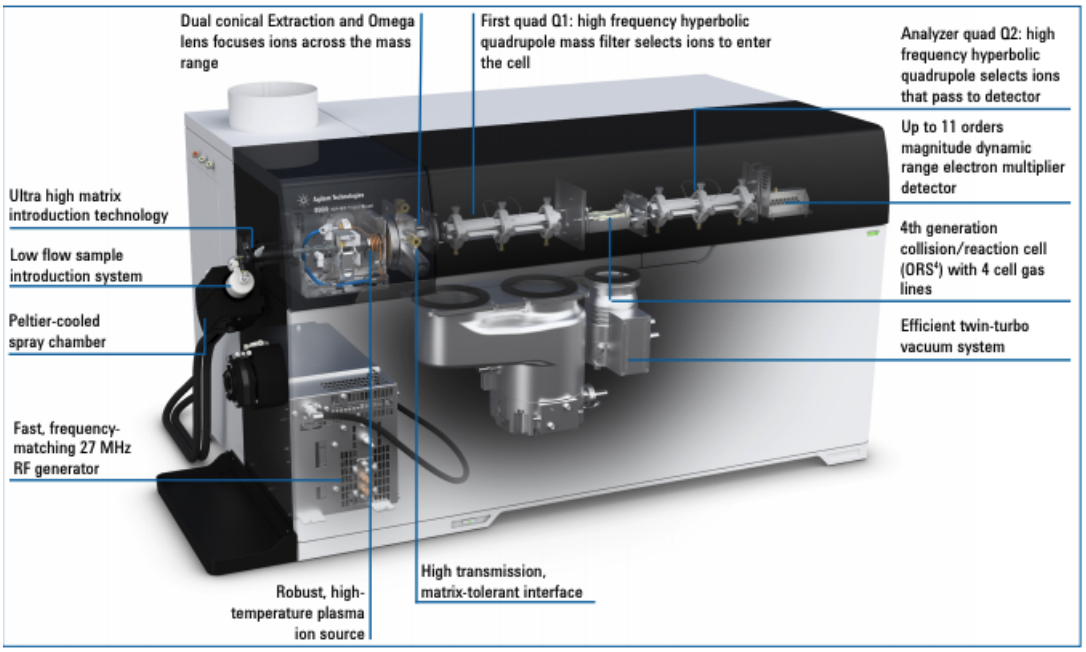

Figure 2.5: ICP-MS Agilent 8900 QQQ

The cell containing the ion guide—the Octopole Reaction System (ORS) in the case of Agilent ICP-QQQ—can be pressurized with a collision or reaction gas to allow the selective attenuation of potential interfering ions. In MS/MS operation, where both quadrupoles are operated as unit mass filters, ions at the target analyte mass are selected by the first quadrupole (Q1) and passed to the ORS cell, where the analyte ions are separated from overlapping interfering ions. The resulting product ions that emerge from the cell are then filtered by the second quadrupole (Q2) before being passed to the detector (Figure 2.5). . This configuration releases the full potential of reaction cell gas methods to resolve spectroscopic interferences including isobaric and doubly-charged interferences, as well as polyatomic ion overlaps. As a result, ICP-QQQ can determine a wider range of analytes at much lower concentrations with greater reliability and higher confidence.

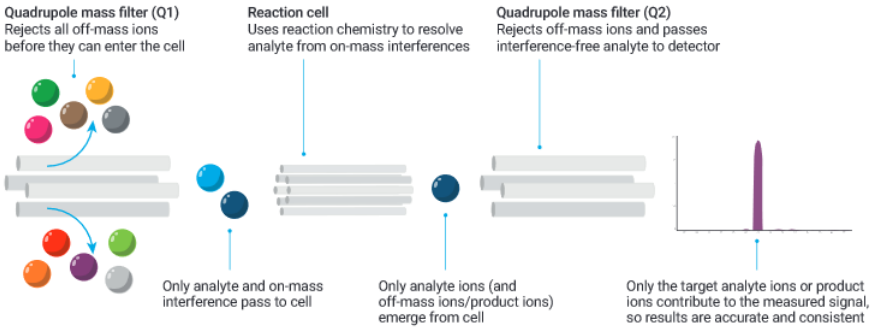

Figure 2.6: Schematics of the ICP-MS/MS system

The tandem MS configuration of Agilent ICP-QQQ instruments – with two fully functioning mass filters, one either side of the ORS cell – allows unprecedented control over the ions that enter the collision/reaction cell (CRC). Q1 rejects all non-target

Institutional Repository - Library & Information Centre - University of Thessaly
19/04/2024 03:53:45 EEST - 18.222.197.243

masses/elements, ensuring more consistent reaction processes in the CRC, even when the sample composition varies. Precise mass selection by the first quadrupole, Q1, is crucial to the accurate analytical performance in MS/MS mode. For reliable, consistent control of reaction processes, Q1 must allow only ions at the target mass-to-charge ratio (m/z) to pass into the cell. Inefficient mass filtering would cause results to be compromised by interferences arising from non-target ions entering the cell. To ensure the most effective mass filtering and the best quality data, Agilent ICP-QQQ instruments use the same hyperbolic quadrupole mass spectrometer for Q1 and Q2. Both quadrupoles are placed in the high vacuum region to ensure optimum mass filtering. This arrangement allows both quadrupoles to operate at unit mass resolution and low abundance sensitivity while maintaining high transmission and sensitivity [18].

The elements under examination were analyzed in no gas mode and in collision-reaction cell (CRC) mode using helium or oxygen with a plasma configuration defined as “General Purpose”.

The instrument was calibrated with standard solutions of known and certified concentration of metals (ICP multi-element standard solution CertiPUR, Merck Chemicals and Reagents), obtaining a calibration line for each metal with the least squares method (Ordinary Least Squares, OLS).

The certified Internal standard mix for ICP-MS systems, 100 ppm of 6 solution was used as an internal standard to correct for changes in instrument operating conditions and sample-specific matrix effects, which could increase or suppress the analyte signal. -Li, Sc, Ge, Rh, In, Tb, Lu, Bi produced by Agilent Technologies.

A parameter strictly connected with the instrumental and analytical performance of the method adopted is the Limit Of Detection (LOD) which indicates the minimum concentration of analyte capable of producing a signal / response, significantly different from that of the blank. LOD was estimated using the slopes of the calibration lines constructed with certified standard solutions of the metals examined (determination with the least squares method using the standard deviation of the residuals of the linear regression Sy/x).

Experimental repeatability was calculated by performing three replicate analyzes of two multi-element standard solutions (1 and 10 μg/L). The % RSDs obtained from the repeatability test of the metal solutions were good and included in the 0.1-10.0% range.

The procedure followed the order listed below:

1. The sample analysis instrument, the triple quadrupole mass ICP, set itself automatically before starting its program (it takes about 30 minutes); first it directed the plasma (8000 Kelvin), then it adjusted the discs inserted between plasma and quadrupole and between the three quadrupoles themselves in order not to disperse ions (provided with a central hole with potential difference).

2. The instrument ebulized the solution under examination; the aerosol that is formed was transported in a high frequency plasma in which the analytes were atomized and ionized. The ions were extracted from the high-frequency plasma through a cone and separated according to their mass-to-charge ratio. The poles were used to differentiate the inherent atom from analytes with equivalent mass.

Institutional Repository - Library & Information Centre - University of Thessaly
19/04/2024 03:53:45 EEST - 18.222.197.243

3. The separation took place at the level of the central octupole, thanks to the use of gases connected to the machinery (for example, it has oxygen, nitrogen and argon available) which through chemical reactions modify the molecules (or ions) consequently varying the weight, allowing so the selection.

4. After separation, they were recorded in a detector and the created signals were evaluated by the software. Quantitative determination was possible after calibration with standard solutions since there is a linear relationship between the intensity of the ionic signals and the concentration of an element.

2.4 Biochemical Analysis

Reactive oxygen species (ROS) are produced in metabolic and physiological processes, and harmful oxidative reactions may occur in organisms, which remove them via enzymatic and non-enzymatic antioxidative mechanisms. Under some conditions, the increase in oxidants and decrease in antioxidants cannot be prevented, and the oxidative/ antioxidative balance shifts toward the oxidative status. Consequently, oxidative stress, which has been implicated in over 100 disorders, develops [19].

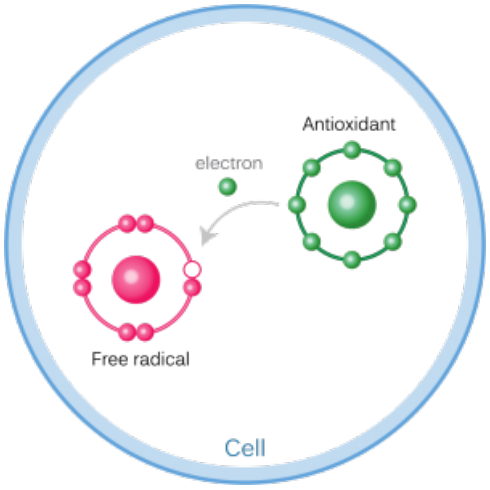

Figure 2.7: Free radical electrons.

Hydroxyl radical ($OH^{\cdot}$) and its subsequent radicals are the most harmful ROS and they are mainly responsible for the oxidative injury of biomolecules. Alone hydrogen peroxide and superoxide molecules cannot directly oxidize lipids, nucleic acids and sugars. These species can lead to oxidative injury in the biomolecules indirectly by producing $OH^{\cdot}$ via Fenton reaction and/or iron-catalyzed Haber– Weiss reaction [20] Oxidized molecules generally form new radicals leading to radical chain reactions or they are neutralized by antioxidants. Antioxidant molecules prevent and/or inhibit these harmful reactions [21].

Institutional Repository - Library & Information Centre - University of Thessaly
19/04/2024 03:53:45 EEST - 18.222.197.243

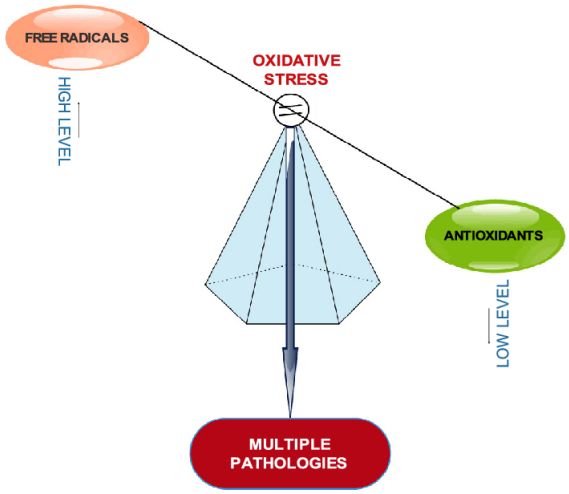

Figure 2.8: Oxidative stress: Imbalance between free radicals and antioxidants.

In this study, we studied the activity of four biomarkers, glutathione (GSH), superoxide dismutase (SOD), catalase (CAT), and glutathione peroxidase (GPx). Mechanisms that involve GSH, and related antioxidants superoxide dismutase (SOD), catalase (CAT), and glutathione peroxidase (GPx) represent important protective metabolic pathways [22], and serve as biomarkers of xenobiotic-mediated oxidative stress. Glutathione in its reduced form is an important non-enzymatic scavenger of oxyradicals, and is involved in metabolism of toxic compounds and endogenous substances [23]. Both SOD and CAT enzymes catalyze the breakdown of ROS-generating O_2^- and hydrogen peroxide (H_2O_2) respectively and are key components within the primary defense system against oxidative stress-induced damage. GPx affects only organic hydroperoxides.

Levels of biomarkers (total GSH^+ 2GSSG levels and activities of SOD, CAT,and GPx) were measured in cytosolic fraction of muscle and hepatopancreas by spectrophotometric analysis (Varian Cary 50 spectrophotometer at 25^{o}C, Figure 2.9). The muscle and hepatopancreas tissue from one individual crab was divided into two portions prior to homogenization with an Ultraturrax homogenizer for different analyses (enzymatic markers and total glutathione). Muscles and hepatopancreas tissues were homogenized in 100 mM KP buffer (pH 7.5) containing 0.1 mg bacitracin/mL, 0.008 TIU aprotinin/ml, 100 μM PMSF (phenylmethylsulphonyl fluoride) and 2.5% NaCl. Homogenates were centrifuged at 18,000 x g (45 min, 4^{o}C) and resulting supernatants further centrifuged at 50,000 x g (90 min, 4^{o}C). Protein concentrations in the cytosol determined [24], were used to normalize enzyme levels. All analyses were performed in triplicate along with blank samples (buffer and reagents only). These absorbance values were subtracted from those of the sample.

1. SOD activity was determined according to an established method [25] following modifications [26]. The analysis was performed at 550 nm in buffer (50 mM Na_2CO_3 0.1 mM EDTA, 500 mM cytochrome C, 1 mM hypoxanthine, and xanthine oxidase, pH 10). A standard curve of SOD units was used. One unit of SOD was defined as the amount of enzyme needed to inhibit 50% of the reduction of cytochrome C.

2. CAT activity was determined by following the decrease in absorbance at 240 nm

Institutional Repository - Library & Information Centre - University of Thessaly
19/04/2024 03:53:45 EEST - 18.222.197.243

Figure 2.9: Picture of Varian Cary 50 spectrophotometer

owing to the consumption of H_2O_2 [27]. The assay was performed in 100 mM sodium phosphate buffer (NaH_2PO_4 + Na_2HPO_4, pH 7, with 12 mM H_2O_2).

3. GPx activity was determined following the oxidation of nicotinamide adenine dinucleotide phosphate reduced form (NADPH) at 340 nm [28]. Each assay was performed in 100 mM sodium phosphate buffer (NaH_2PO_4 + Na_2HPO_4, 1mM EDTA, 0.12 mM NADPH, 2 mM GSH, 1U GR, pH 7.5).
4. Total glutathione (GSH+ 2GSSG) was measured following homogenization in 5% sulfosalicilic acid with 4 mM EDTA (1:3 and 1:4 w/v ratios for muscles and hepatopancreas tissues, respectively). Homogenates were maintained for 30 min on ice and then centrifuged at 30,000 × g for 15 min. Total GSH+ 2GSSG content was determined by the GR recycling assay at 412 nm [29].

2.5 Statistical Analysis

The data were processed using the statistical programming environment R (R Version 3.4.4) and the packages tidyverse, ggplot2 [30], corrgram, corrplot, qwraps2, dplyr, ggpubr and lubridate. In order to verify differences between the biometric variables of males and females, the Student's t test was performed, using a level of statistical significance equal to 0.05. Barlett's test was used for the homogeneity of variances, while comparisons with counting data were carried out using the Shapiro-Wilk hypothesis test.Biomarker levels were compared by one -way ANOVA with post-hoc Tukey test treating each exposure group separately.

Institutional Repository - Library & Information Centre - University of Thessaly
19/04/2024 03:53:45 EEST - 18.222.197.243

Chapter 3

Results & Conclusions

3.1 Statistical Analysis Results with R

With the use of the statistical programming environment R, and in order to see if the samples obtained were following a normal distribution, the following histogram was taken. In addition, the same procedure was followed for all the elements detected, as seen in the B.2.

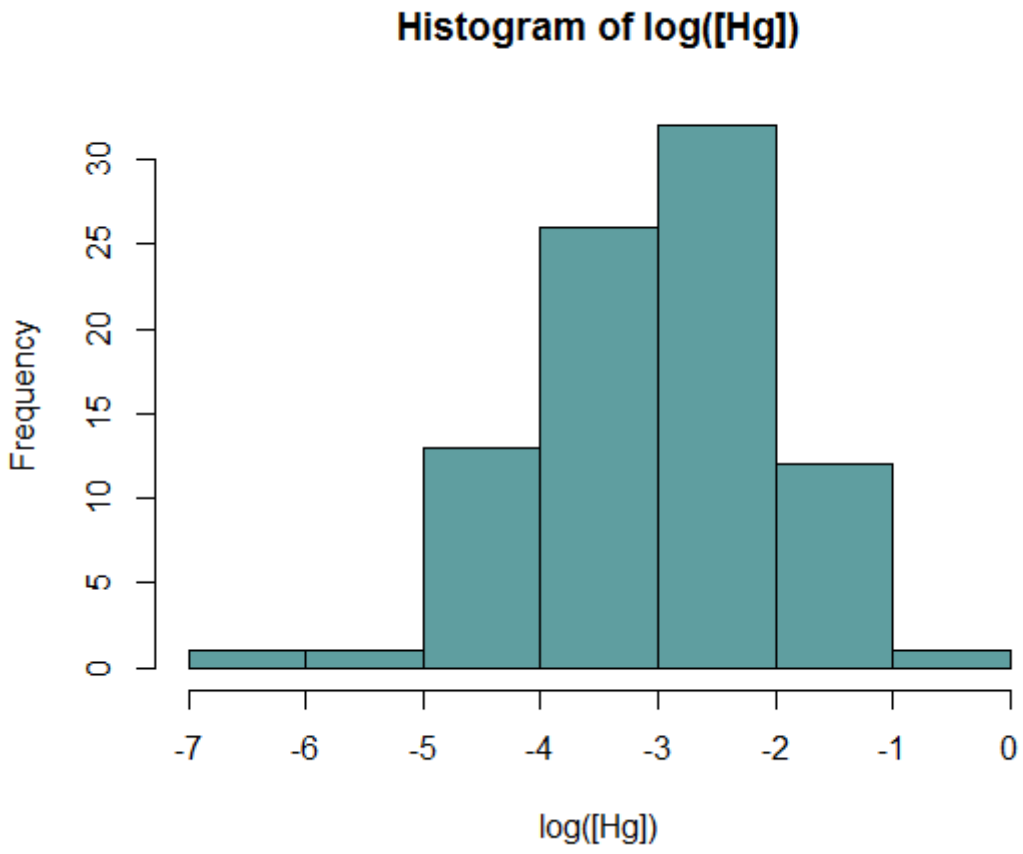

Figure 3.1: Histogram of the logarithm of Hg concentration.

Institutional Repository - Library & Information Centre - University of Thessaly
19/04/2024 03:53:45 EEST - 18.222.197.243

The density plot obtained is used to observe the distribution of the numeric variable (Hg) in the dataset. Thus, the plot is smooth across bins and is not affected by the number of bins created, which helps create a more defined distribution shape. The peaks of the density plot help display where values are concentrated over the interval.

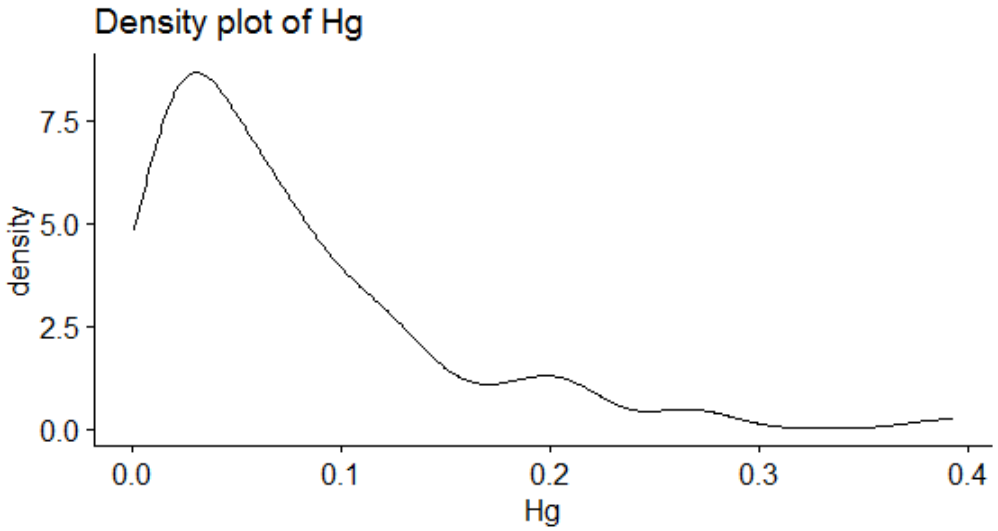

Figure 3.2: Density plot of Hg, obtained from the statistical programming environment R.

The Q-Q plot, or quantile-quantile plot, is a graphical tool to help us assess if a set of data plausibly came from some theoretical distribution such as a normal or exponential. As seen in the tables below, since the points are forming a line that is roughly straight, both sets of quantiles came from the same distribution.

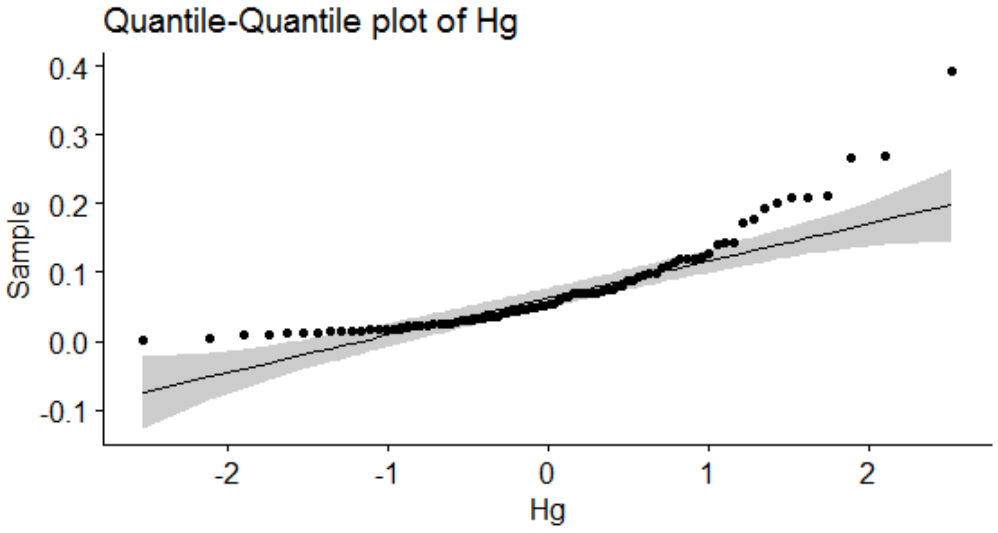

Figure 3.3: Quantile - quantile plot of Hg, obtained from the statistical programming environment R.

Institutional Repository - Library & Information Centre - University of Thessaly
19/04/2024 03:53:45 EEST - 18.222.197.243

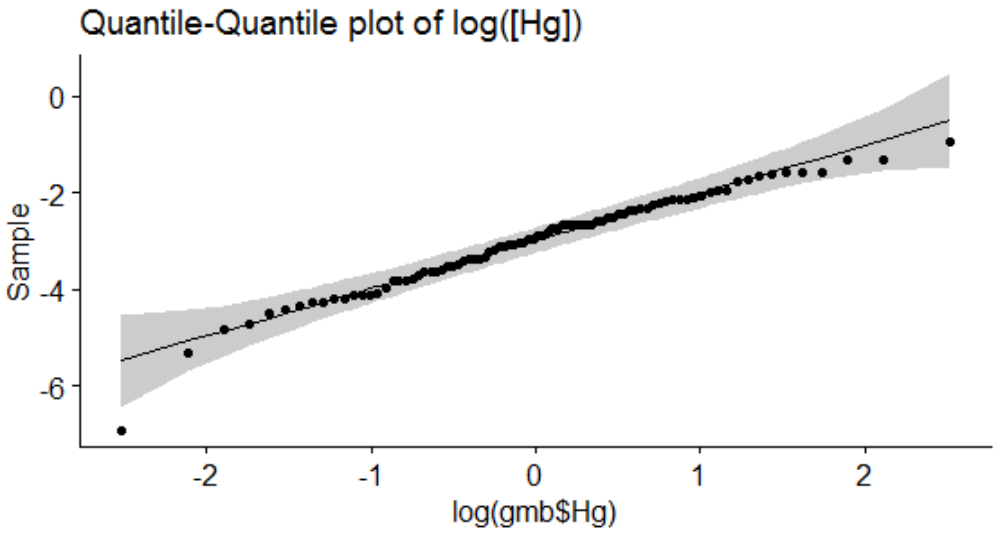

Figure 3.4: Quantile - quantile plot of log ([Hg]), obtained from the statistical programming environment R.

In the process, box plots were conducted in order to provide a visual summary of the data enabling a quick identification of the mean values, the dispersion of the data set, and signs of skewness. Box plots divide the data into sections that each contain approximately 25% of the data in that set.

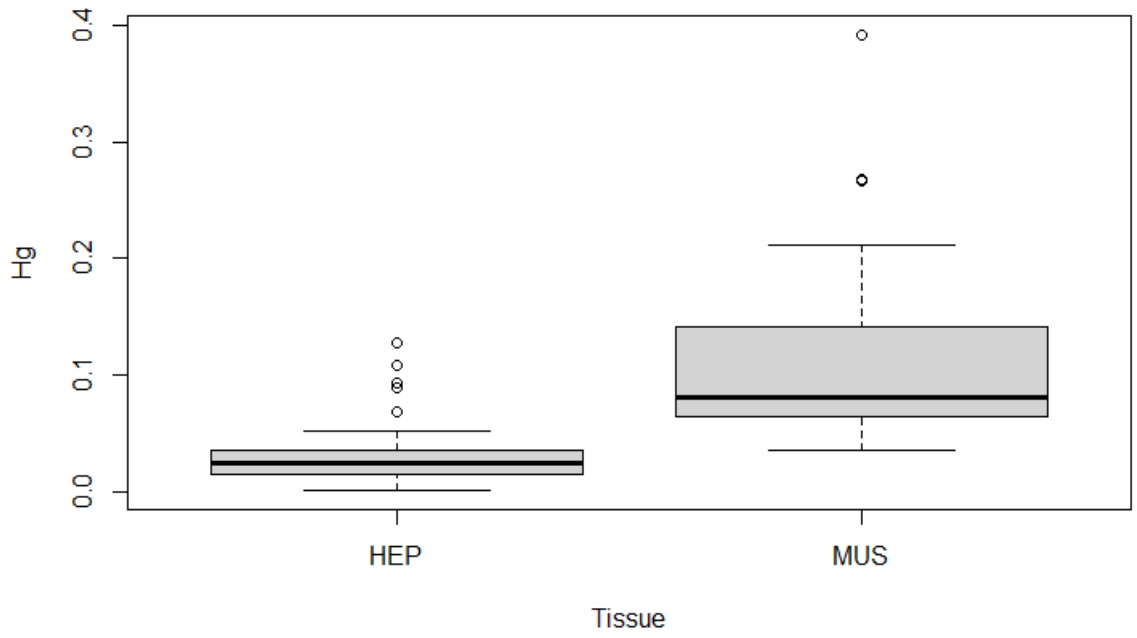

Figure 3.5: Boxplot graph of Hg for hepatopancreas and muscle tissues.

Institutional Repository - Library & Information Centre - University of Thessaly
19/04/2024 03:53:45 EEST - 18.222.197.243

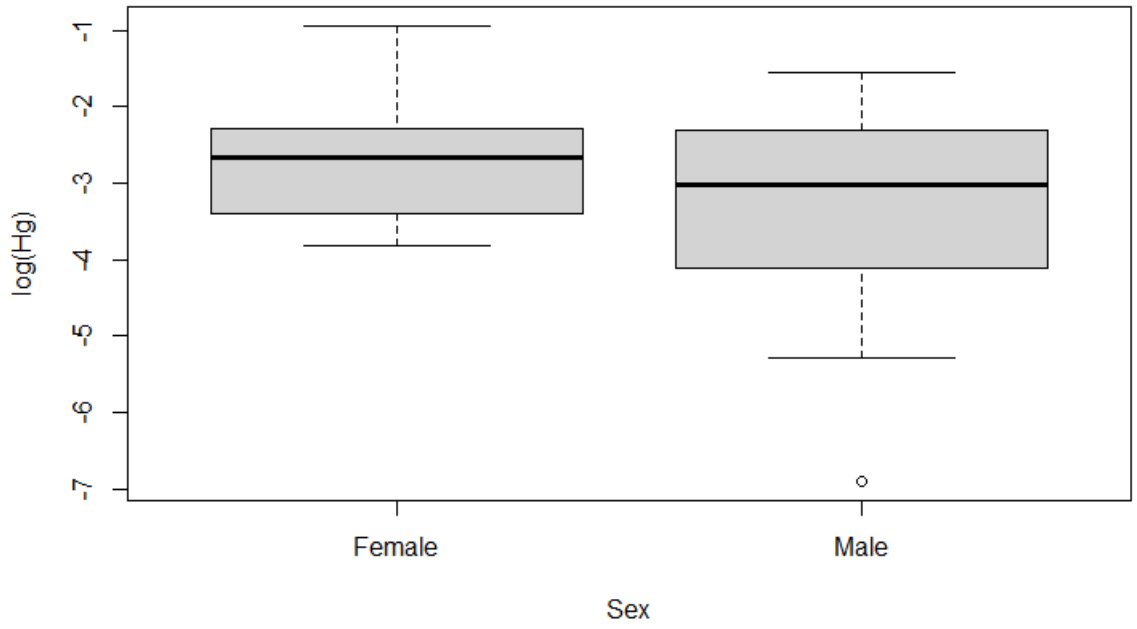

Figure 3.6: Boxplot graph of Hg for hepatopancreas and muscle tissues.

With the use of the statistical programming environment R, the data were processed in order to obtain the correlations matrix. In table 3.1 presented the positive correlations can be seen. Cr and Ni showed a perfect positive correlation. Also As, Mn, Co and Cd showed high positive correlation , while Pb with Zn and Hg with Ni showed low positive correlation.

Table 3.1: Correlation table of metals' concentrations in P.clarkii hepatopancreas and muscle tissues.

Parameters	Mn	Co	Ni	Cu	Zn	Cd	Pb	Hg	As	Cr
Mn	1.00									
Co	0.74	1.00								
Ni	-0.04	0.03	1.00							
Cu	0.16	0.22	-0.24	1.00						
Zn	0.50	0.45	-0.03	0.37	1.00					
Cd	0.62	0.59	-0.22	0.40	0.45	1.00				
Pb	0.09	0.25	-0.04	0.29	0.32	0.19	1.00			
Hg	-0.16	-0.14	0.40	0.04	0.18	-0.32	0.09	1.00		
As	0.77	0.84	-0.15	0.31	0.49	0.80	0.25	-0.28	1.00	
Cr	-0.14	-0.09	0.98	-0.29	-0.08	-0.30	-0.06	0.43	-0.27	1.00

Institutional Repository - Library & Information Centre - University of Thessaly
19/04/2024 03:53:45 EEST - 18.222.197.243

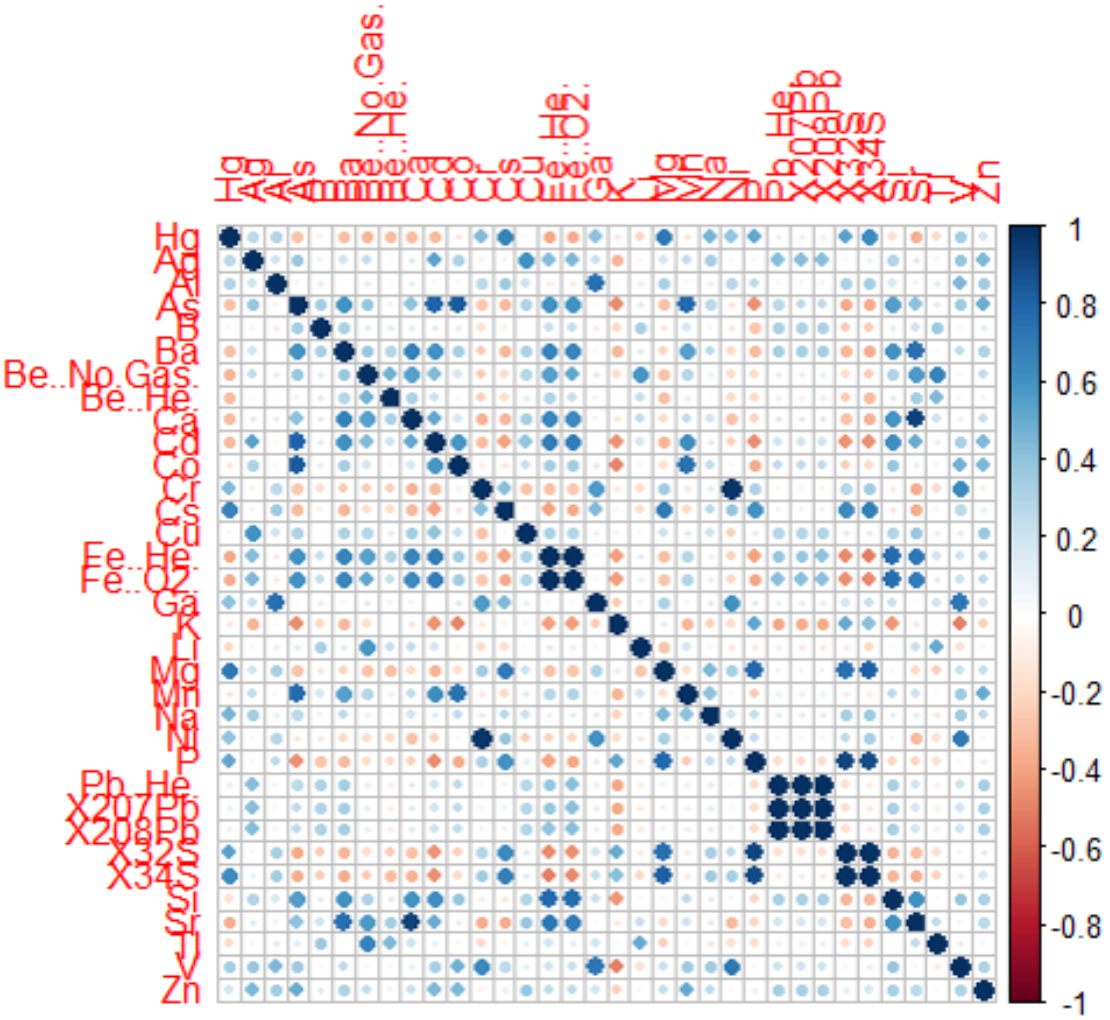

Figure 3.7: Correlations matrix obtained from the statistical programming environment R.

3.2 Chemical Analysis Results

In the tables below, the graphs of Hg concentrations for both sexes, male and female, and for both tissues, muscle and hepatopancreas (y axis = samples, x axis= mean value in ppb) are presented. With respect to the tissue comparison, the difference between muscle and hepatopancreas is directly observd. Hg is accumulated in higher level in muscle, compared to hepatopancreas. As for the comparison between males and females, it is observed that females tend to have higher Hg concentrations compared to males. Moreover, a higher accumulation in the summer months compared to September is also observed.

Institutional Repository - Library & Information Centre - University of Thessaly
19/04/2024 03:53:45 EEST - 18.222.197.243

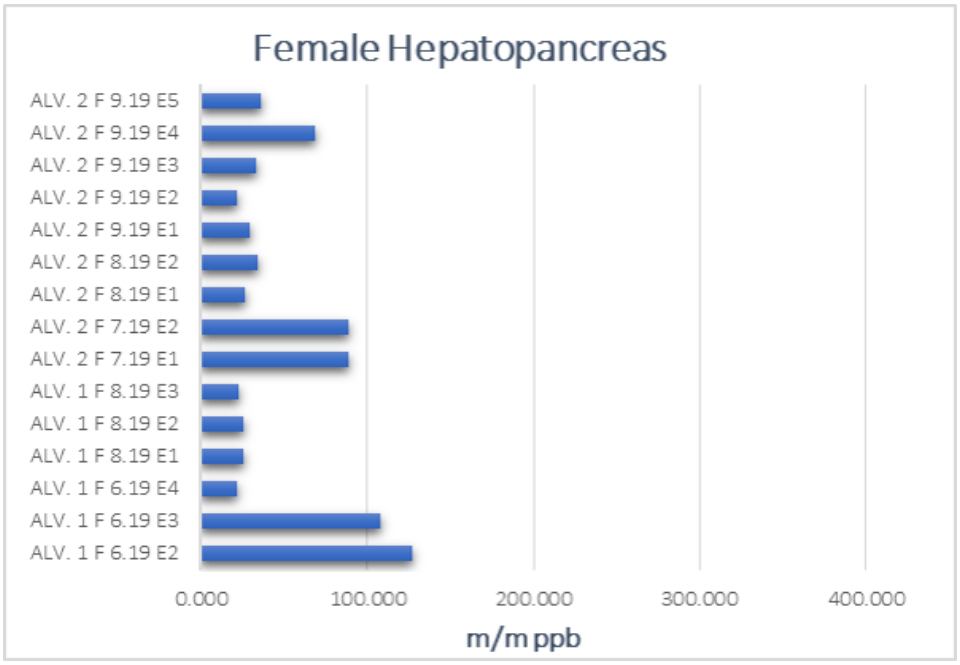

Figure 3.8: Mercury (Hg) concentration in samples of P. clarkii female hepatopancreas tissues.

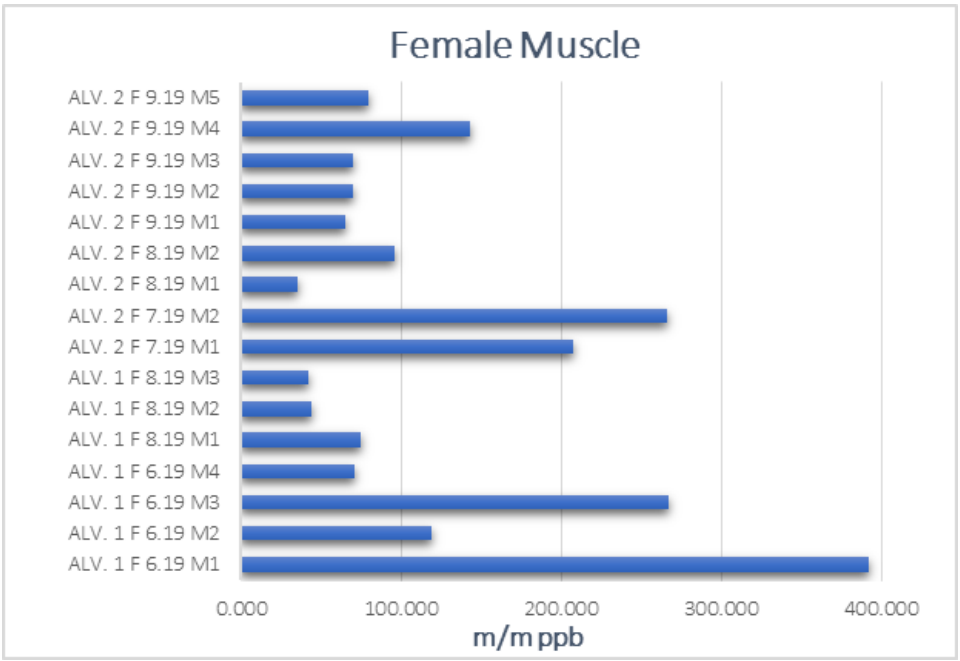

Figure 3.9: Mercury (Hg) concentration in samples of P. clarkii female muscle tissues.

The graphs 3.8, 3.9 above show the accumulation in the female hepatopancreas and muscle tissues respectively. In both tissues, the Hg accumulation is higher in June, while the muscle has significantly higher Hg concentration than the hepatopancreas.

Institutional Repository - Library & Information Centre - University of Thessaly
19/04/2024 03:53:45 EEST - 18.222.197.243

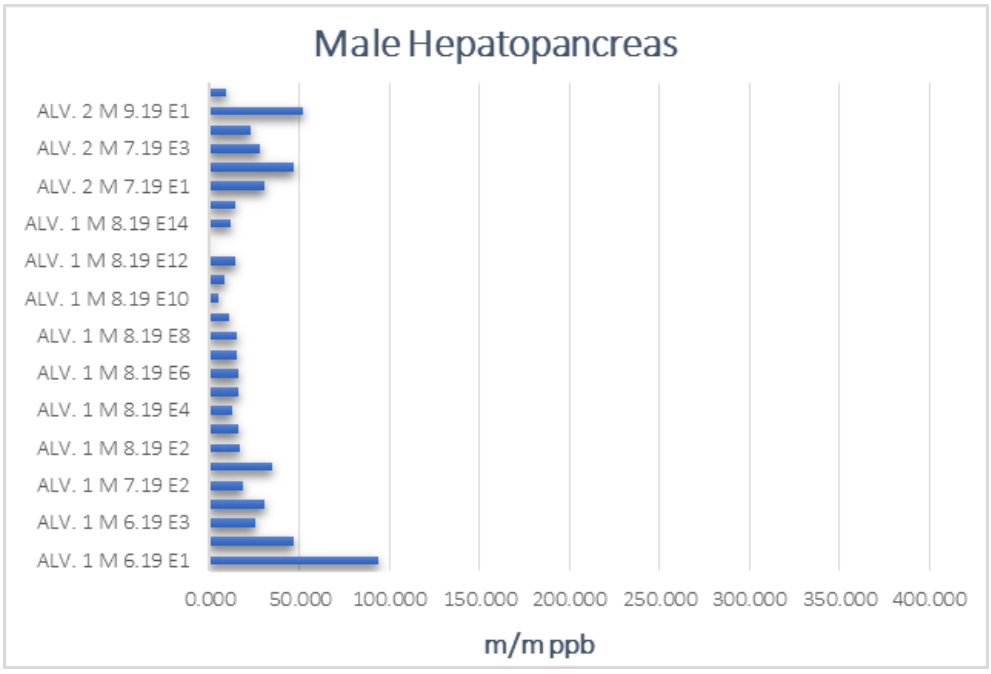

Figure 3.10: Mercury (Hg) concentration in samples of P. clarkii male hepatopancreas tissues.

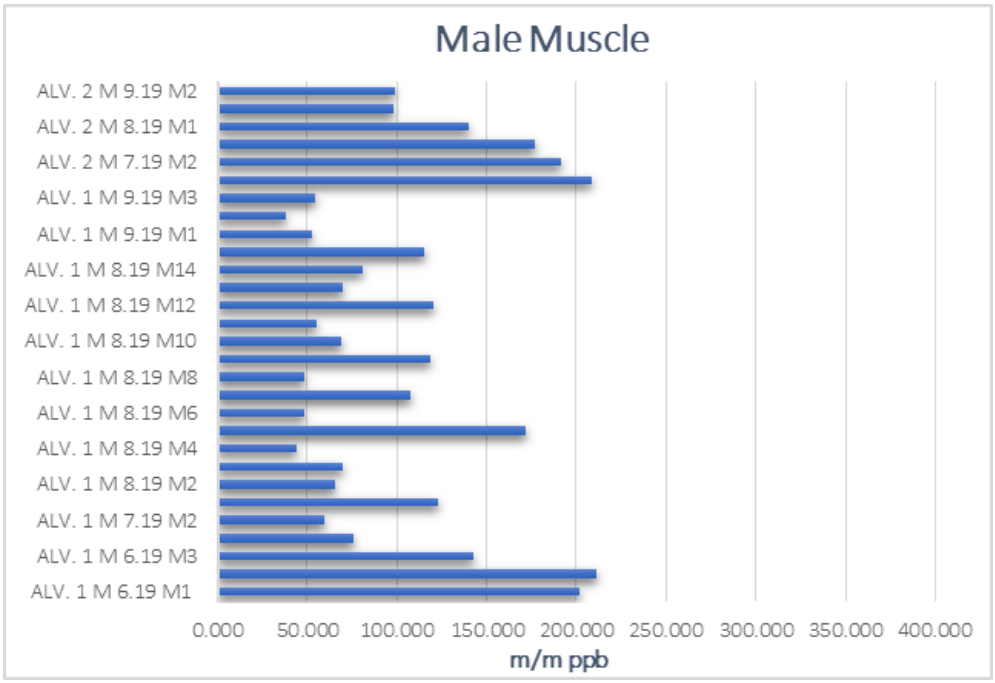

Figure 3.11: Mercury (Hg) concentration in samples of P. clarkii male muscle tissues.

The graphs 3.10, 3.11 above show the accumulation in the male hepatopancreas and muscle tissues respectively. In contrast with the female tissues, a different result is observed.While in the male hepatopancreas the higher concentration is in June too, in the muscle tissue very high concentrations are also observed in also July and August. As for the comparison between the two tissues, as in the female tissues, the

Institutional Repository - Library & Information Centre - University of Thessaly
19/04/2024 03:53:45 EEST - 18.222.197.243

Hg accumulation is higher in the male muscle than in hepatopancreas. Summing up, as seen in table 3.2 the mean Hg concentration in muscle tissues is 0.117 ppm, which is more than three times higher compared to hepatopancreas with 0.037 ppm.

Table 3.2: Comparison of Hg concentrations between sexes and specific tissues of P.clarkii.

	mean	**stdev**	**median**	**rsd**
muscle - female	0.128	0.103	0.077	80%
muscle - male	0.106	0.054	0.098	52%
hepatopancreas - female	0.051	0.036	0.033	71%
hepatopancreas - male	0.023	0.019	0.016	82%
total muscle	0.117	0.075	0.081	64%
total hepatopancreas	0.037	0.029	0.025	79%

Consecutively,using some of the most important elements, the figure 3.13 with the means, medians, standard deviations and relative standard deviations was conducted. As compared with the results of a previous study, in Trasimeno Lake, shown in figure 3.13, it is observed that:

1. Mn is higher concentrated in Alv. Lk compared to Tras.Lk, in both sexes and both tissues;

2. Co in Alviano Lake is in the same amounts as in Trasimeno Lake

3. Ni is in lower concentration in Alviano Lake, and significantly lower in hepatopancreas. The total mean of hepatopancreas in Alviano Lake is 0,73 ppm, when in Trasimeno Lake is 14,4 ppm;

4. Zn is higher concentrated in Alviano Lake than in Trasimeno Lake, with the exception of male hepatopancreas. In Trasimeno Lake the mean concentration of Zn is 28,98 ppm whereas in Alviano Lake it is 16,48 ppm;

5. as for Cd, even though the muscle concentrations in Alviano Lake are lower, the hepatopancreas concentrations are higher;

6. Pb is around the same numbers in both tissues, with the exception of the only higher concentration in female hepatoncreas in Alviano Lake, compared to Trasimeno Lake;

7. Hg is significantly higher in muscle tissues in Alviano Lake compared to Trasimeno Lake. An increase in the concentration in hepatopancreas is also observed in Alviano Lake compared to Trasimeno Lake.

Institutional Repository - Library & Information Centre - University of Thessaly
19/04/2024 03:53:45 EEST - 18.222.197.243

mg/Kg	Mn	Co	Ni	Cu	Zn	Ag	Cd	Pb	Hg
MUSCOLO MASCHIO									
MEDIA	1.13	0.03	4.45	8.42	13.46	0.011	0.004	0.041	0.027
DS	0.57	0.02	5.52	2.51	4.01	0.004	0.004	0.022	0.008
RSD%	51	64	124	30	30	31	95	54	30
MUSCOLO FEMMINA									
MEDIA	1.02	0.03	3.97	8.78	14.06	0.010	0.003	0.060	0.016
DS	0.40	0.02	5.85	4.07	1.24	0.002	0.002	0.043	0.006
RSD%	39	67	148	46	9	15	65	72	38
MUSCOLO TOTALE									
MEDIA	1.08	0.03	4.25	8.56	13.71	0.011	0.004	0.049	0.021
DS	0.51	0.02	5.67	3.25	3.20	0.003	0.004	0.034	0.009
RSD%	47	66	133	38	23	27	92	70	43
EPATOPANCREAS MASCHIO									
MEDIA	16.79	0.60	19.62	17.84	28.98	0.035	0.101	0.114	0.011
DS	9.75	0.29	29.96	21.16	17.40	0.051	0.040	0.178	0.006
RSD%	58	48	153	119	60	145	39	155	52
EPATOPANCREAS FEMMINA									
MEDIA	9.32	0.36	5.10	11.16	19.41	0.023	0.128	0.084	0.015
DS	4.39	0.10	3.42	6.64	4.53	0.018	0.060	0.066	0.007
RSD%	47	29	67	60	23	81	47	80	48
EPATOPANCREAS TOTALE									
MEDIA	14.10	0.51	14.40	15.44	25.53	0.031	0.111	0.103	0.013
DS	8.98	0.26	25.05	17.69	14.91	0.043	0.050	0.148	0.007
RSD%	64	51	174	115	58	139	45	143	53
LOD	0.0002	0.00002	0.0028	0.0003	0.0063	0.00002	0.00003	0.00004	0.00004

Figure 3.12: Metals concentration in P. clarkii hepatopancreas and muscle tissues in Trasimeno Lake.

Institutional Repository - Library & Information Centre - University of Thessaly
19/04/2024 03:53:45 EEST - 18.222.197.243

mg/kg (ppm)	Mn	Co	Ni	Cu	Zn	Cd	Pb	Hg	As	Cr
Muscle - Male										
Mean	2.17	0.05	2.19	6.14	14.76	0.01	0.04	0.11	0.25	3.47
Median	2.37	0.04	0.80	6.00	14.15	0.01	0.03	0.10	0.23	1.19
SD	1.91	0.05	3.60	2.17	3.28	0.00	0.03	0.05	0.11	5.97
RSD%	87.82	93.74	164.21	35.29	22.22	52.53	98.32	51.60	43.29	171.97
Muscle- Female										
Mean	1.74	0.05	2.43	7.53	16.21	0.01	0.05	0.13	0.20	3.76
Median	1.44	0.04	2.08	6.87	16.21	0.01	0.02	0.08	0.18	3.28
SD	1.50	0.03	1.97	1.71	2.87	0.01	0.09	0.10	0.06	3.21
RSD%	86.34	59.25	80.95	22.74	17.71	73.17	168.27	80.35	29.92	85.28
Muscle Total										
Mean	2.02	0.05	2.28	6.63	15.28	0.01	0.04	0.11	0.23	3.58
Median	1.46	0.04	0.92	6.41	15.66	0.01	0.03	0.08	0.22	1.42
SD	1.77	0.04	3.09	2.11	3.19	0.00	0.06	0.07	0.10	5.12
RSD%	87.67	83.40	135.96	31.77	20.85	62.64	142.87	65.94	41.50	143.24
Hepatopancreas - Male										
Mean	23.25	0.33	0.77	6.55	16.48	0.16	0.08	0.02	0.77	0.19
Median	12.81	0.20	0.60	6.68	12.43	0.14	0.07	0.02	0.75	0.03
SD	28.13	0.41	0.63	3.03	12.75	0.10	0.06	0.02	0.45	0.36
RSD%	120.97	124.80	81.72	46.23	77.33	63.03	66.51	82.37	58.32	190.32
Hepatopancreas - Female										
Mean	11.70	0.30	0.67	10.48	23.28	0.17	0.30	0.05	0.72	0.23
Median	8.60	0.22	0.62	9.87	21.51	0.15	0.05	0.03	0.69	0.05
SD	11.18	0.18	0.31	2.90	8.36	0.11	0.47	0.04	0.24	0.33
RSD%	95.62	61.35	45.88	27.65	35.89	62.85	157.26	70.89	33.15	144.68
Hepatopancreas Total										
Mean	19.02	0.32	0.73	7.99	18.97	0.16	0.17	0.03	0.75	0.20
Median	11.29	0.21	0.62	7.86	15.21	0.15	0.07	0.03	0.73	0.04
SD	23.88	0.34	0.53	3.51	11.70	0.10	0.30	0.03	0.38	0.34
RSD%	125.50	107.65	72.51	43.98	61.69	62.30	178.00	87.82	50.90	169.89
LOD	0.00004	0.000000004	0.00001	0.00001	0.00003	0.000001	0.000003	0.000002	0.000002	0.000004

Figure 3.13: Metals concentration in P. clarkii hepatopancreas and muscle tissues in Alviano Lake.

As seen in figure 3.14 both Ni and Cr are higher concentrated in muscle tissues, and higher concentrated in females compared to hepatopancreas and males, respectively. In figure 3.15 Hg shows significantly higher concentrations in muscle tissues, with higher concentration in females, while Cd shows significantly higher concentrations in hepatopancreas, with higher concentration in females. Figure 3.16 shows the concentrations of As, Co and Pb in both sexes and both tissues detected. As and Co are significantly higher concentrated in hepatopancreas, with higher concentration in males. However, although Pb is also significantly higher concentrated in hepatopancreas, higher concentration is observed in females compared to males. Moreover, as observed in figure 3.17 Cu and Zn are higher concentrated in hepatopancreas, with significantly higher concentration in female hepatopancreas compared to male hepatopancreas. Mn is significantly higher concentrations in hepatopancreas, with higher concentration in males.

Institutional Repository - Library & Information Centre - University of Thessaly
19/04/2024 03:53:45 EEST - 18.222.197.243

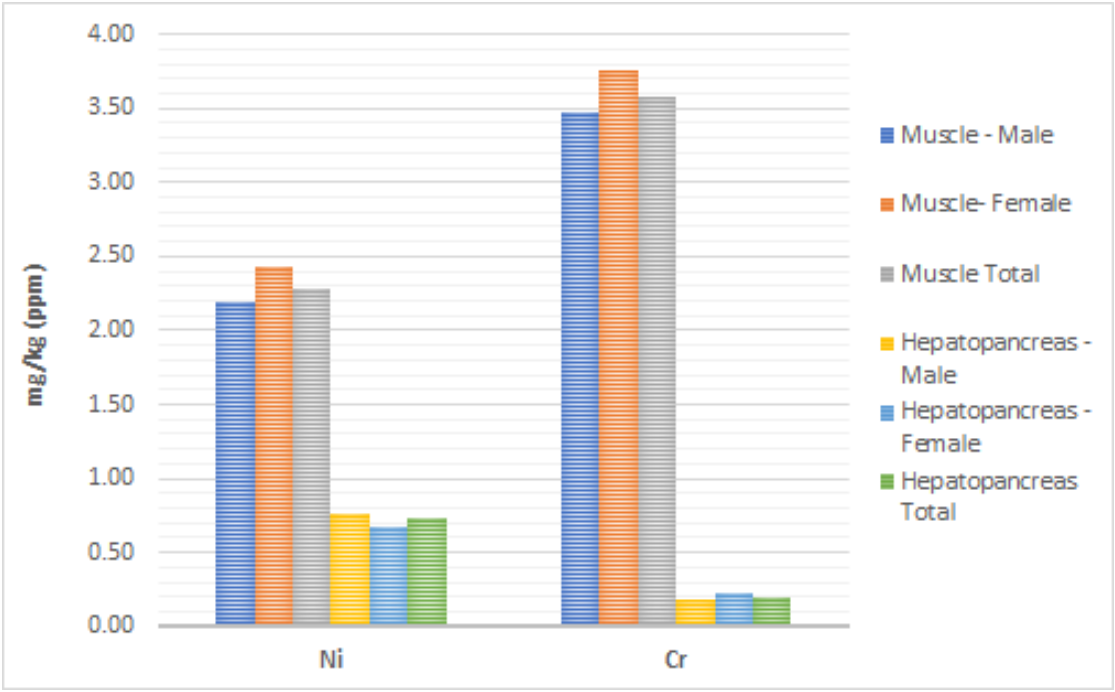

Figure 3.14: Concentrations of Ni and Cr in abdominal muscle tissues and hepatopancreas of P. clarkii in Alviano Lake.

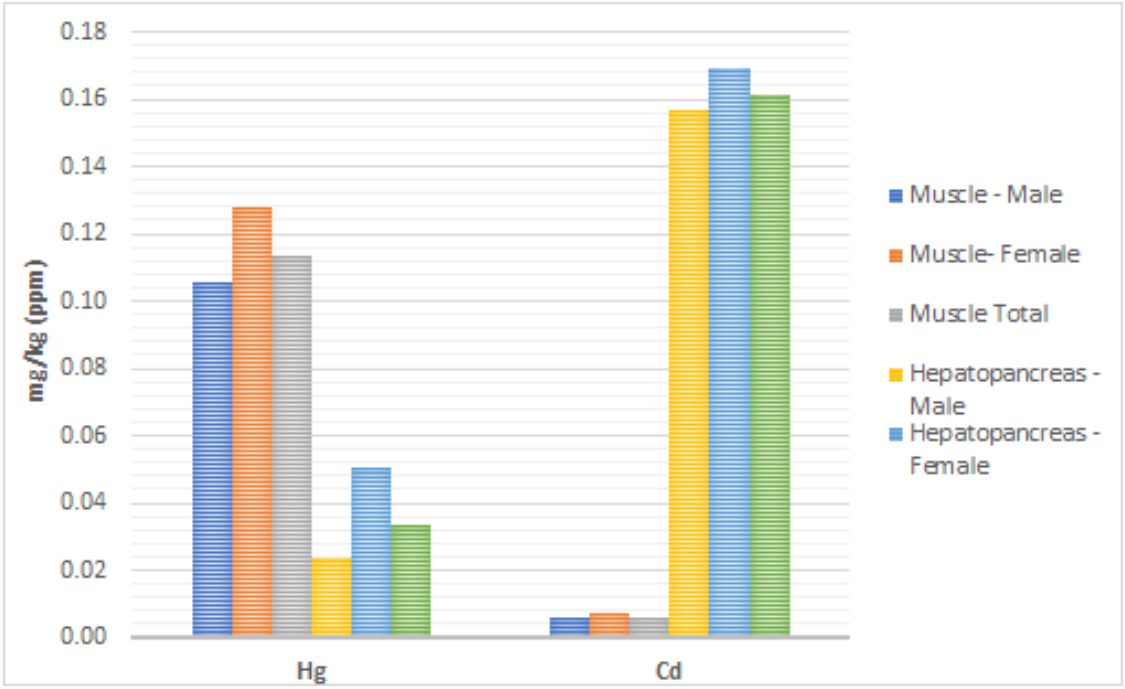

Figure 3.15: Concentrations of Hg and Cd in abdominal muscle tissues and hepatopancreas of P. clarkii in Alviano Lake.

Institutional Repository - Library & Information Centre - University of Thessaly
19/04/2024 03:53:45 EEST - 18.222.197.243

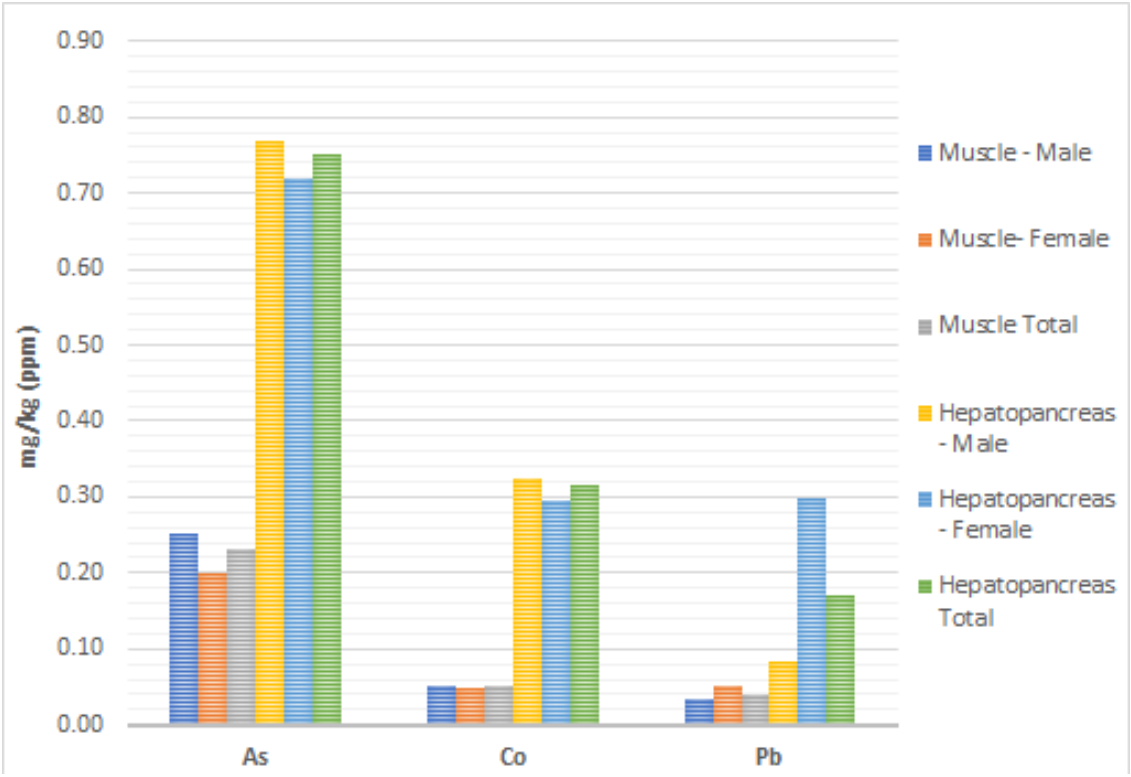

Figure 3.16: Concentrations of As, Co and Pb in abdominal muscle tissues and hepatopancreas of P. clarkii in Alviano Lake.

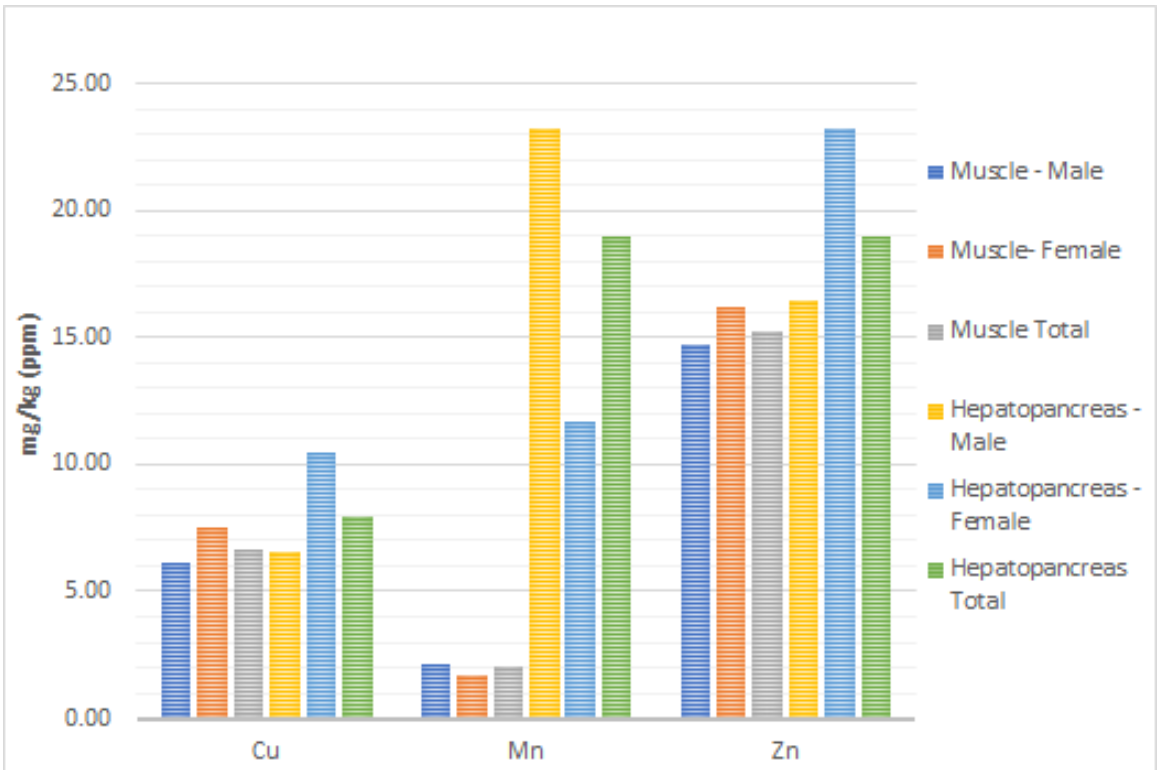

Figure 3.17: Concentrations of Cu, Mn and Zn in abdominal muscle tissues and hepatopancreas of P. clarkii in Alviano Lake.

Institutional Repository - Library & Information Centre - University of Thessaly
19/04/2024 03:53:45 EEST - 18.222.197.243

In table 3.2, an examination of the total average concentration data shows that the levels of accumulation are always greater in the muscle tissue, which is know to reflect a chronic exposure to pollutant inputs, while hepatopancreas, major tissue for detoxification, is the organ that reflects short term contaminant exposure. Total mean concentrations decrease in the following order: Zn> Cu> Cr> Ni> Mn> As> Hg> Co> Pb> Cd in the muscle and Mn> Zn> Cu> As> Ni> Co> Cr> Pb> Cd> Hg in hepatopancreas.

Table 3.3: Mean values of elements accumulation in different tissues of the crayfish species P. clarkii.

Species	**Tissue**	**Order**
P. clarkii	Muscle	Zn >Cu >Cr >Ni >Mn >As >Hg >Co >Pb >Cd
P. clarkii	Hepatopancreas	Mn >Zn >Cu >As >Ni >Co >Cr >Pb >Cd >Hg

Table 3.4: Elements accumulation in different tissues of the crayfish species P.clarkii.

Species	**Sex**	**Tissue**	**Order**
P. clarkii	Female	Muscle	Zn >Cu >Cr >Mn >As >Hg >Pb >Cd
P. clarkii	Male	Muscle	Zn >Cu >Cr >Mn >As >Hg >Pb >Cd
P. clarkii	Female	Hepatopancreas	Zn >Mn >Cu >As >Pb >Cr >Cd >Hg
P. clarkii	Male	Hepatopancreas	Mn >Zn >Cu >As >Cr >Cd >Pb >Hg

As regards the trends with respect to sex, the average concentrations of metals in the muscle are almost equal and decrease as follows: Zn> Cu> Ni> Mn> Pb> Co> Hg> Ag> Cd in the muscle of male specimens and Zn> Cu > Ni> Mn> Pb> Co> Ag> Hg> Cd in that of females.

Differences in concentration are instead observed in the muscles with higher values in the tissues of female specimens with the exception of Ag and Hg which have higher concentrations in males. In the hepatopancreas the average concentrations of metals decrease in the following order: Zn> Ni> Cu> Mn> Co> Pb> Cd> Ag> Hg in males and Zn> Cu> Mn> Ni> Co> Cd> Pb> Ag> Hg in females.

The results obtained are generally comparable with the values reported in the literature. There are some exceptions with some of the studies reporting lower or higher values than those observed in this study, for the same species, which could be justified by the different geological nature and biovailability of the metals in the study area.

Finally, it should be noted that the average concentrations of mercury, cadmium and lead in the muscle and in the hepatopancreas for both genders are below the maximum permissible limits (0.5 mg / kg of fresh weight) prescribed by Regulation (EC) No. 1881/2006 and 2014.

Institutional Repository - Library & Information Centre - University of Thessaly
19/04/2024 03:53:45 EEST - 18.222.197.243

Standard's	Cu	Cr	Pb	Cd	Zn	Mn	Hg	As
WHO (1989)	30	50	2	1	100	0.5-1	–	
CFHC (1994)	50	2	0.5	0.1	50	–	0.5	0.1
FAO (1983)	30	–	0.5	0.5	40	–	0.5	1.4
HKG (1987)							0.5	2.3
USEPA (2000)	120	8	4	2	120	–	–	
EC (2014)	–	–	0.3	0.5	30	–	–	
FSSAI (2015)	–	–	0.3	0.3	–	–	–	

Figure 3.18: Maximum Permissible Limit of trace metals in fish muscles (mg kg^{-1}) according to International Guideline values.

Additionally, in figure 3.18 the Maximum Permissible Limit (MPL) of trace metals in fish muscles according to International Guideline values is shown.In accordance with table 3.1 which presents the mean, median and standard deviation values of metals concentrations in crayfish tissues of this study, Mn reaches the Maximum Permissible Limit based on the World's Health Organization Standard. In contrast, both Cr and As exceed the MPL of Chinese Food Health Criterions Standard. Notably, the MPL of Hg, Cd and Pb based on EC/2006, is 0,5 pmm of fresh fish. So these elements concentrations in this study, even though are higher compared to the Trasimeno Lake results, they are not exceeding the MPL based on the European and Internaltional Standards.

Table 3.5: Mean, median and standard deviation (SD) values of metals concentrations (mg kg^{-1}) in P.clarkii hepatopancreas and muscle tissues.

		Cu	**Zn**	**Mn**	**Cr**	**Cd**	**Pb**	**Hg**	**As**
Hepatopancreas	**Mean**	7.99	18.97	19.02	0.20	0.16	0.17	0.03	0.75
	Median	7.86	15.21	11.29	0.04	0.15	0.07	0.03	0.73
	SD	3.51	11.70	23.88	0.34	0.10	0.30	0.03	0.38
Abdominal muscle	**Mean**	6.63	15.28	2.02	3.58	0.01	0.04	0.11	0.23
	Median	6.41	15.66	1.46	1.42	0.01	0.03	0.08	0.22
	SD	2.11	3.19	1.77	5.12	0.00	0.06	0.07	0.10

Table 3.6 shows the total mean concentrations by gender, the median values, the standard deviation and the RSD% values of the metals detected in the abdominal muscle and hepatopancreas tissues of P. clarkii and the respective LODs. All metal concentrations are expressed in mg/kg of wet weight and each metal investigated has a defined instrumental detection limit (LOD).

Institutional Repository - Library & Information Centre - University of Thessaly
19/04/2024 03:53:45 EEST - 18.222.197.243

Table 3.6: Mean (mg/kg) and median values by gender, the standard deviation,the RSD% and LOD values of metals in abdomincal muscle and hepatopancreas tissues.

mg/kg (ppm)	Mn	Co	Ni	Cu	Zn	Cd	Pb	Hg	As	Cr
Muscle - Male										
Mean	2.17	0.05	2.19	6.14	14.76	0.01	0.04	0.11	0.25	3.47
Median	2.37	0.04	0.80	6.00	14.15	0.01	0.03	0.10	0.23	1.19
SD	1.91	0.05	3.60	2.17	3.28	0.00	0.03	0.05	0.11	5.97
RSD%	87.82	93.74	164.21	35.29	22.22	52.53	98.32	51.60	43.29	171.97
Muscle- Female										
Mean	1.74	0.05	2.43	7.53	16.21	0.01	0.05	0.13	0.20	3.76
Median	1.44	0.04	2.08	6.87	16.21	0.01	0.02	0.08	0.18	3.28
SD	1.50	0.03	1.97	1.71	2.87	0.01	0.09	0.10	0.06	3.21
RSD%	86.34	59.25	80.95	22.74	17.71	73.17	168.27	80.35	29.92	85.28
Muscle Total										
Mean	2.02	0.05	2.28	6.63	15.28	0.01	0.04	0.11	0.23	3.58
Median	1.46	0.04	0.92	6.41	15.66	0.01	0.03	0.08	0.22	1.42
SD	1.77	0.04	3.09	2.11	3.19	0.00	0.06	0.07	0.10	5.12
RSD%	87.67	83.40	135.96	31.77	20.85	62.64	142.87	65.94	41.50	143.24
Hepatopancreas - Male										
Mean	23.25	0.33	0.77	6.55	16.48	0.16	0.08	0.02	0.77	0.19
Median	12.81	0.20	0.60	6.68	12.43	0.14	0.07	0.02	0.75	0.03
SD	28.13	0.41	0.63	3.03	12.75	0.10	0.06	0.02	0.45	0.36
RSD%	120.97	124.80	81.72	46.23	77.33	63.03	66.51	82.37	58.32	190.32
Hepatopancreas - Female										
Mean	11.70	0.30	0.67	10.48	23.28	0.17	0.30	0.05	0.72	0.23
Median	8.60	0.22	0.62	9.87	21.51	0.15	0.05	0.03	0.69	0.05
SD	11.18	0.18	0.31	2.90	8.36	0.11	0.47	0.04	0.24	0.33
RSD%	95.62	61.35	45.88	27.65	35.89	62.85	157.26	70.89	33.15	144.68
Hepatopancreas Total										
Mean	19.02	0.32	0.73	7.99	18.97	0.16	0.17	0.03	0.75	0.20
Median	11.29	0.21	0.62	7.86	15.21	0.15	0.07	0.03	0.73	0.04
SD	23.88	0.34	0.53	3.51	11.70	0.10	0.30	0.03	0.38	0.34
RSD%	125.50	107.65	72.51	43.98	61.69	62.30	178.00	87.82	50.90	169.89
LOD	0.00004	0.000000004	0.00001	0.00001	0.00003	0.000001	0.000003	0.000002	0.000002	0.000004

Furthermore, in figure 3.19, there is a comparison of the elemental concentrations in the muscle tissues between this study and studies from other regions. Generally, it is observed that Alviano Lake is not as contaminated as other areas, like Ebro river in Spain ([Hg] = 0,76-1,64 ppm), Chech Republic area ([Hg] = 1,18 ppm) and Luisiana in USA with Cu concentration as high as 204 ppm.

Location	Sex	Tissue	Cu	Zn	Mn	Cr	Cd	Pb	Hg	As
Present Study	*Female*	*Muscle*	*7.53*	*16.21*	*1.74*	*3.76*	*0.01*	*0.05*	*0.13*	*0.20*
Present Study	*Female*	*Hepatopancreas*	*10.48*	*23.28*	*11.70*	*0.23*	*0.17*	*0.30*	*0.05*	*0.72*
Present Study	*Male*	*Muscle*	*6.14*	*14.76*	*2.17*	*3.47*	*0.01*	*0.04*	*0.11*	*0.25*
Present Study	*Male*	*Hepatopancreas*	*6.55*	*16.48*	*23.25*	*0.19*	*0.16*	*0.08*	*0.02*	*0.77*
Czech Republic	-	*Muscle*	*32.9*	*76.9*	-	*4.2*	*0.05*	*<0.5*	*1.18*	-
Luisiana, USA	-	*Muscle*	*31*	*61*	-	-	*0.06*	*4.5*	-	*0.2-3.7*
Luisiana, USA	-	*Gill*	*204*	*113*	-	-	*0.23*	*4.2*	-	*0.6-8.7*
Ebro river, Spain	-	*Muscle*	*12.1-82.3*	*49.2-127*	*1.7-2.6*	-	*0.03-0.41*	*0.22-3.1*	*0.76-1.64*	*12.1-82.3*
Egypt	-	*Muscle*	*32.7*	*125*	-	*5.1*	-	*15.9*	-	-
South- Western Sicily, Italy	-	*Muscle*	*17.3*	*74.9*	-	*0.81*	-	*0.2*	-	-
California, USA	-	*Muscle*	*44.6*	*76.9*	-	*0.43*	-	*0.2*	-	*0.7*
China	-	*Muscle*	*10.7*	*11.7*	-	*0.4*	*0.1*	*0.72*	*0.024*	*0.028*

Figure 3.19: Comparison of elemental concentrations (mg kg^{-1} dry weight) in the muscle tissues of P.clarkii from the present study with other regions.

Institutional Repository - Library & Information Centre - University of Thessaly
19/04/2024 03:53:45 EEST - 18.222.197.243

3.3 Biochemical Analysis Results

Superoxide dismutase (SOD): is known to catalyze the dismutation of superoxide (O_2^-) to hydrogen peroxide (H_2O_2) and O_2. SOD is present in most aerobic organisms and is assumed to play a central role in providing defense against oxidative stress.

In the first graph 3.20 we observe that the SOD activity in hepatopancreas, is lower in summer and higher in autumn, both in males and females. Based also on the chemical analysis results, where we observed higher concentrations of Hg and other metals in summer, we could interpret that the decrease in SOD activity, in summer, is due to the presence of free radicals. In the second graph 3.21, compared to hepatopancreas results, we observe a more persistent decrease in the SOD activity in muscle, in both seasons, to both males and females. We could assume that this result is logical since muscle is a tissue that reflects chronic exposure, while hepatopancreas is the major tissue for detoxification.

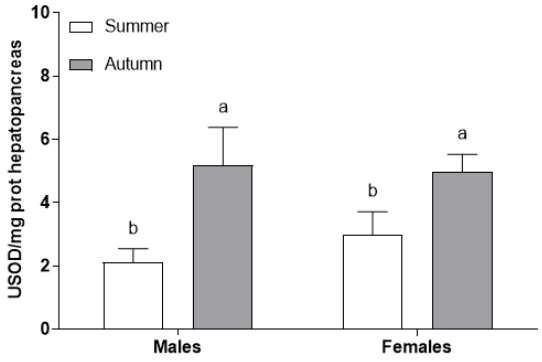

Figure 3.20: Superoxide dismutase activity (mean values ±SD) in hepatopancreas of both sexes of P. clarkii. Different lower case letters indicate statistically significant differences among seasons (Two-way ANOVA with Tukey's multiple comparisons test P<0.05).

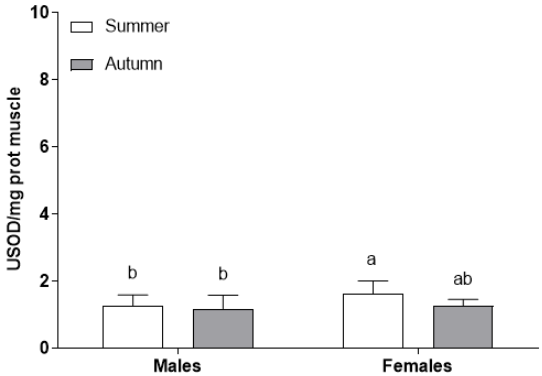

Figure 3.21: Superoxide dismutase activity (mean values ±SD) in muscle of both sexes of P. clarkii. Different lower case letters indicate statistically significant differences among seasons (Two-way ANOVA with Tukey's multiple comparisons test P<0.05).

Institutional Repository - Library & Information Centre - University of Thessaly
19/04/2024 03:53:45 EEST - 18.222.197.243

Catalase is a common enzyme found in nearly all living organisms exposed to oxygen (such as bacteria, plants, and animals) which catalyzes the decomposition of hydrogen peroxide to water and oxygen. It is a very important enzyme in protecting the cell from oxidative damage by reactive oxygen species (ROS).

Similarly to SOD activity, the graph 3.22 shows that the CAT activity in hepatopancreas, is lower in summer and higher in autumn, both in males and females. Therefore, it would appear that, in summer, crayfishes, especially females, are subjected to more harmful effects of free radicals and lipid peroxidation. Continuously, the muscle graph 3.23, shows again a lower activity of CAT to both sexes and seasons compared to hepatopancreas.

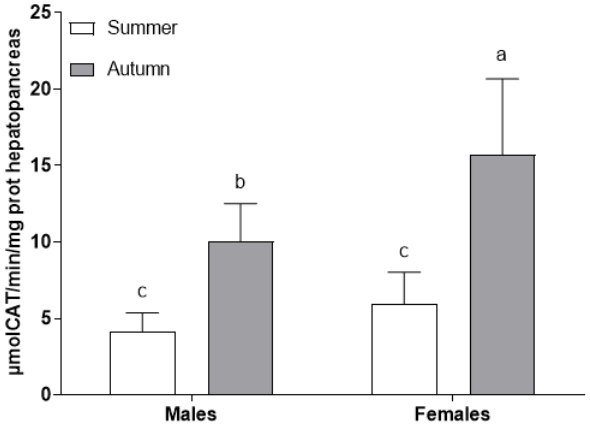

Figure 3.22: Catalase activity (mean values ±SD) in hepatopancreas of both sexes of P. clarkii. Different lower case letters indicate statistically significant differences among seasons (Two-way ANOVA with Tukey's multiple comparisons test P<0.05).

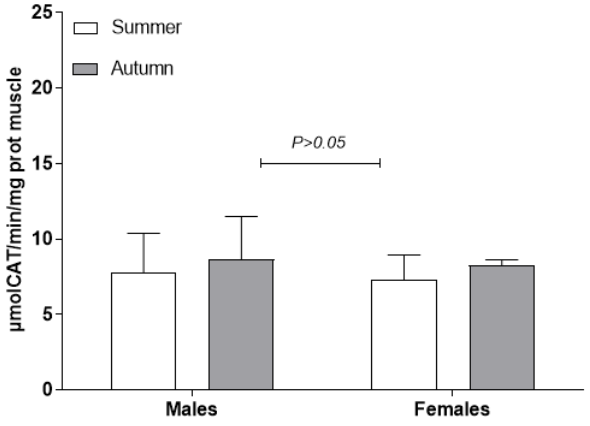

Figure 3.23: Catalase activity (mean values ±SD) in muscle of both sexes of P. clarkii. Different lower case letters indicate statistically significant differences among seasons (Two-way ANOVA with Tukey's multiple comparisons test P<0.05).

Glutathione peroxidase (GPx) is a cytosolic enzyme that catalyzes the reduction of hydrogen peroxide to water and oxygen as well as catalyzing the reduction of peroxide radicals to alcohols and oxygen.

Institutional Repository - Library & Information Centre - University of Thessaly
19/04/2024 03:53:45 EEST - 18.222.197.243

As seen in graph 3.24, the GPx activity in hepatopancreas, is lower in summer and higher in autumn, both in males and females. Therefore, it would appear that crayfishes, especially females, are subjected to more harmful effects of free radicals and consequently to oxidative stress. As for the graph 3.25, in comparison with the graph 3.24, a smaller decrease in the GPx activity to both male and female muscle tissues is observed, between summer and autumn.

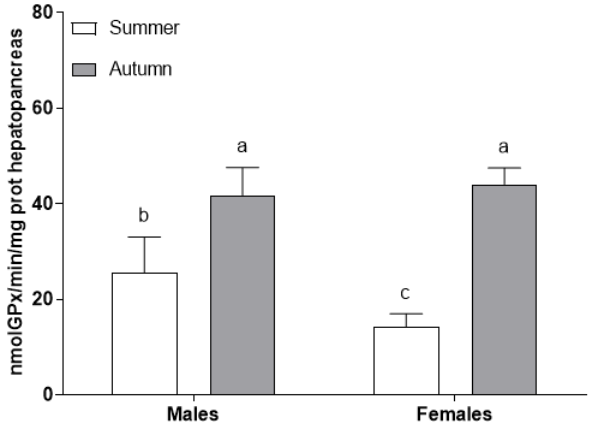

Figure 3.24: Glutathione peroxidase activity (mean values ±SD) in hepatopancreas of both sexes of P. clarkii. Different lower case letters indicate statistically significant differences among seasons (Two-way ANOVA with Tukey's multiple comparisons test P<0.05).

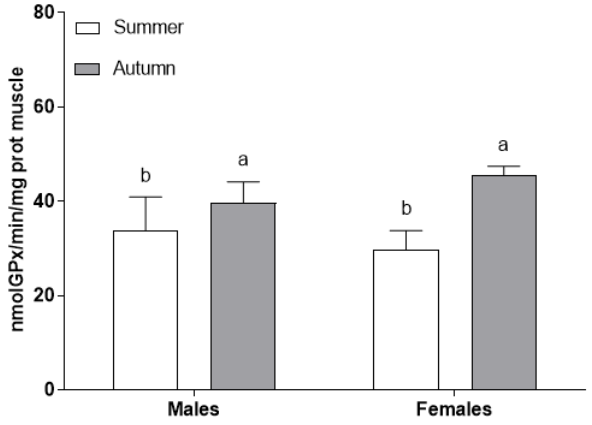

Figure 3.25: Glutathione peroxidase activity (mean values ±SD) in muscle of both sexes of P. clarkii. Different lower case letters indicate statistically significant differences among seasons (Two-way ANOVA with Tukey's multiple comparisons test P<0.05).

Glutathione S- transferase is best known for its ability to catalyze the conjugation of the reduced form of glutathione (GSH) to xenobiotic substrates for the purpose of detoxification.

Additionally, in the graph 3.26 the GST activity in hepatopancreas, is lower in summer and higher in autumn, both in males and females. So we could interpret that

Institutional Repository - Library & Information Centre - University of Thessaly
19/04/2024 03:53:45 EEST - 18.222.197.243

the result of lower GST activity, in summer, is explained of a potential defense mechanism against free radicals. Similarly to the other enzymes activity, as seen in the muscle graph 3.27, a lower activity of GST is observed to both sexes and seasons compared to hepatopancreas.

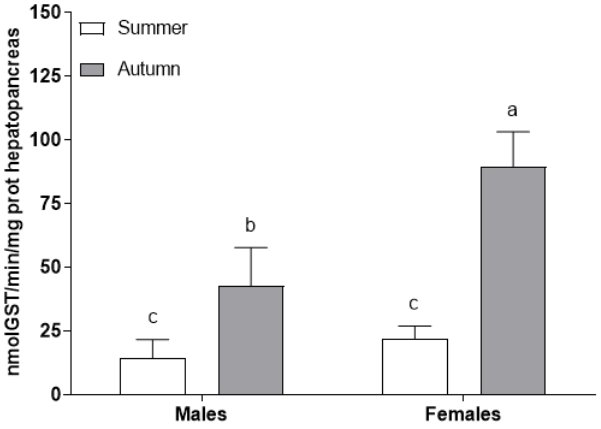

Figure 3.26: Glutathione S- transferase activity (mean values ±SD) in hepatopancreas of both sexes of P. clarkii. Different lower case letters indicate statistically significant differences among seasons (Two-way ANOVA with Tukey's multiple comparisons test P<0.05).

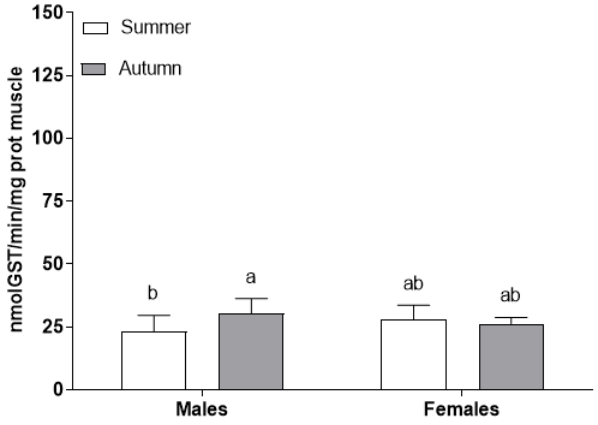

Figure 3.27: Glutathione S- transferase activity (mean values ±SD) in muscle of both sexes of P. clarkii. Different lower case letters indicate statistically significant differences among seasons (Two-way ANOVA with Tukey's multiple comparisons test P<0.05)..

As for the biochemical analysis results, in the hepatopancreas, all four biomarkers showed a decrease in the activity in summer, and an increase in autumn for both sexes, with bigger concentrations in females compared to males. Generally, in muscle tissues, even though there was not a significant difference among seasons and sexes,lower enzymes activities were observed compared to the activity in hepatopancreas.

The mode and action of chemicals, like heavy metals, play different role in the ac-

Institutional Repository - Library & Information Centre - University of Thessaly
19/04/2024 03:53:45 EEST - 18.222.197.243

tion of antioxidant enzymes. Different researchers point out that metals decrease the antioxidant's activity which is time dependent, and it also depends on the study area and the animal model used. But, generally, lots of literature and experimental analysis proves that, the level of antioxidant enzyme decreases as the level of free radicals increase. Because decrease of antioxidant level means, increase of free radicals, which ultimately increase the oxidative stress.

So based on both chemical and biochemical analysis, the results are consistent with each other. In chemical analysis higher contamination was found in summer months, and this explains the decrease in biomarkers' activity, which are considered the first defense line against oxyradicals, which triggers an interdependent enzymes cascade that offsets oxidative stress.

Moreover, the invasive red swamp crayfish, Procambarus clarkii, poses a serious threat to native freshwater species, causing significant economic damage every year. The high ecological value, resistance to environmental stresses, plasticity of the reproductive cycle, aggressiveness, ability to locomotion and dispersion and parental care make its eradication almost impossible and successful only if the diffusion environment is very limited spatially. Consequently, in large lakes such as Alviano, its eradication does not seem possible to date. Currently, the only way to mitigate the adverse effects of this alien species on lake ecosystems is to implement containment maneuvers, mainly based on large-scale sampling. These actions have produced positive environmental implications, but also led to the reconversion of this invasive species into a resource of considerable economic value for the fish market and the food chain. In fact, both recreational and professional fishing is rapidly increasing and is expanding all over the world, thanks also to the high economic performance of this species.

For the red shrimp population, which has settled in Alviano for 20 years and difficult to eradicate, a feasible and economically convenient choice is to adopt a policy of containment and control of the population through fishing, as a source of income. additional for lake fishermen. The adequate assessment of the chemical contamination of meat is therefore crucial for the maintenance and implementation of production, in order to support the seafood sector with a product of excellent quality and high commercial value.

The reported dataset from the present study clearly documents that the muscle tissue is the main storage organs for analyzed elements in the P.clarkii species followed by walking leg and abdominal muscle tissues. Compared to the international (WHO/-FAO) fishery products guidelines the accumulation of elements in the muscle tissues of crayfish were below the maximum permissible limits (0.5 mg / kg of fresh weight) prescribed by the regulation, (EC) No. 1881/2006, with few exceptions and considered safe for human consumption by avoiding the muscle tissues because these tissues contains elevated concentration of As, Mn and Cr. Since, the crayfish is an invasive species and have the capacity to tolerate high level of metal content compared to the native species. The both analyzed species from the study area can be consumed safely by humans and it can be used as a sentinel species for assessing the heavy metals contamination in freshwater ecosystems and culturing areas.

This study represents a first monitoring of the metal accumulaton in P. clarkii in the Alviano Lake. In the later stages of this research, you will need:

Institutional Repository - Library & Information Centre - University of Thessaly
19/04/2024 03:53:45 EEST - 18.222.197.243

1. increase the number of samples analyzed,
2. extend the sampling area to other sites in order to have more data available,
3. use comparison populations also from other continents and already available in the literature.

Institutional Repository - Library & Information Centre - University of Thessaly
19/04/2024 03:53:45 EEST - 18.222.197.243

Institutional Repository - Library & Information Centre - University of Thessaly
19/04/2024 03:53:45 EEST - 18.222.197.243

Bibliography

[1] Schroeder, W. H., K. Anlauf, L. A. Barrie, J. Y. Lu, A. Steffen,D. R. Schneeberger, and T, Berg. 1998. Arctic springtime depletion of mercury. Nature 394: 331–332.

[2] Lin C.and Pehkonen, S.O. 1999. The chemistry of atmospheric mercury: a review. Atmospheric Environment,33: 2067–2079.

[3] Boudou, A., and F. Ribeyre. 1997. Mercury in the food web: accumulation and transfer mechanisms, in metal ions in biological systems, Vol. 34, Mercury and Its Effects on Environment and Biology, Sigel, A. and Sigel, H., Eds., Marcel Dekker, New York, 1997, 289–319.

[4] United Nations Environment Programme. "Chapter 7: current production and use of mercury." in Global Mercury Assessment. pp. 117–134. Geneva, Switzerland: UNEP Chemicals, 2002. http://new.unep.org/gc/gc22/Document/UNEP-GC22-INF3.pdf (accessed February 5,2008).

[5] Chen, C., A. Amirbahman, N. Fisher, G. Harding, C. Lamborg, D. Nacci, and D. Taylor. 2008. Methylmercury in Marine Ecosystems: Spatial Patterns and Processes of Production, Bioaccumulation, and Biomagnification. EcoHealth doi:10.1007/s10393-008-0201-1.

[6] Fitzgerald, W. F., C. H. Lamborg, and C. R. Hammerschmidt. 2007. Marine biogeochemical cycling of mercury. Chemical Reviews 107: 641–662.

[7] Landis, M. S., R. K. Stevens, F. Schaedlich, and E. M. Prestbo. 2002. Development and characterization of an annular denuder methodology for the measurement of divalent inorganic reactive gaseous mercury in ambient air. Environmental Science and Technology 36: 3000–3009.

[8] Adriano, D. C. (2001). Trace elements in terrestrial environments. New York: Springer-Verlag. Agnan, Y., Le Dantec, T., Moore, C. W., Edwards, G. C., and Obrist, D. (2016). New Constraints on Terrestrial Surface¡Atmosphere Fluxes of Gaseous Elemental Mercury Using a Global Database. Environ. Sci. Technol. 50:507–524.

[9] Hazen, R. M., Golden, J., Downs, R. T., Hystad, G., Grew, E. S., Azzolini, D., and Sverjensky, D.A. (2012). Mercury (Hg) mineral evolution: A mineralogical record of supercontinent assembly, changing ocean geochemistry, and the emerging terrestrial biosphere. Am. Miner.97:1013–1042.

[10] Gilmour CC, Riedel GS, Ederington MC, Bell JT, Benoit JM, et al. 1998. Methylmercury concentrations and production rates across a trophic gradient in the northern everglades. Biogeochemistry 40:327–45

Institutional Repository - Library & Information Centre - University of Thessaly
19/04/2024 03:53:45 EEST - 18.222.197.243

[11] Benoit JM, Gilmour CC, Heyes A, Mason RP, Miller C. 2003. Geochemical and biological controls over methylmercury production and degradation in aquatic ecosystems. In ACS Symp. Ser. 835, ed. Y Chai, OC Braids, pp. 262–97.Washington, DC: Am. Chem. Soc.

[12] Kerin EJ, Gilmour CC, Roden E, Suzuki MT, Coates JD, Mason RP. 2006. Mercury methylation by dissimilatory iron-reducing bacteria. Appl. Environ. Microbiol. 72:7919

[13] Website:Lago di Alviano | WWF Italy

[14] Alcorlo, P., Otero, M., Crehuet, M., Baltanás, A., Montes, C., 2006. The use of the red swamp crayfish (Procambarus clarkii, Girard) as indicator of the bioavailability of heavy metals in environmental monitoring in the River Guadiamar (SW, Spain). Sci. Total Environ. 366 (1), 380–390. https://doi.org/10.1016/j.scitotenv.2006.02.023.

[15] Suárez-Serrano, A., Alcaraz, C., Ibáñez, C., Trobajo, R., Barata, C., 2010. Procambarus clarkii as a bioindicator of heavy metal pollution sources in the lower Ebro River and Delta. Ecotoxicol. Environ. Saf. 73 (3), 280–286. https://doi.org/10.1016/j.ecoenv.2009.11.001.

[16] Gedik, K., Kongchum, M., DeLaune, R.D., Sonnier, J.J., 2017. Distribution of arsenic and other metals in crayfish tissues (Procambarus clarkii) under different production practices. Sci. Total Environ. 574, 322–331. https://doi.org/10.1016/j.scitotenv.2016.09.060.

[17] Gherardi, F., 2006. Crayfish invading Europe: the case study of Procambarus clarkii. Mar. Freshw. Behav. Physiol. 39 (3), 175–191. https://doi.org/10.1080/10236240600869702.

[18] Handbook of ICP-QQQ Applications using the Agilent 8800 and 8900 - 4th Edition

[19] Halliwell B, Gutteridge JMC, editors. Free radicals in biology and medicine. Third ed. Oxford: Oxford Science Publications; 2000.p. 617– 24.

[20] Thomas CE, Morehouse LA, Aust SD. Ferritin and superoxide-dependent lipid peroxidation. J Biol Chem 1995;260(6):3275– 80.

[21] Young IS, Woodside JV. Antioxidants in health and disease. J Clin Pathol 2001;54:176–86.

[22] Livingstone, David W. "Adults' informal learning: Definitions, findings, gaps and future research." (2001).

[23] Meister, Alton, and Mary E. Anderson. "Glutathione." Annual review of biochemistry 52.1 (1983): 711-760.

[24] Lowry, Oliver H., et al. "Protein measurement with the Folin phenol reagent." Journal of biological chemistry 193 (1951): 265-275.

[25] McCord, Joe M., and Irwin Fridovich. "Superoxide dismutase: an enzymic function for erythrocuprein (hemocuprein)." Journal of Biological chemistry 244.22 (1969): 6049-6055.

Institutional Repository - Library & Information Centre - University of Thessaly
19/04/2024 03:53:45 EEST - 18.222.197.243

[26] Pacini, Nicole, et al. "Antioxidant response versus selenium accumulation in the liver and kidney of the Siberian sturgeon (Acipenser baeri)." Chemosphere 93.10 (2013): 2405-2412.

[27] Beutler, B., et al. "Identity of tumour necrosis factor and the macrophage-secreted factor cachectin." Nature 316.6028 (1985): 552-554.

[28] Lawrence, Richard A., and Raymond F. Burk. "Glutathione peroxidase activity in selenium-deficient rat liver." Biochemical and biophysical research communications 71.4 (1976): 952-958.

[29] Akerboom, Theodorus PM, and Helmut Sies. "[48] Assay of glutathione, glutathione disulfide, and glutathione mixed disulfides in biological samples." Methods in enzymology. Vol. 77. Academic Press, 1981. 373-382.

[30] Wickham, Hadley, and Garrett Grolemund. R for data science: import, tidy, transform, visualize, and model data. " O'Reilly Media, Inc.", 2016.

Institutional Repository - Library & Information Centre - University of Thessaly
19/04/2024 03:53:45 EEST - 18.222.197.243

Institutional Repository - Library & Information Centre - University of Thessaly
19/04/2024 03:53:45 EEST - 18.222.197.243

Appendix A

Tables

A.1 Female Data

Table A.1: Elements concentrations(mg/kg) in female hepatopancreas and muscle tissues.

Sample Name	Sex	Tissue	Ca	Cd	Co	Cr	Cs	Cu	Fe [He]	Fe [O2]
ALV. 1 F 6.19 M1	F	m	307,665	0,022	0,106	3,997	0,012	10,380	30,718	30,491
ALV. 1 F 6.19 M2	F	m	98,673	0,012	0,088	5,814	0,026	5,831	29,749	39,635
ALV. 1 F 6.19 M3	F	m	65,996	0,004	0,109	12,515	0,029	5,433	44,602	59,357
ALV. 1 F 6.19 M4	F	m	95,300	0,004	0,017	0,049	0,019	8,751	10,383	8,444
ALV. 1 F 8.19 M1	F	m	141,475	0,011	0,038	1,736	0,015	9,562	25,635	23,871
ALV. 1 F 8.19 M2	F	m	137,562	0,010	0,035	1,610	0,012	7,596	16,334	16,550
ALV. 1 F 8.19 M3	F	m	145,460	0,003	0,030	2,468	0,011	6,036	17,514	16,890
ALV. 2 F 7.19 M1	F	m	140,277	0,007	0,039	0,112	0,030	10,302	8,534	9,402
ALV. 2 F 7.19 M2	F	m	188,203	0,003	0,024	0,912	0,041	6,410	13,406	14,030
ALV. 2 F 8.19 M1	F	m	109,581	0,003	0,032	1,203	0,012	7,893	10,686	8,451
ALV. 2 F 8.19 M2	F	m	125,025	0,005	0,029	3,443	0,031	5,653	21,479	21,166
ALV. 2 F 9.19 M1	F	m	130,952	0,003	0,035	5,255	0,016	6,577	36,267	35,504
ALV. 2 F 9.19 M2	F	m	288,097	0,007	0,059	5,504	0,023	9,841	51,207	50,313
ALV. 2 F 9.19 M3	F	m	135,104	0,004	0,072	7,514	0,017	6,790	39,500	40,513
ALV. 2 F 9.19 M4	F	m	162,807	0,005	0,046	4,930	0,015	6,521	26,903	26,493
ALV. 2 F 9.19 M5	F	m	208,217	0,007	0,028	3,114	0,014	6,950	22,091	19,817
ALV. 1 F 6.19 E2	F	h	218,074	0,504	0,616	0,400	0,007	14,766	1118,963	1543,630
ALV. 1 F 6.19 E3	F	h	87,393	0,142	0,413	1,174	0,010	11,417	173,011	227,689
ALV. 1 F 6.19 E4	F	h	161,017	0,063	0,112	0,048	0,005	8,150	153,528	129,144
ALV. 1 F 8.19 E1	F	h	287,987	0,207	0,211	0,050	0,004	14,531	387,855	434,913
ALV. 1 F 8.19 E2	F	h	287,696	0,179	0,210	0,109	0,007	9,144	296,623	348,401
ALV. 1 F 8.19 E3	F	h	298,704	0,136	0,215	0,042	0,006	9,733	401,979	462,004
ALV. 2 F 7.19 E1	F	h	675,000	0,198	0,772	0,341	0,010	7,864	469,638	594,374
ALV. 2 F 7.19 E2	F	h	351,427	0,065	0,312	0,733	0,017	10,031	1057,043	1382,928
ALV. 2 F 8.19 E1	F	h	142,389	0,137	0,347	0,013	0,005	10,469	328,712	365,345
ALV. 2 F 8.19 E2	F	h	219,546	0,055	0,162	0,040	0,008	7,166	372,053	417,393
ALV. 2 F 9.19 E1	F	h	473,226	0,212	0,197	0,050	0,007	12,405	734,054	838,934
ALV. 2 F 9.19 E2	F	h	271,717	0,212	0,294	0,038	0,008	9,055	770,273	822,785
ALV. 2 F 9.19 E3	F	h	236,198	0,119	0,210	0,054	0,011	16,201	132,195	144,987
ALV. 2 F 9.19 E4	F	h	377,347	0,164	0,247	0,053	0,008	9,868	526,505	574,479
ALV. 2 F 9.19 E5	F	h	330,964	0,148	0,134	0,267	0,007	6,341	552,713	608,795

Institutional Repository - Library & Information Centre - University of Thessaly
19/04/2024 03:53:45 EEST - 18.222.197.243

Table A.2: Elements concentrations(mg/kg) in female hepatopancreas and muscle tissues.

Sample Name	Sex	Tissue	Ca	Cd	Co	Cr	Cs	Cu	Fe [He]	Fe [O2]
ALV. 1 F 6.19 M1	F	m	307.665	0.022	0.106	3.997	0.012	10.380	30.718	30.491
ALV. 1 F 6.19 M2	F	m	98.673	0.012	0.088	5.814	0.026	5.831	29.749	39.635
ALV. 1 F 6.19 M3	F	m	65.996	0.004	0.109	12.515	0.029	5.433	44.602	59.357
ALV. 1 F 6.19 M4	F	m	95.300	0.004	0.017	0.049	0.019	8.751	10.383	8.444
ALV. 1 F 8.19 M1	F	m	141.475	0.011	0.038	1.736	0.015	9.562	25.635	23.871
ALV. 1 F 8.19 M2	F	m	137.562	0.010	0.035	1.610	0.012	7.596	16.334	16.550
ALV. 1 F 8.19 M3	F	m	145.460	0.003	0.030	2.468	0.011	6.036	17.514	16.890
ALV. 2 F 7.19 M1	F	m	140.277	0.007	0.039	0.112	0.030	10.302	8.534	9.402
ALV. 2 F 7.19 M2	F	m	188.203	0.003	0.024	0.912	0.041	6.410	13.406	14.030
ALV. 2 F 8.19 M1	F	m	109.581	0.003	0.032	1.203	0.012	7.893	10.686	8.451
ALV. 2 F 8.19 M2	F	m	125.025	0.005	0.029	3.443	0.031	5.653	21.479	21.166
ALV. 2 F 9.19 M1	F	m	130.952	0.003	0.035	5.255	0.016	6.577	36.267	35.504
ALV. 2 F 9.19 M2	F	m	288.097	0.007	0.059	5.504	0.023	9.841	51.207	50.313
ALV. 2 F 9.19 M3	F	m	135.104	0.004	0.072	7.514	0.017	6.790	39.500	40.513
ALV. 2 F 9.19 M4	F	m	162.807	0.005	0.046	4.930	0.015	6.521	26.903	26.493
ALV. 2 F 9.19 M5	F	m	208.217	0.007	0.028	3.114	0.014	6.950	22.091	19.817
ALV. 1 F 6.19 E2	F	h	218.074	0.504	0.616	0.400	0.007	14.766	1118.963	1543.630
ALV. 1 F 6.19 E3	F	h	87.393	0.142	0.413	1.174	0.010	11.417	173.011	227.689
ALV. 1 F 6.19 E4	F	h	161.017	0.063	0.112	0.048	0.005	8.150	153.528	129.144
ALV. 1 F 8.19 E1	F	h	287.987	0.207	0.211	0.050	0.004	14.531	387.855	434.913
ALV. 1 F 8.19 E2	F	h	287.696	0.179	0.210	0.109	0.007	9.144	296.623	348.401
ALV. 1 F 8.19 E3	F	h	298.704	0.136	0.215	0.042	0.006	9.733	401.979	462.004
ALV. 2 F 7.19 E1	F	h	675.000	0.198	0.772	0.341	0.010	7.864	469.638	594.374
ALV. 2 F 7.19 E2	F	h	351.427	0.065	0.312	0.733	0.017	10.031	1057.043	1382.928
ALV. 2 F 8.19 E1	F	h	142.389	0.137	0.347	0.013	0.005	10.469	328.712	365.345
ALV. 2 F 8.19 E2	F	h	219.546	0.055	0.162	0.040	0.008	7.166	372.053	417.393
ALV. 2 F 9.19 E1	F	h	473.226	0.212	0.197	0.050	0.007	12.405	734.054	838.934
ALV. 2 F 9.19 E2	F	h	271.717	0.212	0.294	0.038	0.008	9.055	770.273	822.785
ALV. 2 F 9.19 E3	F	h	236.198	0.119	0.210	0.054	0.011	16.201	132.195	144.987
ALV. 2 F 9.19 E4	F	h	377.347	0.164	0.247	0.053	0.008	9.868	526.505	574.479
ALV. 2 F 9.19 E5	F	h	330.964	0.148	0.134	0.267	0.007	6.341	552.713	608.795

Table A.3: Elements concentrations(mg/kg) in female hepatopancreas and muscle tissues.

Sample Name	Sex	Tissue	Ga	K	Li	Mg	Mn	Na	Ni	P
ALV. 1 F 6.19 M1	F	m	0,0053	1584,819	<DL	334,796	6,909	1601,710	2,494	1646,518
ALV. 1 F 6.19 M2	F	m	0,0033	1504,490	<DL	292,828	1,589	671,328	4,283	1533,789
ALV. 1 F 6.19 M3	F	m	0,0063	2100,710	<DL	328,776	2,463	785,831	7,636	1980,472
ALV. 1 F 6.19 M4	F	m	0,0010	26483,080	0,070	285,703	2,038	749,395	0,172	2173,706
ALV. 1 F 8.19 M1	F	m	0,0011	27795,556	0,029	277,957	1,221	579,716	1,293	1978,889
ALV. 1 F 8.19 M2	F	m	0,0002	24007,383	<DL	228,352	1,451	778,360	1,166	1940,612
ALV. 1 F 8.19 M3	F	m	0,0013	23110,835	0,022	222,930	0,724	540,754	1,583	1818,249
ALV. 2 F 7.19 M1	F	m	0,0006	2557,827	<DL	535,250	0,780	988,328	0,205	2419,830
ALV. 2 F 7.19 M2	F	m	0,0038	1836,383	<DL	386,441	0,847	1147,025	0,603	1635,544
ALV. 2 F 8.19 M1	F	m	0,0009	30494,693	<DL	309,808	0,600	562,641	0,808	2143,246
ALV. 2 F 8.19 M2	F	m	0,0021	26402,240	<DL	255,146	0,874	525,995	2,215	2218,332
ALV. 2 F 9.19 M1	F	m	0,0050	22615,685	0,006	252,203	2,143	580,674	3,108	1864,456
ALV. 2 F 9.19 M2	F	m	0,0098	26540,681	0,064	311,108	2,249	684,828	3,578	2128,868
ALV. 2 F 9.19 M3	F	m	0,0044	25972,822	0,152	273,220	1,540	674,495	4,741	2467,033
ALV. 2 F 9.19 M4	F	m	0,0023	17331,004	0,108	217,137	1,428	669,279	3,021	1565,366
ALV. 2 F 9.19 M5	F	m	0,0009	26442,831	0,062	296,960	0,928	741,076	1,936	1986,936
ALV. 1 F 6.19 E2	F	h	0,0036	1220,968	0,019	263,253	46,205	1140,910	0,991	1072,016
ALV. 1 F 6.19 E3	F	h	0,0027	726,635	<DL	112,685	11,735	498,383	1,003	676,769
ALV. 1 F 6.19 E4	F	h	0,0033	12696,551	0,309	113,237	18,863	816,790	1,275	823,650
ALV. 1 F 8.19 E1	F	h	0,0013	17587,287	<DL	160,190	11,515	472,063	0,620	1085,984
ALV. 1 F 8.19 E2	F	h	0,0038	13630,033	<DL	134,729	22,493	609,322	0,518	831,605
ALV. 1 F 8.19 E3	F	h	0,0038	12872,244	0,091	149,495	5,439	590,992	0,671	987,921
ALV. 2 F 7.19 E1	F	h	0,0095	745,673	<DL	214,528	11,295	550,726	1,149	824,606
ALV. 2 F 7.19 E2	F	h	0,0018	1087,470	<DL	340,406	6,284	936,591	0,565	1251,514
ALV. 2 F 8.19 E1	F	h	0,0014	12052,424	0,040	116,621	2,789	386,453	0,380	1066,305
ALV. 2 F 8.19 E2	F	h	0,0027	11021,891	<DL	143,505	4,829	415,548	0,425	926,141
ALV. 2 F 9.19 E1	F	h	0,0027	15517,509	0,060	281,303	12,496	657,549	0,238	1742,595
ALV. 2 F 9.19 E2	F	h	0,0010	11766,867	0,073	204,182	8,179	462,289	0,511	1541,316
ALV. 2 F 9.19 E3	F	h	0,0012	15088,090	0,027	182,084	2,366	571,097	0,764	1182,729
ALV. 2 F 9.19 E4	F	h	0,0099	13473,606	0,127	237,615	8,601	759,683	0,617	1148,813
ALV. 2 F 9.19 E5	F	h	0,0013	12497,303	<DL	219,856	2,344	470,028	0,335	1350,366

Institutional Repository - Library & Information Centre - University of Thessaly
19/04/2024 03:53:45 EEST - 18.222.197.243

Table A.4: Elements concentrations(mg/kg) in female hepatopancreas and muscle tissues.

Sample Name	Sex	Tissue	Ga	K	Li	Mg	Mn	Na	Ni	P
ALV. 1 F 6.19 M1	F	m	0,0053	1584,819	<DL	334,796	6,909	1601,710	2,494	1646,518
ALV. 1 F 6.19 M2	F	m	0,0033	1504,490	<DL	292,828	1,589	671,328	4,283	1533,789
ALV. 1 F 6.19 M3	F	m	0,0063	2100,710	<DL	328,776	2,463	785,831	7,636	1980,472
ALV. 1 F 6.19 M4	F	m	0,0010	26483,080	0,070	285,703	2,038	749,395	0,172	2173,706
ALV. 1 F 8.19 M1	F	m	0,0011	27795,556	0,029	277,957	1,221	579,716	1,293	1978,889
ALV. 1 F 8.19 M2	F	m	0,0002	24007,383	<DL	228,352	1,451	778,360	1,166	1940,612
ALV. 1 F 8.19 M3	F	m	0,0013	23110,835	0,022	222,930	0,724	540,754	1,583	1818,249
ALV. 2 F 7.19 M1	F	m	0,0006	2557,827	<DL	535,250	0,780	988,328	0,205	2419,830
ALV. 2 F 7.19 M2	F	m	0,0038	1836,383	<DL	386,441	0,847	1147,025	0,603	1635,544
ALV. 2 F 8.19 M1	F	m	0,0009	30494,693	<DL	309,808	0,600	562,641	0,808	2143,246
ALV. 2 F 8.19 M2	F	m	0,0021	26402,240	<DL	255,146	0,874	525,995	2,215	2218,332
ALV. 2 F 9.19 M1	F	m	0,0050	22615,685	0,006	252,203	2,143	580,674	3,108	1864,456
ALV. 2 F 9.19 M2	F	m	0,0098	26540,681	0,064	311,108	2,249	684,828	3,578	2128,868
ALV. 2 F 9.19 M3	F	m	0,0044	25972,822	0,152	273,220	1,540	674,495	4,741	2467,033
ALV. 2 F 9.19 M4	F	m	0,0023	17331,004	0,108	217,137	1,428	669,279	3,021	1565,366
ALV. 2 F 9.19 M5	F	m	0,0009	26442,831	0,062	296,960	0,928	741,076	1,936	1986,936
ALV. 1 F 6.19 E2	F	h	0,0036	1220,968	0,019	263,253	46,205	1140,910	0,991	1072,016
ALV. 1 F 6.19 E3	F	h	0,0027	726,635	<DL	112,685	11,735	498,383	1,003	676,769
ALV. 1 F 6.19 E4	F	h	0,0033	12696,551	0,309	113,237	18,863	816,790	1,275	823,650
ALV. 1 F 8.19 E1	F	h	0,0013	17587,287	<DL	160,190	11,515	472,063	0,620	1085,984
ALV. 1 F 8.19 E2	F	h	0,0038	13630,033	<DL	134,729	22,493	609,322	0,518	831,605
ALV. 1 F 8.19 E3	F	h	0,0038	12872,244	0,091	149,495	5,439	590,992	0,671	987,921
ALV. 2 F 7.19 E1	F	h	0,0095	745,673	<DL	214,528	11,295	550,726	1,149	824,606
ALV. 2 F 7.19 E2	F	h	0,0018	1087,470	<DL	340,406	6,284	936,591	0,565	1251,514
ALV. 2 F 8.19 E1	F	h	0,0014	12052,424	0,040	116,621	2,789	386,453	0,380	1066,305
ALV. 2 F 8.19 E2	F	h	0,0027	11021,891	<DL	143,505	4,829	415,548	0,425	926,141
ALV. 2 F 9.19 E1	F	h	0,0027	15517,509	0,060	281,303	12,496	657,549	0,238	1742,595
ALV. 2 F 9.19 E2	F	h	0,0010	11766,867	0,073	204,182	8,179	462,289	0,511	1541,316
ALV. 2 F 9.19 E3	F	h	0,0012	15088,090	0,027	182,084	2,366	571,097	0,764	1182,729
ALV. 2 F 9.19 E4	F	h	0,0099	13473,606	0,127	237,615	8,601	759,683	0,617	1148,813
ALV. 2 F 9.19 E5	F	h	0,0013	12497,303	<DL	219,856	2,344	470,028	0,335	1350,366

Table A.5: Elements concentrations(mg/kg) in female hepatopancreas and muscle tissues.

Sample Name	Sex	Tissue	Tl	V	Zn
ALV. 1 F 6.19 M1	F	m	0,0003	0,082	22,648
ALV. 1 F 6.19 M2	F	m	<DL	0,058	18,444
ALV. 1 F 6.19 M3	F	m	<DL	0,147	16,598
ALV. 1 F 6.19 M4	F	m	0,0009	0,017	14,895
ALV. 1 F 8.19 M1	F	m	0,0009	0,014	15,813
ALV. 1 F 8.19 M2	F	m	0,0006	0,012	12,586
ALV. 1 F 8.19 M3	F	m	0,0008	0,027	12,732
ALV. 2 F 7.19 M1	F	m	<DL	0,038	19,662
ALV. 2 F 7.19 M2	F	m	<DL	0,051	16,667
ALV. 2 F 8.19 M1	F	m	0,0012	0,017	16,640
ALV. 2 F 8.19 M2	F	m	0,0017	0,041	15,692
ALV. 2 F 9.19 M1	F	m	0,0007	0,057	13,206
ALV. 2 F 9.19 M2	F	m	0,0013	0,085	18,343
ALV. 2 F 9.19 M3	F	m	0,0007	0,051	15,683
ALV. 2 F 9.19 M4	F	m	0,0015	0,037	11,706
ALV. 2 F 9.19 M5	F	m	0,0003	0,028	18,006
ALV. 1 F 6.19 E2	F	h	0,0007	0,117	36,765
ALV. 1 F 6.19 E3	F	h	0,0002	0,076	18,918
ALV. 1 F 6.19 E4	F	h	0,0013	0,047	15,210
ALV. 1 F 8.19 E1	F	h	<DL	0,035	14,324
ALV. 1 F 8.19 E2	F	h	0,0031	0,080	12,818
ALV. 1 F 8.19 E3	F	h	0,0048	0,048	15,990
ALV. 2 F 7.19 E1	F	h	0,0002	0,105	29,832
ALV. 2 F 7.19 E2	F	h	<DL	0,046	31,115
ALV. 2 F 8.19 E1	F	h	0,0020	0,023	14,918
ALV. 2 F 8.19 E2	F	h	0,0025	0,022	30,171
ALV. 2 F 9.19 E1	F	h	0,0031	0,047	21,507
ALV. 2 F 9.19 E2	F	h	0,0028	0,042	19,959
ALV. 2 F 9.19 E3	F	h	0,0019	0,036	27,301
ALV. 2 F 9.19 E4	F	h	0,0070	0,073	37,983
ALV. 2 F 9.19 E5	F	h	0,0018	0,035	22,443

Institutional Repository - Library & Information Centre - University of Thessaly
19/04/2024 03:53:45 EEST - 18.222.197.243

A.2 Male Data

Table A.6: Elements concentrations(mg/kg) in males hepatopancreas and muscle tissues.

Sample Name	Sex	Tissue	Hg	Ag	Al	As	B	Ba	Be [No Gas]	Be [He]
ALV. 1 M 6.19 M1	M	m	0,201	0,020	9,158	0,291	0,442	0,645	<DL	0,000
ALV. 1 M 6.19 M2	M	m	0,211	0,018	6,101	0,297	0,414	0,466	<DL	0,000
ALV. 1 M 6.19 M3	M	m	0,142	0,009	10,265	0,221	0,312	0,612	<DL	0,000
ALV. 1 M 7.19 M1	M	m	0,076	0,016	3,925	0,265	0,416	1,247	<DL	0,007
ALV. 1 M 7.19 M2	M	m	0,060	0,010	1,783	0,148	0,256	0,379	0,0016	0,003
ALV. 1 M 7.19 M3	M	m	0,123	0,011	10,402	0,162	0,182	0,240	0,0023	0,001
ALV. 1 M 8.19 M2	M	m	0,065	0,012	2,938	0,262	0,170	0,482	<DL	0,000
ALV. 1 M 8.19 M3	M	m	0,069	0,017	3,588	0,165	0,149	0,313	<DL	0,001
ALV. 1 M 8.19 M4	M	m	0,044	0,007	2,134	0,169	0,253	0,471	<DL	0,000
ALV. 1 M 8.19 M5	M	m	0,172	0,009	1,936	0,158	0,423	0,234	<DL	0,000
ALV. 1 M 8.19 M6	M	m	0,048	0,010	3,088	0,278	0,342	1,286	<DL	0,000
ALV. 1 M 8.19 M7	M	m	0,107	0,023	2,258	0,219	0,333	0,810	<DL	0,001
ALV. 1 M 8.19 M8	M	m	0,049	0,012	0,809	0,152	0,191	0,261	<DL	0,000
ALV. 1 M 8.19 M9	M	m	0,119	0,008	2,408	0,236	0,278	0,672	<DL	0,001
ALV. 1 M 8.19 M10	M	m	0,069	0,009	2,895	0,262	0,294	0,863	<DL	0,001
ALV. 1 M 8.19 M11	M	m	0,055	0,012	2,595	0,212	0,273	1,035	<DL	0,000
ALV. 1 M 8.19 M12	M	m	0,120	0,019	1,719	0,158	0,362	1,041	<DL	<DL
ALV. 1 M 8.19 M13	M	m	0,070	0,009	1,335	0,184	0,230	0,735	<DL	0,000
ALV. 1 M 8.19 M14	M	m	0,081	0,019	0,324	0,708	2,865	0,197	0,0009	0,010
ALV. 1 M 8.19 M15	M	m	0,115	0,023	1,717	0,423	1,272	0,800	<DL	0,004
ALV. 1 M 9.19 M1	M	m	0,052	0,013	3,988	0,311	0,661	1,005	<DL	0,001
ALV. 1 M 9.19 M2	M	m	0,040	0,012	3,580	0,195	0,407	0,885	<DL	0,001
ALV. 1 M 9.19 M3	M	m	0,055	0,018	3,866	0,283	0,419	1,004	<DL	0,003
ALV. 2 M 7.19 M1	M	m	0,209	0,020	9,112	0,337	0,510	0,366	0,0017	0,003
ALV. 2 M 7.19 M2	M	m	0,192	0,017	3,618	0,230	0,327	0,556	<DL	0,000
ALV. 2 M 7.19 M3	M	m	0,177	0,034	3,938	0,235	0,394	0,990	<DL	0,000
ALV. 2 M 8.19 M1	M	m	0,140	0,016	3,906	0,264	0,660	0,248	<DL	0,004
ALV. 2 M 9.19 M1	M	m	0,098	0,014	7,270	0,223	0,173	0,262	<DL	0,003
ALV. 2 M 9.19 M2	M	m	0,099	0,010	3,986	0,216	0,766	0,849	<DL	0,001
ALV. 1 M 6.19 E1	M	h	0,094	0,027	8,518	1,689	0,873	5,488	<DL	<DL
ALV. 1 M 6.19 E2	M	h	0,047	0,024	1,959	2,262	0,621	1,467	0,0014	0,001
ALV. 1 M 6.19 E3	M	h	0,026	0,014	3,113	0,908	0,340	1,590	<DL	<DL
ALV. 1 M 7.19 E1	M	h	0,030	0,024	11,015	0,814	0,412	4,741	0,0077	0,014
ALV. 1 M 7.19 E2	M	h	0,019	0,016	0,754	0,353	0,003	1,088	0,0109	0,023
ALV. 1 M 7.19 E3	M	h	0,035	0,012	2,026	0,391	0,104	0,616	0,0081	0,016
ALV. 1 M 8.19 E2	M	h	0,017	0,017	0,469	0,714	0,440	1,786	0,0024	0,002
ALV. 1 M 8.19 E3	M	h	0,016	0,007	-0,006	0,727	0,291	0,724	0,0002	<DL
ALV. 1 M 8.19 E4	M	h	0,013	0,015	2,228	0,761	1,039	4,554	0,0046	0,007
ALV. 1 M 8.19 E5	M	h	0,016	0,008	-0,231	0,592	0,512	0,883	<DL	<DL
ALV. 1 M 8.19 E6	M	h	0,016	0,013	0,572	0,845	0,638	3,100	0,0028	0,004
ALV. 1 M 8.19 E7	M	h	0,015	0,018	2,074	0,839	1,018	4,587	0,0040	0,013
ALV. 1 M 8.19 E8	M	h	0,015	0,029	1,161	0,883	0,726	3,967	0,0018	0,016
ALV. 1 M 8.19 E9	M	h	0,011	0,008	0,252	0,448	0,430	0,517	0,0001	0,002
ALV. 1 M 8.19 E10	M	h	0,005	0,009	0,025	1,148	0,604	1,558	0,0010	0,006
ALV. 1 M 8.19 E11	M	h	0,008	0,015	0,193	0,797	-0,005	3,768	0,0033	<DL
ALV. 1 M 8.19 E12	M	h	0,014	0,014	1,330	0,334	0,429	2,123	0,0012	0,018
ALV. 1 M 8.19 E13	M	h	0,001	0,003	0,097	0,107	0,166	0,447	0,0009	0,000
ALV. 1 M 8.19 E14	M	h	0,012	0,021	0,932	0,446	0,596	2,769	0,0031	0,005
ALV. 1 M 8.19 E15	M	h	0,014	0,016	0,799	0,584	0,658	1,972	0,0006	0,000
ALV. 2 M 7.19 E1	M	h	0,031	0,017	5,920	0,991	1,372	2,457	0,0141	<DL
ALV. 2 M 7.19 E2	M	h	0,047	0,019	2,520	0,940	0,958	1,352	0,0003	0,001
ALV. 2 M 7.19 E3	M	h	0,028	0,024	2,840	1,005	0,757	1,678	0,0002	0,000
ALV. 2 M 8.19 E1	M	h	0,023	0,024	3,031	0,428	0,316	1,173	0,0013	0,003
ALV. 2 M 9.19 E1	M	h	0,052	0,045	13,361	0,748	0,189	2,693	0,0052	0,005
ALV. 2 M 9.19 E2	M	h	0,009	0,003	1,363	0,233	1,361	2,873	0,0007	0,007

Institutional Repository - Library & Information Centre - University of Thessaly
19/04/2024 03:53:45 EEST - 18.222.197.243

Table A.7: Elements concentrations(mg/kg) in males hepatopancreas and muscle tissues.

Sample Name	Sex	Tissue	Ca	Cd	Co	Cr	Cs	Cu	Fe [He]	Fe [O2]
ALV. 1 M 6.19 M1	M	m	103,407	0,004	0,237	23,431	0,022	3,114	93,981	135,185
ALV. 1 M 6.19 M2	M	m	98,914	0,004	0,046	1,618	0,025	4,849	16,220	17,493
ALV. 1 M 6.19 M3	M	m	90,926	0,002	0,157	19,122	0,023	2,834	66,019	90,579
ALV. 1 M 7.19 M1	M	m	285,088	0,007	0,059	0,356	0,019	7,567	16,670	14,709
ALV. 1 M 7.19 M2	M	m	151,975	0,002	0,045	0,054	0,019	6,552	7,503	6,174
ALV. 1 M 7.19 M3	M	m	111,136	0,009	0,017	0,078	0,012	6,266	17,498	14,852
ALV. 1 M 8.19 M2	M	m	112,020	0,005	0,064	12,156	0,010	5,367	41,961	52,866
ALV. 1 M 8.19 M3	M	m	109,740	0,011	0,019	0,695	0,008	7,318	11,600	11,004
ALV. 1 M 8.19 M4	M	m	125,545	0,007	0,032	1,222	0,002	4,909	20,294	18,676
ALV. 1 M 8.19 M5	M	m	128,698	0,001	0,027	2,772	0,008	6,230	18,725	17,996
ALV. 1 M 8.19 M6	M	m	203,420	0,005	0,056	4,165	0,008	5,997	34,810	33,234
ALV. 1 M 8.19 M7	M	m	168,493	0,006	0,052	1,792	0,007	10,504	23,499	23,461
ALV. 1 M 8.19 M8	M	m	100,907	0,002	0,023	0,433	0,005	5,797	14,148	13,683
ALV. 1 M 8.19 M9	M	m	171,968	0,002	0,030	1,187	0,012	7,200	18,841	17,359
ALV. 1 M 8.19 M10	M	m	151,759	0,005	0,050	1,197	0,007	4,715	23,418	20,519
ALV. 1 M 8.19 M11	M	m	144,732	0,008	0,043	2,802	0,007	5,944	32,812	30,134
ALV. 1 M 8.19 M12	M	m	212,068	0,006	0,032	1,272	0,004	10,496	15,707	14,170
ALV. 1 M 8.19 M13	M	m	145,488	0,006	0,050	4,289	0,007	5,750	34,933	30,664
ALV. 1 M 8.19 M14	M	m	60,289	0,009	0,018	0,248	0,014	2,596	5,502	4,741
ALV. 1 M 8.19 M15	M	m	164,909	0,011	0,066	1,416	0,011	9,039	21,048	18,693
ALV. 1 M 9.19 M1	M	m	187,720	0,010	0,042	1,058	0,006	6,923	21,056	18,983
ALV. 1 M 9.19 M2	M	m	120,252	0,004	0,017	0,437	0,010	4,774	12,368	10,797
ALV. 1 M 9.19 M3	M	m	151,867	0,007	0,029	0,900	0,015	6,197	14,365	15,403
ALV. 2 M 7.19 M1	M	m	187,530	0,006	0,021	0,090	0,019	10,152	15,420	12,474
ALV. 2 M 7.19 M2	M	m	96,454	0,006	0,144	14,688	0,018	3,823	50,412	66,700
ALV. 2 M 7.19 M3	M	m	184,642	0,011	0,089	0,574	0,021	7,815	22,205	23,113
ALV. 2 M 8.19 M1	M	m	146,749	0,005	0,022	0,654	0,016	7,683	15,895	13,965
ALV. 2 M 9.19 M1	M	m	122,959	0,001	0,018	1,152	0,018	4,417	15,929	14,108
ALV. 2 M 9.19 M2	M	m	183,534	0,002	0,019	0,879	0,009	3,102	19,971	18,098
ALV. 1 M 6.19 E1	M	h	193,056	0,447	0,854	1,154	0,010	7,278	153,245	199,521
ALV. 1 M 6.19 E2	M	h	97,327	0,224	2,048	0,424	0,011	9,216	173,753	241,244
ALV. 1 M 6.19 E3	M	h	79,182	0,061	0,771	1,188	0,008	5,649	263,072	348,010
ALV. 1 M 7.19 E1	M	h	532,610	0,156	0,424	0,042	0,010	12,675	397,220	472,455
ALV. 1 M 7.19 E2	M	h	361,675	0,080	0,182	0,024	0,012	7,460	164,972	185,780
ALV. 1 M 7.19 E3	M	h	168,966	0,179	0,203	0,025	0,006	4,163	247,798	209,325
ALV. 1 M 8.19 E2	M	h	277,795	0,246	0,239	0,025	0,006	7,936	473,005	627,351
ALV. 1 M 8.19 E3	M	h	355,324	0,263	0,108	0,019	0,004	4,591	89,820	84,361
ALV. 1 M 8.19 E4	M	h	395,040	0,206	0,207	0,039	0,005	6,507	502,273	640,466
ALV. 1 M 8.19 E5	M	h	306,204	0,050	0,189	0,036	0,003	3,617	347,147	455,417
ALV. 1 M 8.19 E6	M	h	388,302	0,100	0,239	0,028	0,006	5,387	381,380	537,504
ALV. 1 M 8.19 E7	M	h	461,574	0,191	0,203	0,030	0,004	7,962	546,632	588,842
ALV. 1 M 8.19 E8	M	h	428,382	0,227	0,144	0,021	0,003	10,022	911,527	1143,909
ALV. 1 M 8.19 E9	M	h	240,888	0,052	0,111	0,008	0,007	3,716	126,898	149,026
ALV. 1 M 8.19 E10	M	h	244,855	0,116	0,229	0,021	0,007	4,777	326,982	424,487
ALV. 1 M 8.19 E11	M	h	452,802	0,140	0,196	0,020	0,007	4,398	861,612	1214,718
ALV. 1 M 8.19 E12	M	h	287,833	0,147	0,113	0,045	0,003	3,797	581,105	739,175
ALV. 1 M 8.19 E13	M	h	44,185	0,013	0,030	0,018	0,002	0,648	97,604	106,380
ALV. 1 M 8.19 E14	M	h	375,542	0,106	0,119	0,042	0,004	7,033	438,376	543,594
ALV. 1 M 8.19 E15	M	h	230,220	0,103	0,202	0,027	0,004	6,857	384,125	479,408
ALV. 2 M 7.19 E1	M	h	515,912	0,092	0,198	0,020	0,009	7,799	529,778	657,501
ALV. 2 M 7.19 E2	M	h	279,409	0,285	0,558	0,912	0,007	4,915	334,973	463,865
ALV. 2 M 7.19 E3	M	h	200,432	0,201	0,508	0,586	0,008	9,101	696,840	932,629
ALV. 2 M 8.19 E1	M	h	331,444	0,105	0,102	0,039	0,005	9,450	381,145	484,460
ALV. 2 M 9.19 E1	M	h	508,699	0,266	0,242	0,068	0,011	13,445	531,432	657,939
ALV. 2 M 9.19 E2	M	h	222,899	0,015	0,049	0,028	0,004	1,887	447,338	590,735

Institutional Repository - Library & Information Centre - University of Thessaly
19/04/2024 03:53:45 EEST - 18.222.197.243

Table A.8: Elements concentrations(mg/kg) in males hepatopancreas and muscle tissues.

Sample Name	Sex	Tissue	Ga	K	Li	Mg	Mn	Na	Ni	P
ALV. 1 M 6.19 M1	M	m	0,0115	1930,844	<DL	352,618	7,497	1025,438	16,029	1948,250
ALV. 1 M 6.19 M2	M	m	0,0030	2070,624	<DL	374,820	8,172	893,630	0,905	2030,047
ALV. 1 M 6.19 M3	M	m	0,0095	1992,581	<DL	302,774	5,162	832,452	10,290	1512,067
ALV. 1 M 7.19 M1	M	m	0,0003	26484,324	<DL	288,615	3,088	725,946	0,544	2114,099
ALV. 1 M 7.19 M2	M	m	0,0021	24103,515	0,055	223,701	1,766	648,647	0,207	1659,500
ALV. 1 M 7.19 M3	M	m	0,0044	22916,451	<DL	242,746	1,918	581,486	0,308	1810,191
ALV. 1 M 8.19 M2	M	m	0,0021	24938,787	<DL	245,985	1,616	619,213	6,473	1543,033
ALV. 1 M 8.19 M3	M	m	0,0004	22499,056	0,054	226,350	1,244	657,948	0,484	1292,870
ALV. 1 M 8.19 M4	M	m	<DL	21273,248	0,001	238,034	1,456	851,891	0,801	1255,433
ALV. 1 M 8.19 M5	M	m	0,0004	28701,959	<DL	238,726	1,220	790,189	1,707	1736,826
ALV. 1 M 8.19 M6	M	m	0,0013	21245,986	0,020	279,538	2,063	704,917	2,542	1435,877
ALV. 1 M 8.19 M7	M	m	0,0000	26143,549	<DL	277,415	2,102	760,831	1,278	1582,631
ALV. 1 M 8.19 M8	M	m	<DL	20754,854	<DL	194,888	0,620	722,363	0,367	1257,376
ALV. 1 M 8.19 M9	M	m	0,0004	27517,041	<DL	310,291	0,843	747,493	0,807	1961,857
ALV. 1 M 8.19 M10	M	m	0,0008	20490,373	0,003	193,701	1,008	692,025	0,913	1273,700
ALV. 1 M 8.19 M11	M	m	0,0011	24522,938	<DL	205,164	1,513	530,101	1,655	1523,999
ALV. 1 M 8.19 M12	M	m	<DL	34108,881	<DL	341,080	1,224	683,483	0,924	2308,713
ALV. 1 M 8.19 M13	M	m	0,0004	20110,438	<DL	218,529	1,400	518,369	2,623	1360,023
ALV. 1 M 8.19 M14	M	m	0,0009	13382,165	0,214	114,321	0,463	542,670	0,328	673,824
ALV. 1 M 8.19 M15	M	m	0,0004	22384,301	0,114	239,782	1,157	767,764	1,284	1654,788
ALV. 1 M 9.19 M1	M	m	0,0007	18427,673	0,037	244,369	3,098	699,904	0,717	1410,236
ALV. 1 M 9.19 M2	M	m	0,0009	21166,231	0,071	199,399	1,667	570,421	0,365	1350,076
ALV. 1 M 9.19 M3	M	m	0,0018	26947,388	0,029	235,144	4,077	648,740	0,682	1971,204
ALV. 2 M 7.19 M1	M	m	0,0051	36250,942	0,076	312,725	1,593	707,435	0,532	2519,197
ALV. 2 M 7.19 M2	M	m	0,0059	1668,348	<DL	272,630	3,560	697,475	8,184	1669,853
ALV. 2 M 7.19 M3	M	m	0,0014	1817,456	<DL	393,209	0,830	960,787	0,690	2044,775
ALV. 2 M 8.19 M1	M	m	0,0009	27811,933	0,026	339,563	0,683	873,027	0,526	2111,100
ALV. 2 M 9.19 M1	M	m	0,0026	22264,760	0,037	187,533	1,026	612,012	0,740	1328,331
ALV. 2 M 9.19 M2	M	m	0,0015	23491,632	0,108	226,851	0,993	483,631	0,642	1658,444
ALV. 1 M 6.19 E1	M	h	0,0009	1090,367	0,092	244,095	116,276	1028,673	1,486	1379,974
ALV. 1 M 6.19 E2	M	h	0,0025	1177,756	<DL	184,856	98,173	1153,951	2,186	893,081
ALV. 1 M 6.19 E3	M	h	0,0022	797,628	<DL	133,622	19,335	695,436	1,364	720,395
ALV. 1 M 7.19 E1	M	h	0,0071	15964,831	0,131	266,610	50,341	868,612	1,984	1023,072
ALV. 1 M 7.19 E2	M	h	0,0028	13041,395	<DL	164,635	26,206	1334,148	0,905	1423,571
ALV. 1 M 7.19 E3	M	h	0,0041	9734,767	0,351	94,727	13,993	526,496	0,751	1012,922
ALV. 1 M 8.19 E2	M	h	0,0012	12794,381	0,021	138,110	3,280	544,447	0,551	1084,304
ALV. 1 M 8.19 E3	M	h	0,0000	8737,624	0,182	106,605	11,618	725,267	0,192	632,765
ALV. 1 M 8.19 E4	M	h	0,0020	15145,349	0,067	131,527	24,887	1044,667	0,423	1096,941
ALV. 1 M 8.19 E5	M	h	<DL	13517,268	<DL	118,191	43,913	824,487	0,400	1090,057
ALV. 1 M 8.19 E6	M	h	<DL	15566,613	0,062	162,591	20,218	909,527	0,965	1029,571
ALV. 1 M 8.19 E7	M	h	0,0020	12013,631	0,006	185,984	31,843	796,357	0,653	1014,866
ALV. 1 M 8.19 E8	M	h	<DL	13366,723	0,099	158,579	25,643	1142,238	0,137	1430,492
ALV. 1 M 8.19 E9	M	h	<DL	12922,351	<DL	129,442	6,481	593,322	0,355	541,303
ALV. 1 M 8.19 E10	M	h	<DL	12514,487	<DL	137,759	8,021	598,975	0,761	915,765
ALV. 1 M 8.19 E11	M	h	0,0007	16157,239	<DL	180,015	14,336	895,990	0,544	1816,866
ALV. 1 M 8.19 E12	M	h	0,0003	7234,228	0,063	110,744	8,853	475,561	0,084	917,290
ALV. 1 M 8.19 E13	M	h	0,0004	1581,914	0,095	22,572	2,469	111,015	0,089	148,567
ALV. 1 M 8.19 E14	M	h	0,0001	9549,041	0,104	138,888	8,883	720,116	0,217	1023,140
ALV. 1 M 8.19 E15	M	h	<DL	8901,047	0,038	105,135	8,925	400,159	0,875	714,887
ALV. 2 M 7.19 E1	M	h	0,0017	10804,504	0,549	185,982	37,542	826,030	1,209	1517,007
ALV. 2 M 7.19 E2	M	h	0,0024	863,355	<DL	213,898	6,372	699,845	1,564	692,729
ALV. 2 M 7.19 E3	M	h	0,0033	802,341	<DL	239,706	1,946	821,204	1,811	863,412
ALV. 2 M 8.19 E1	M	h	0,0001	9173,094	0,114	139,637	2,025	638,293	0,193	909,117
ALV. 2 M 9.19 E1	M	h	0,0042	11097,147	0,110	167,451	9,715	663,015	0,238	1420,467
ALV. 2 M 9.19 E2	M	h	0,0011	7982,929	<DL	112,131	3,283	361,490	0,093	759,345

Institutional Repository - Library & Information Centre - University of Thessaly
19/04/2024 03:53:45 EEST - 18.222.197.243

Table A.9: Elements concentrations(mg/kg) in males hepatopancreas and muscle tissues.

Sample Name	Sex	Tissue	Pb (206)	Pb (207)	Pb (208)	32 –>68 S [O2]	34 –>50 S [O2]	Si	Sr
ALV. 1 M 6.19 M1	M	m	0,081	0,073	0,070	1239,711171	1521,567438	25,172	1,556
ALV. 1 M 6.19 M2	M	m	0,104	0,107	0,097	1324,611303	1594,082036	19,369	1,627
ALV. 1 M 6.19 M3	M	m	0,045	0,056	0,046	1056,418476	1266,620286	32,433	1,413
ALV. 1 M 7.19 M1	M	m	0,062	0,061	0,064	1353,607093	1478,621703	11,148	5,780
ALV. 1 M 7.19 M2	M	m	0,095	0,103	0,098	1005,041077	1088,212692	7,352	2,638
ALV. 1 M 7.19 M3	M	m	0,097	0,081	0,095	1286,270266	1407,421921	18,053	1,773
ALV. 1 M 8.19 M2	M	m	<DL	<DL	<DL	1030,35723	1222,195308	10,637	2,198
ALV. 1 M 8.19 M3	M	m	0,004	0,002	0,003	1012,418429	1171,598554	8,848	2,090
ALV. 1 M 8.19 M4	M	m	0,007	0,003	0,003	899,3817749	1076,163673	6,625	2,767
ALV. 1 M 8.19 M5	M	m	0,021	0,025	0,022	1393,106997	1618,851885	6,685	2,171
ALV. 1 M 8.19 M6	M	m	0,012	0,016	0,012	1073,018934	1239,765157	11,724	4,472
ALV. 1 M 8.19 M7	M	m	0,001	0,000	0,002	1275,225477	1477,210294	9,940	3,851
ALV. 1 M 8.19 M8	M	m	<DL	<DL	<DL	933,7615494	1067,03716	5,000	2,081
ALV. 1 M 8.19 M9	M	m	0,041	0,039	0,039	1182,186251	1336,937936	7,848	3,422
ALV. 1 M 8.19 M10	M	m	0,004	0,010	0,005	992,8411619	1111,905003	11,101	3,184
ALV. 1 M 8.19 M11	M	m	0,010	0,011	0,011	1097,448361	1209,671725	11,312	3,211
ALV. 1 M 8.19 M12	M	m	0,041	0,032	0,040	1360,186641	1502,570049	18,856	4,088
ALV. 1 M 8.19 M13	M	m	0,001	0,002	0,002	979,3712053	1061,763857	9,246	3,256
ALV. 1 M 8.19 M14	M	m	0,025	0,034	0,031	430,1413605	481,5646308	1,292	1,114
ALV. 1 M 8.19 M15	M	m	0,019	0,018	0,022	1185,782158	1322,978432	7,082	3,496
ALV. 1 M 9.19 M1	M	m	0,087	0,068	0,082	1126,758123	1256,606299	7,887	4,348
ALV. 1 M 9.19 M2	M	m	0,060	0,065	0,061	1123,815558	1225,876105	8,364	3,143
ALV. 1 M 9.19 M3	M	m	0,004	0,005	0,005	1384,910834	1572,641231	8,060	3,450
ALV. 2 M 7.19 M1	M	m	0,018	0,008	0,015	1705,698884	1835,103743	18,141	3,367
ALV. 2 M 7.19 M2	M	m	0,046	0,034	0,035	1119,871749	1318,459394	15,729	1,703
ALV. 2 M 7.19 M3	M	m	0,085	0,095	0,084	1265,770527	1480,022916	19,517	4,095
ALV. 2 M 8.19 M1	M	m	0,054	0,059	0,058	1479,362044	1655,241694	18,841	2,978
ALV. 2 M 9.19 M1	M	m	0,021	0,002	0,013	1089,326932	1193,758597	12,342	2,419
ALV. 2 M 9.19 M2	M	m	0,023	0,016	0,022	1193,664829	1327,073055	10,854	5,055
ALV. 1 M 6.19 E1	M	h	0,182	0,175	0,159	1041,540605	1215,011315	49,673	3,531
ALV. 1 M 6.19 E2	M	h	0,089	0,081	0,078	1100,75118	1308,826938	18,597	2,203
ALV. 1 M 6.19 E3	M	h	0,206	0,205	0,203	607,9007829	706,2941066	26,804	1,564
ALV. 1 M 7.19 E1	M	h	0,103	0,113	0,114	1003,769377	1090,782799	37,499	10,452
ALV. 1 M 7.19 E2	M	h	0,024	0,027	0,026	1064,736386	1162,650174	9,465	6,741
ALV. 1 M 7.19 E3	M	h	0,032	0,036	0,035	678,2709989	621,5784742	21,237	2,715
ALV. 1 M 8.19 E2	M	h	0,043	0,042	0,042	611,2195822	687,3096292	33,766	6,020
ALV. 1 M 8.19 E3	M	h	0,027	0,020	0,038	395,2416563	368,4506298	8,139	5,859
ALV. 1 M 8.19 E4	M	h	0,177	0,147	0,175	862,417305	791,1747028	35,196	8,897
ALV. 1 M 8.19 E5	M	h	0,113	0,086	0,113	935,1494482	887,3233249	11,506	4,944
ALV. 1 M 8.19 E6	M	h	0,147	0,110	0,126	862,783268	928,1584785	46,127	8,588
ALV. 1 M 8.19 E7	M	h	0,057	0,033	0,053	815,4449536	854,8954555	35,555	9,955
ALV. 1 M 8.19 E8	M	h	0,058	0,059	0,061	701,8139771	645,5823863	59,374	8,245
ALV. 1 M 8.19 E9	M	h	0,010	0,009	0,007	474,4559086	529,6222659	23,341	3,614
ALV. 1 M 8.19 E10	M	h	0,043	0,048	0,043	639,5731893	699,207147	38,759	4,900
ALV. 1 M 8.19 E11	M	h	0,140	0,162	0,140	1239,510733	1180,738628	62,804	10,347
ALV. 1 M 8.19 E12	M	h	0,052	0,067	0,053	524,2006045	480,3537623	26,001	5,784
ALV. 1 M 8.19 E13	M	h	0,033	0,022	0,032	138,0793072	129,7628981	4,549	0,909
ALV. 1 M 8.19 E14	M	h	0,066	0,067	0,079	648,7298412	610,1454286	23,148	7,744
ALV. 1 M 8.19 E15	M	h	0,042	0,046	0,043	650,3174536	708,3433831	26,611	4,937
ALV. 2 M 7.19 E1	M	h	0,276	0,196	0,211	1175,592838	1092,224226	23,839	10,251
ALV. 2 M 7.19 E2	M	h	0,121	0,099	0,100	705,5008033	837,7401068	44,955	6,410
ALV. 2 M 7.19 E3	M	h	0,115	0,119	0,116	592,1959971	703,8892645	72,935	4,773
ALV. 2 M 8.19 E1	M	h	0,054	0,068	0,069	612,8391038	673,9857127	38,571	7,182
ALV. 2 M 9.19 E1	M	h	0,114	0,103	0,119	883,2014642	964,4125123	45,147	11,553
ALV. 2 M 9.19 E2	M	h	0,046	0,046	0,054	484,2155275	540,8159304	22,247	8,389

Institutional Repository - Library & Information Centre - University of Thessaly
19/04/2024 03:53:45 EEST - 18.222.197.243

Table A.10: Elements concentrations(mg/kg) in males hepatopancreas and muscle tissues.

Sample Name	Sex	Tissue	Tl	V	Zn
ALV. 1 M 6.19 M1	M	m	<DL	0,224	15,659
ALV. 1 M 6.19 M2	M	m	0,0000	0,033	20,725
ALV. 1 M 6.19 M3	M	m	<DL	0,150	12,461
ALV. 1 M 7.19 M1	M	m	<DL	0,021	18,674
ALV. 1 M 7.19 M2	M	m	0,0013	0,006	15,700
ALV. 1 M 7.19 M3	M	m	0,0015	0,031	13,722
ALV. 1 M 8.19 M2	M	m	0,0001	0,050	14,025
ALV. 1 M 8.19 M3	M	m	<DL	0,018	10,650
ALV. 1 M 8.19 M4	M	m	<DL	0,013	12,420
ALV. 1 M 8.19 M5	M	m	<DL	0,018	16,667
ALV. 1 M 8.19 M6	M	m	<DL	0,032	14,384
ALV. 1 M 8.19 M7	M	m	<DL	0,018	13,489
ALV. 1 M 8.19 M8	M	m	<DL	0,013	9,551
ALV. 1 M 8.19 M9	M	m	<DL	0,016	18,204
ALV. 1 M 8.19 M10	M	m	<DL	0,025	13,964
ALV. 1 M 8.19 M11	M	m	<DL	0,026	12,372
ALV. 1 M 8.19 M12	M	m	<DL	0,019	19,753
ALV. 1 M 8.19 M13	M	m	<DL	0,023	11,780
ALV. 1 M 8.19 M14	M	m	0,0093	0,005	6,811
ALV. 1 M 8.19 M15	M	m	0,0013	0,011	17,339
ALV. 1 M 9.19 M1	M	m	0,0002	0,015	14,150
ALV. 1 M 9.19 M2	M	m	0,0004	0,014	11,786
ALV. 1 M 9.19 M3	M	m	0,0001	0,017	13,924
ALV. 2 M 7.19 M1	M	m	0,0016	0,023	20,475
ALV. 2 M 7.19 M2	M	m	<DL	0,106	14,376
ALV. 2 M 7.19 M3	M	m	<DL	0,017	17,943
ALV. 2 M 8.19 M1	M	m	0,0006	0,013	17,819
ALV. 2 M 9.19 M1	M	m	<DL	0,026	13,465
ALV. 2 M 9.19 M2	M	m	0,0001	0,017	15,844
ALV. 1 M 6.19 E1	M	h	<DL	0,101	58,650
ALV. 1 M 6.19 E2	M	h	<DL	0,128	32,053
ALV. 1 M 6.19 E3	M	h	<DL	0,052	7,705
ALV. 1 M 7.19 E1	M	h	0,0026	0,097	11,156
ALV. 1 M 7.19 E2	M	h	0,0041	0,012	15,479
ALV. 1 M 7.19 E3	M	h	0,0050	0,022	11,797
ALV. 1 M 8.19 E2	M	h	0,0004	0,031	12,551
ALV. 1 M 8.19 E3	M	h	0,0008	0,014	6,174
ALV. 1 M 8.19 E4	M	h	0,0014	0,057	12,313
ALV. 1 M 8.19 E5	M	h	0,0007	0,018	25,083
ALV. 1 M 8.19 E6	M	h	0,0009	0,058	13,003
ALV. 1 M 8.19 E7	M	h	0,0010	0,068	8,555
ALV. 1 M 8.19 E8	M	h	0,0006	0,072	10,215
ALV. 1 M 8.19 E9	M	h	0,0000	0,023	5,547
ALV. 1 M 8.19 E10	M	h	0,0004	0,034	15,316
ALV. 1 M 8.19 E11	M	h	0,0009	0,040	10,713
ALV. 1 M 8.19 E12	M	h	0,0006	0,038	6,073
ALV. 1 M 8.19 E13	M	h	0,0004	0,006	2,012
ALV. 1 M 8.19 E14	M	h	0,0002	0,026	6,811
ALV. 1 M 8.19 E15	M	h	0,0001	0,034	7,779
ALV. 2 M 7.19 E1	M	h	0,0079	0,010	29,163
ALV. 2 M 7.19 E2	M	h	<DL	0,075	28,230
ALV. 2 M 7.19 E3	M	h	0,0000	0,045	13,167
ALV. 2 M 8.19 E1	M	h	0,0004	0,024	12,562
ALV. 2 M 9.19 E1	M	h	0,0014	0,094	38,603
ALV. 2 M 9.19 E2	M	h	0,0006	0,013	27,891

Institutional Repository - Library & Information Centre - University of Thessaly
19/04/2024 03:53:45 EEST - 18.222.197.243

A.3 Other Data

Table A.11: Blanck, LOD and BEC for every element detected.

	blank	**LOD**	**BEC**
Hg	2,0255E-11	1,83439E-06	3,37403E-06
Ag	2,95505E-11	9,98463E-07	1,81006E-06
Al	1,51094E-09	0,000119378	0,000273011
As	4,71745E-09	1,54377E-06	7,63991E-06
B	4,55306E-09	0,000184689	0,000235547
Ba	3,69905E-10	4,3823E-06	1,40202E-05
Be [No Gas]	8,2924E-12	0,0000009	2,17722E-07
Be [He]	7,34841E-11	2,09741E-05	4,03646E-06
Ca	2,82777E-09	0,000258511	0,000949723
Cd	3,38791E-13	8,46624E-07	1,62933E-07
Co	5,49521E-11	3,83485E-09	2,65009E-07
Cr	3,33669E-09	3,85381E-06	1,78237E-05
Cs	5,903E-11	5,57734E-07	2,30612E-06
Cu	6,7533E-09	5,00735E-06	1,73658E-05
Fe [He]	6,12649E-08	1,01971E-05	0,00044106
Fe [O2]	6,04217E-10	1,09523E-05	0,000212916
Ga	1,78266E-12	1,1125E-06	2,14101E-07
K	1,96735E-07	0,000885362	0,014044422
Li [No Gas]	1,28036E-07	0,000387188	0,001486685
Li [He]	1,00303E-07	0,000346815	0,001447383
Mg	1,12131E-09	4,35519E-05	0,000100657
Mn	4,42461E-10	1,96455E-06	2,34695E-06
Na	1,05499E-07	0,000757013	0,005738938
Ni	1,3811E-09	8,308E-06	1,18327E-05
P	3,31722E-10	8,77145E-06	0,000356353
Pb [206 He]	1,10289E-10	2,2422E-06	9,29442E-06
Pb [207 He]	1,09582E-10	3,34748E-06	1,05844E-05
Pb [208 He]	2,56475E-10	1,92498E-06	9,61753E-06
Rb	1,92E-10	1,70338E-06	1,74774E-06
S [32–>48 O2]	4,17977E-09	0,000103426	0,002567758
S [34–>50 O2]	3,38917E-10	3,41462E-05	0,004076492
Si	4,48981E-09	6,02674E-05	0,00152253
Sr	1,12715E-10	9,345832E-07	1,196012E-05
TI	1,11039E-11	4,93195E-08	2,45594E-07
V	3,70275E-11	8,43923E-09	2,57059E-07
Zn	7,59703E-09	2,70913E-05	8,75219E-05
Sn	1,3902E-11	0,021915541	0,016787822

Institutional Repository - Library & Information Centre - University of Thessaly
19/04/2024 03:53:45 EEST - 18.222.197.243

Table A.12: Standard concentrations in every element detected.

(ppm)	STD-FISH1	STD-FISH2	STD-FISH3	STD-FISH4	mean STD	SD
Hg	0,490	0,525	0,475	0,420	0,478	0,043
Ag	0,003	0,003	0,006	0,007	0,005	0,002
Al	0,254	0,359	0,851	0,382	0,461	0,265
As	8,864	9,183	8,779	8,081	8,727	0,465
B	0,610	0,648	0,577	0,651	0,622	0,035
Ba	0,096	0,020	0,271	0,166	0,138	0,107
Be [No Gas]	0,005	0,004	0,004	0,005	0,005	0,001
Be [He]	0,000	0,003	0,003	0,000	0,001	0,002
Ca	65,042	70,720	65,194	53,804	63,690	7,100
Cd	0,008	0,009	0,007	0,004	0,007	0,002
Co	0,014	0,015	0,012	0,011	0,013	0,001
Cr	0,024	0,026	0,039	0,065	0,038	0,019
Cs	0,138	0,140	0,139	0,118	0,134	0,011
Cu	1,622	1,519	8,901	8,594	5,159	4,146
Fe [He]	5,964	7,019	6,750	5,748	6,370	0,610
Fe [O2]	4,908	5,767	5,499	5,178	5,338	0,374
Ga	0,001	0,001	0,000	0,001	0,001	0,000
Li [He]	0,099	0,073	0,000	0,062	0,058	0,042
Mg	804,898	849,897	798,827	696,948	787,642	64,612
Mn	0,244	0,273	0,259	0,219	0,249	0,023
Na	835,657	868,682	845,598	749,588	824,881	52,067
Ni	0,051	0,050	0,071	0,055	0,057	0,010
P	6997,818	7478,344	6704,825	6438,704	6904,923	445,287
Pb [206 He]	0,028	0,022	0,339	0,331	0,180	0,179
Pb [207 He]	0,028	0,028	0,349	0,311	0,179	0,175
Pb [208 He]	0,034	0,023	0,341	0,312	0,177	0,172
Rb	2,677	2,859	2,714	2,294	2,636	0,241
S [32–>48 O2]	6791,612	6782,419	6268,712	6103,476	6486,555	353,459
S [34–>50 O2]	7138,702	7363,642	6880,096	6748,210	7032,663	273,850
Si	7,465	5,729	14,012	12,206	9,853	3,896
Sr	0,926	0,994	0,962	0,803	0,922	0,083
TI	0,002	0,002	0,002	0,001	0,002	0,000
V	0,018	0,016	0,021	0,013	0,017	0,003
Zn	12,385	14,092	17,408	15,440	14,831	2,124
Sn	58,506	28,664	195,461	180,356	115,747	84,436

Institutional Repository - Library & Information Centre - University of Thessaly
19/04/2024 03:53:45 EEST - 18.222.197.243

Institutional Repository - Library & Information Centre - University of Thessaly
19/04/2024 03:53:45 EEST - 18.222.197.243

Appendix B

R Results

B.1 Bartlett tests

Table B.1: Bartlett test tissue results for all the elements detected.

Bartlett test	K - squared	df	P-value
Hg	31.196	1	<0.05
Ag	35.030	1	<0.05
Al	0.024	1	0.877
As	63.755	1	<0.05
B	0.589	1	0.443
Ba	50.383	1	0.000
Be (No gas)	26.084	1	0.000
Be (He)	35.485	1	0.000
Ca	32.886	1	0.000
Cd	222.510	1	<0.05
Co	119.830	1	<0.05
Cr	160.080	1	<0.05
Cs	34.447	1	<0.05
Cu	10.731	1	0.001
Fe (He)	175.700	1	<0.05
Fe (O_2)	169.360	1	<0.05
Ga	0.515	1	0.473
K	15.330	1	<0.05
Li	29.930	1	<0.05
Mg	0.848	1	0.357
Mn	165.190	1	<0.05
Na	2.878	1	0.090
Ni	87.737	1	<0.05
P	0.938	1	0.333
Pb (206 ->206)	80.228	1	<0.05
Pb (207 ->207)	83.967	1	<0.05
Pb (208 ->208)	81.764	1	<0.05
S (32 ->48)	0.204	1	0.652
S (34 ->50)	0.175	1	0.675
Si	28.530	1	<0.05
Sr	22.814	1	<0.05
Tl	0.610	1	0.435
V	3.826	1	0.050
Zn	57.997	1	<0.05

Institutional Repository - Library & Information Centre - University of Thessaly
19/04/2024 03:53:45 EEST - 18.222.197.243

Table B.2: Bartlett test sex results for all the elements detected.

Bartlett test	**K - squared**	**df**	**P-value**
Hg	6.029	1	0.014
Ag	46.732	1	<0.05
Al	11.475	1	0.001
As	2.510	1	0.113
B	4.256	1	0.039
Ba	3.184	1	0.074
Be (No gas)	1.538	1	0.215
Be (He)	0.002	1	0.968
Ca	0.017	1	0.895
Cd	0.262	1	0.609
Co	10.253	1	0.001
Cr	7.316	1	0.007
Cs	7.785	1	0.005
Cu	0.155	1	0.694
Fe (He)	3.213	1	0.073
Fe (O_2)	2.537	1	0.111
Ga	0.081	1	0.776
K	0.065	1	0.799
Li	6.973	1	0.008
Mg	0.757	1	0.384
Mn	22.429	1	<0.05
Na	1.608	1	0.205
Ni	8.138	1	0.004
P	0.133	1	0.715
Pb (206 ->206)	127.800	1	<0.05
Pb (207 ->207)	133.940	1	<0.05
Pb (208 ->208)	133.490	1	<0.05
S (32 ->48)	0.563	1	0.453
S (34 ->50)	0.284	1	0.594
Si	0.955	1	0.328
Sr	0.046	1	0.830
Tl	0.234	1	0.629
V	2.412	1	0.120
Zn	2.172	1	0.141

Institutional Repository - Library & Information Centre - University of Thessaly
19/04/2024 03:53:45 EEST - 18.222.197.243

B.2 Histograms

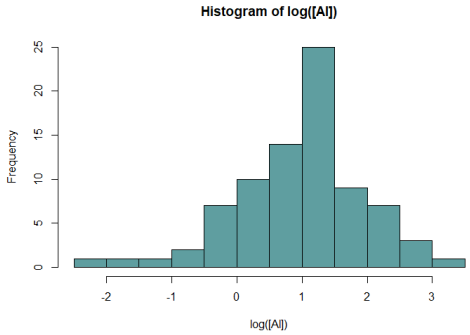

Figure B.1: Histogram of log([Al]).

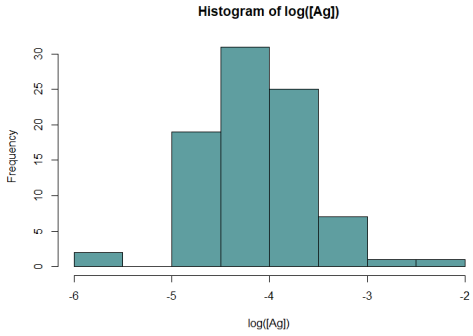

Figure B.2: Histogram of log([Ag]).

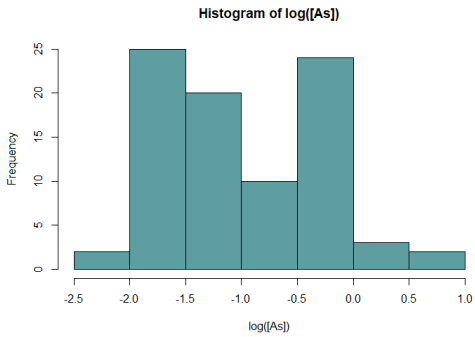

Figure B.3: Histogram of log([As]).

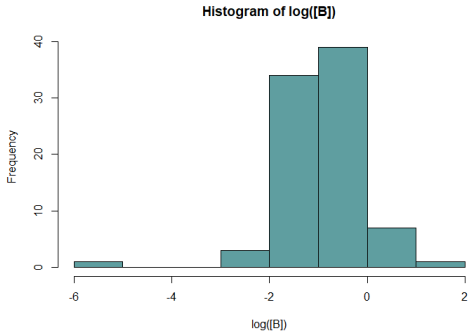

Figure B.4: Histogram of log([B]).

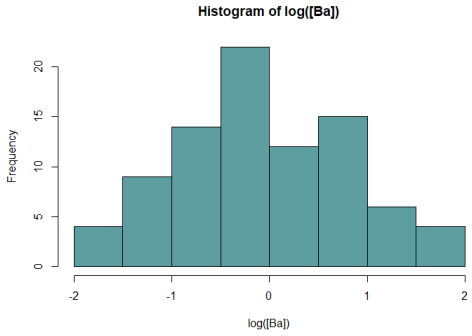

Figure B.5: Histogram of log([Ba]).

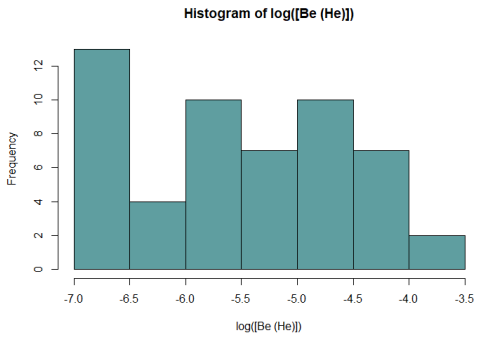

Figure B.6: Histogram of log([Be (He)]).

Institutional Repository - Library & Information Centre - University of Thessaly
19/04/2024 03:53:45 EEST - 18.222.197.243

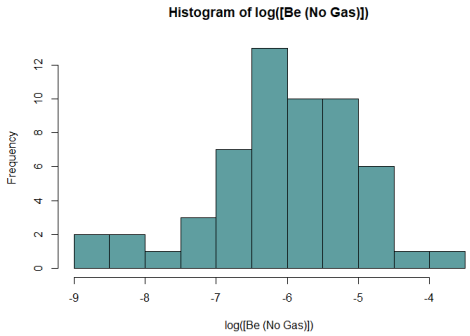

Figure B.7: Histogram of log([Be (No Gas)]).

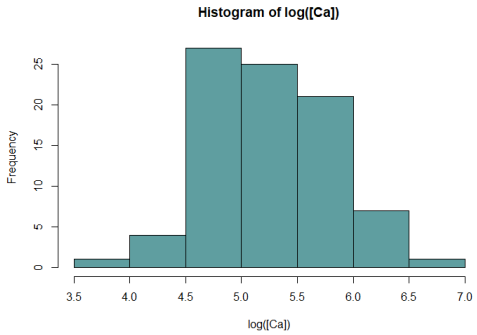

Figure B.8: Histogram of log([Ca]).

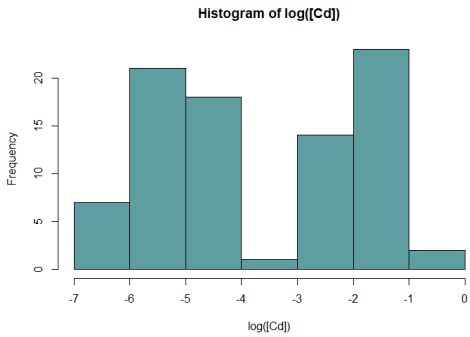

Figure B.9: Histogram of log([Cd]).

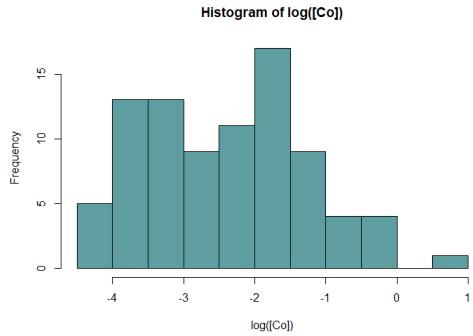

Figure B.10: Histogram of log([Co]).

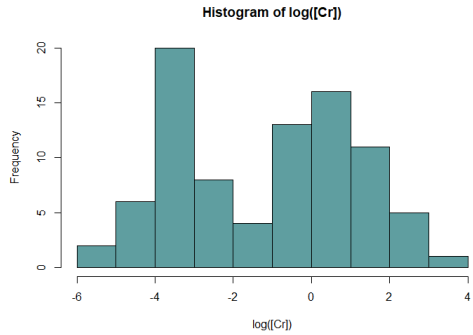

Figure B.11: Histogram of log([Cr]).

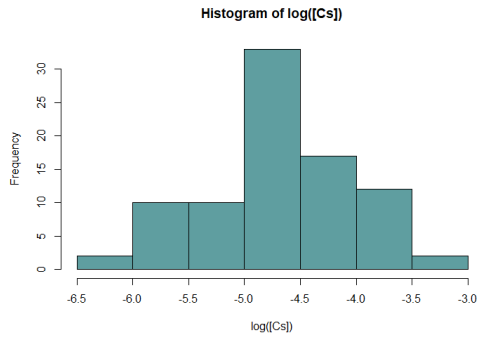

Figure B.12: Histogram of log([Cs]).

Institutional Repository - Library & Information Centre - University of Thessaly
19/04/2024 03:53:45 EEST - 18.222.197.243

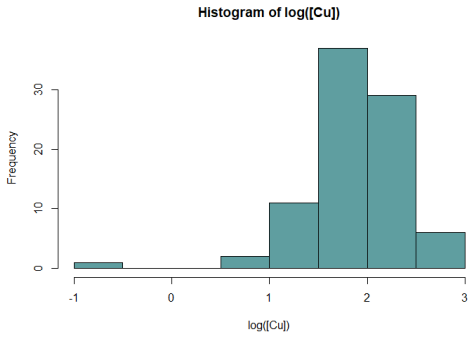

Figure B.13: Histogram of log([Cu]).

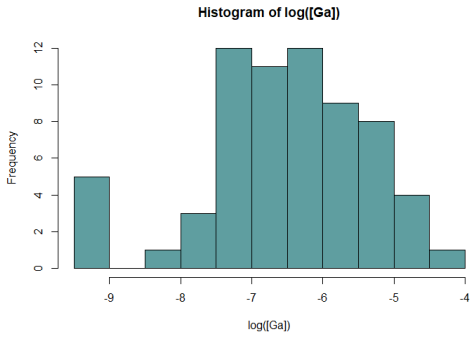

Figure B.16: Histogram of log([Ga]).

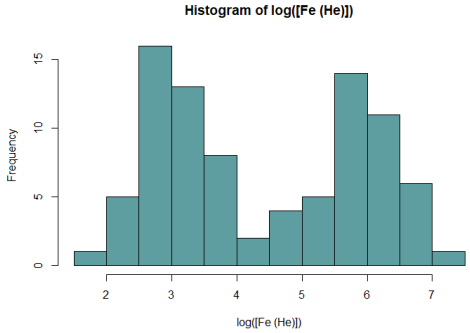

Figure B.14: Histogram of log([Fe (He)]).

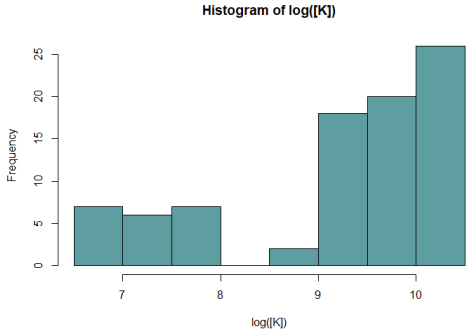

Figure B.17: Histogram of log([K]).

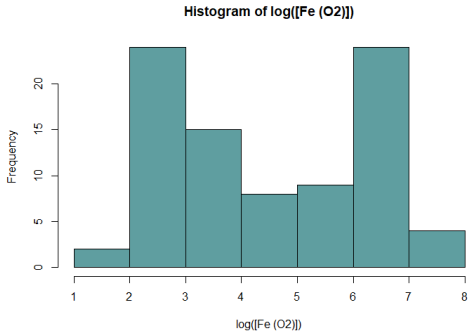

Figure B.15: Histogram of log([Fe O_2]).

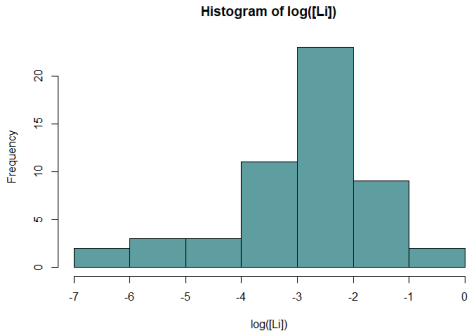

Figure B.18: Histogram of log([Li]).

Institutional Repository - Library & Information Centre - University of Thessaly
19/04/2024 03:53:45 EEST - 18.222.197.243

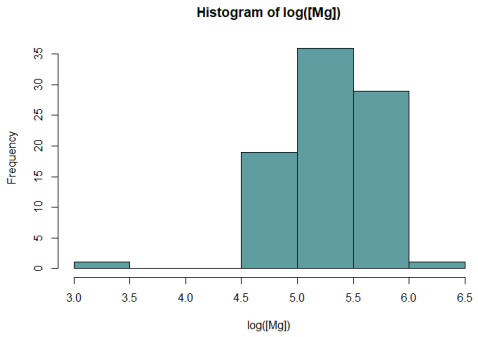

Figure B.19: Histogram of log([Mg]).

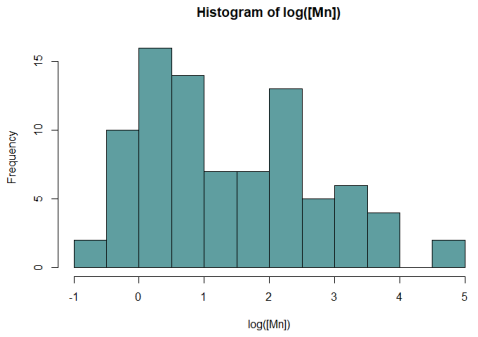

Figure B.20: Histogram of log([Mn]).

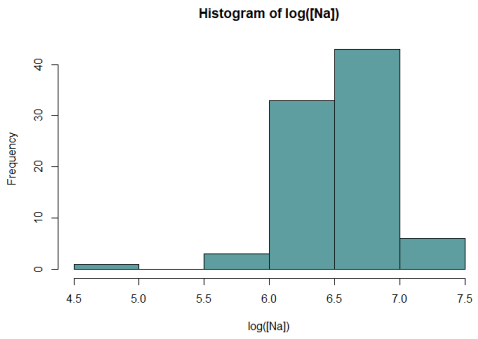

Figure B.21: Histogram of log([Na]).

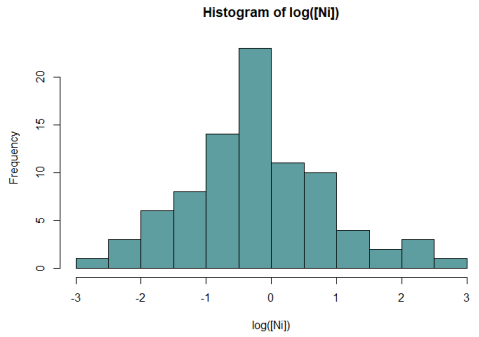

Figure B.22: Histogram of log([Ni]).

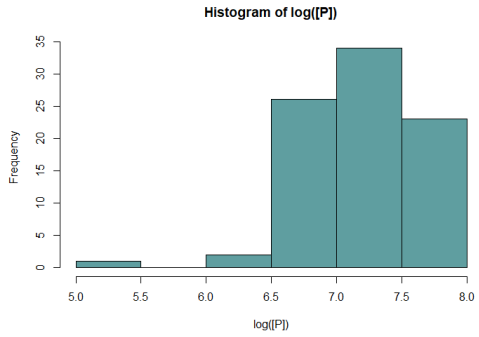

Figure B.23: Histogram of log([P]).

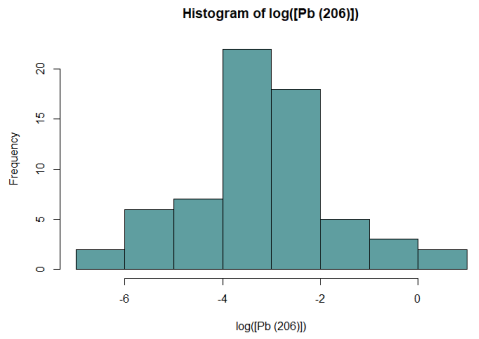

Figure B.24: Histogram of log([Pb (206)]).

Institutional Repository - Library & Information Centre - University of Thessaly
19/04/2024 03:53:45 EEST - 18.222.197.243

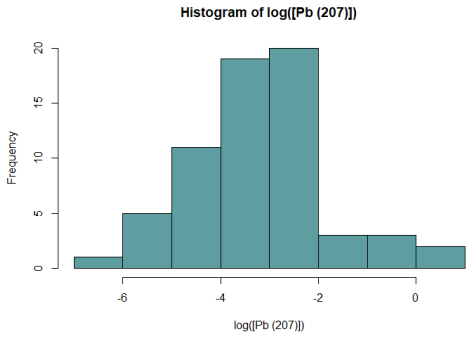

Figure B.25: Histogram of log([Pb (207)]).

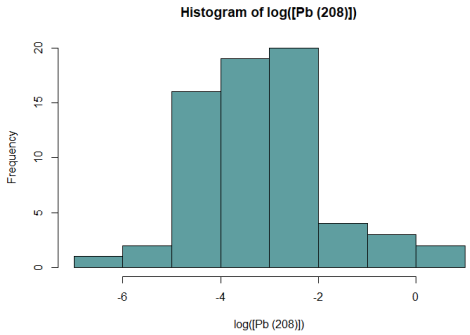

Figure B.26: Histogram of log([Pb (208)]).

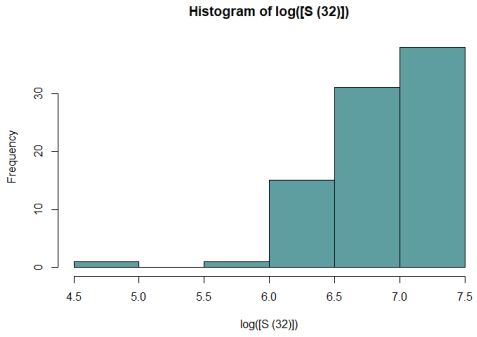

Figure B.27: Histogram of log([S (32)]).

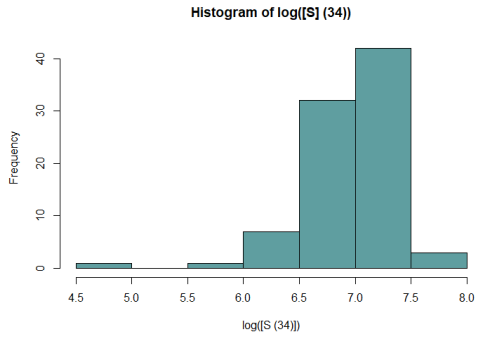

Figure B.28: Histogram of log([S (34)]).

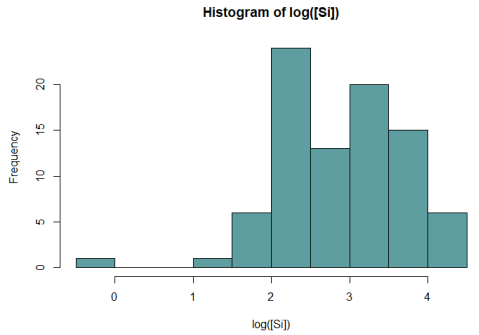

Figure B.29: Histogram of log([Si]).

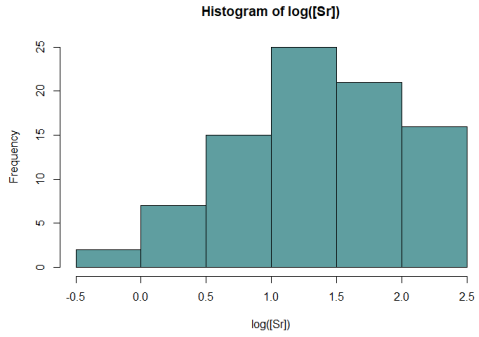

Figure B.30: Histogram of log([Sr]).

Institutional Repository - Library & Information Centre - University of Thessaly
19/04/2024 03:53:45 EEST - 18.222.197.243

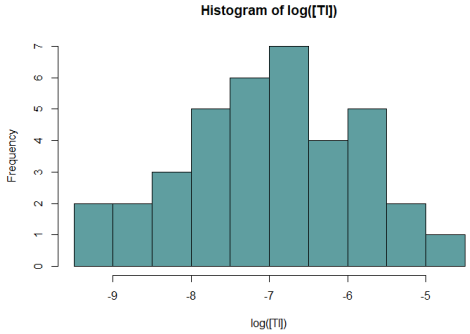

Figure B.31: Histogram of log([Tl]).

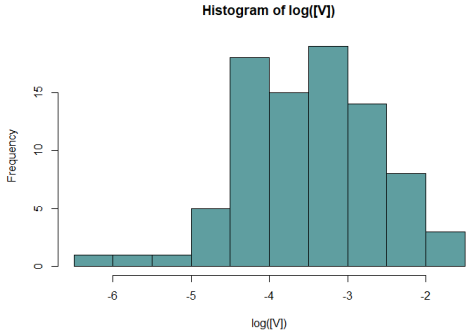

Figure B.32: Histogram of log([V]).

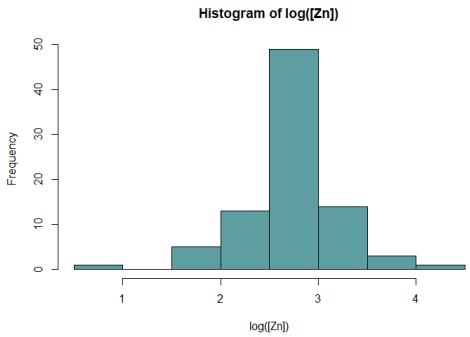

Figure B.33: Histogram of log([Zn]).

Institutional Repository - Library & Information Centre - University of Thessaly
19/04/2024 03:53:45 EEST - 18.222.197.243

B.3 Density plots

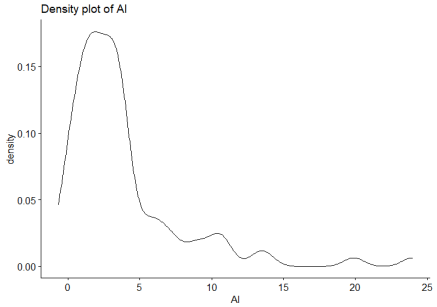

Figure B.34: Density plot of Al.

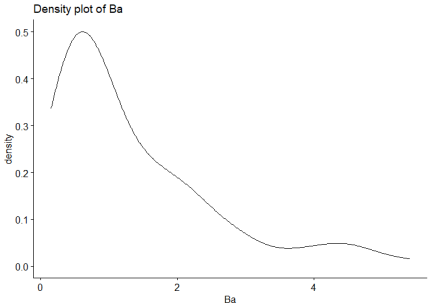

Figure B.38: Density plot of Ba.

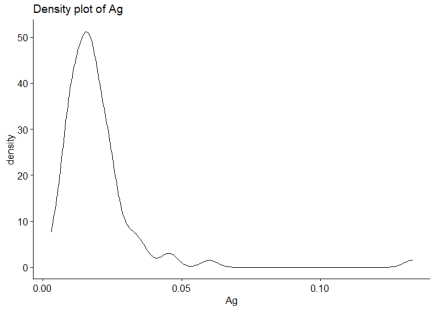

Figure B.35: Density plot of Ag.

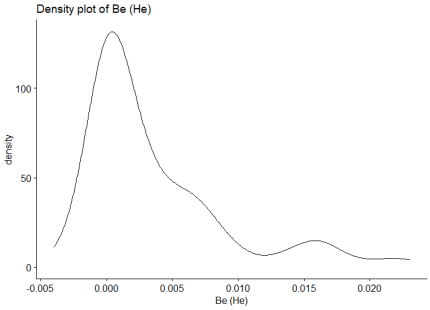

Figure B.39: Density plot of Be (He).

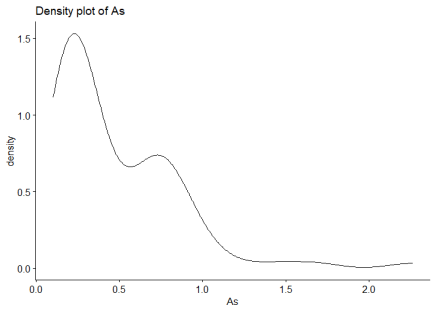

Figure B.36: Density plot of As.

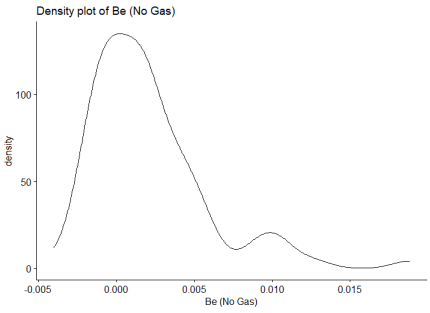

Figure B.40: Density plot of Be (No Gas).

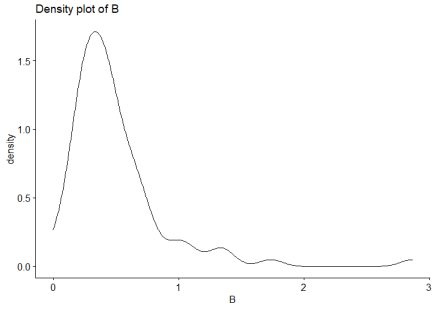

Figure B.37: Density plot of B.

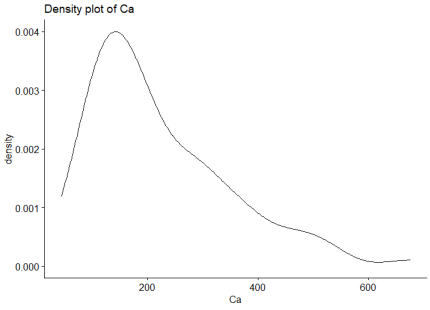

Figure B.41: Density plot of Ca.

Institutional Repository - Library & Information Centre - University of Thessaly
19/04/2024 03:53:45 EEST - 18.222.197.243

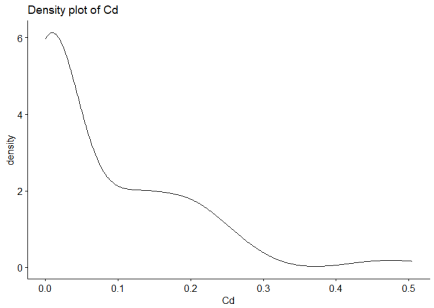

Figure B.42: Density plot of Cd.

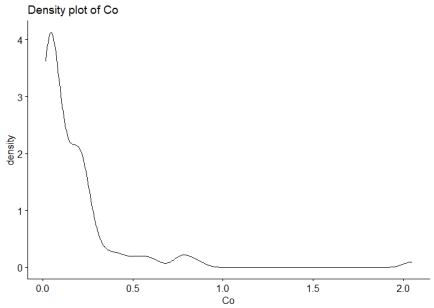

Figure B.43: Density plot of Co.

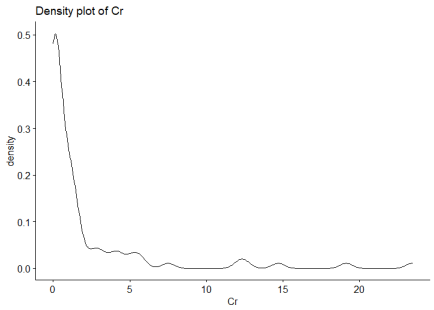

Figure B.44: Density plot of Cr.

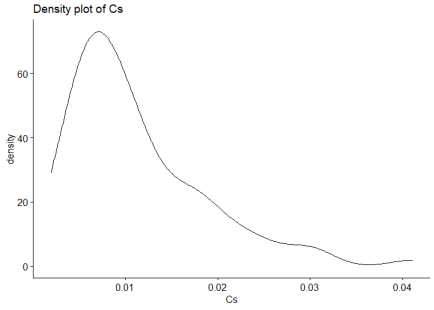

Figure B.45: Density plot of Cs.

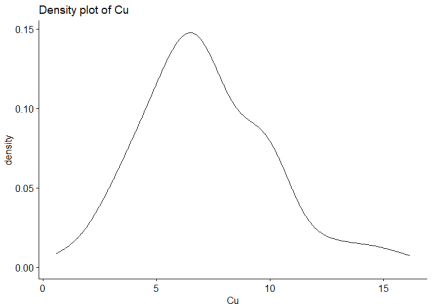

Figure B.46: Density plot of Cr.

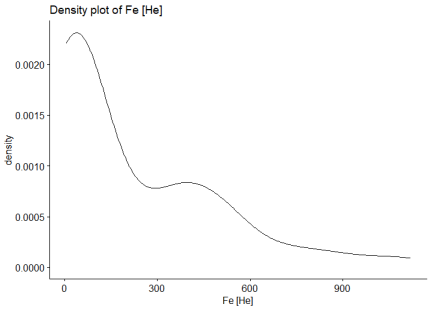

Figure B.47: Density plot of Fe (He).

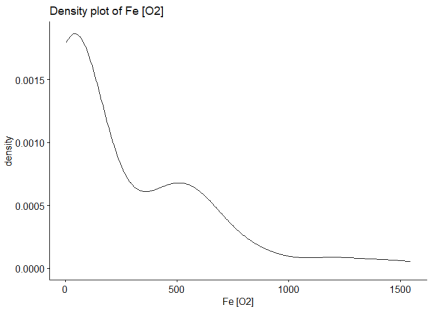

Figure B.48: Density plot of Fe (O_2).

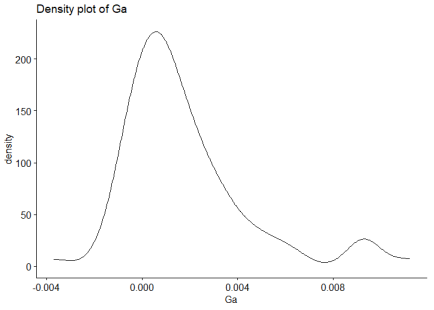

Figure B.49: Density plot of Ga.

Institutional Repository - Library & Information Centre - University of Thessaly
19/04/2024 03:53:45 EEST - 18.222.197.243

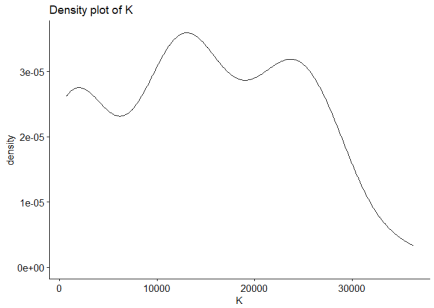

Figure B.50: Density plot of K.

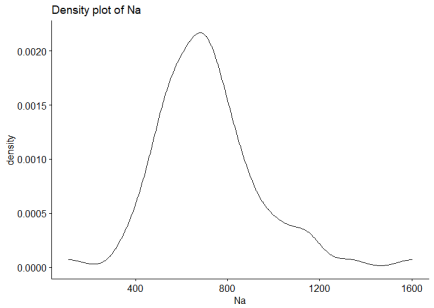

Figure B.54: Density plot of Na.

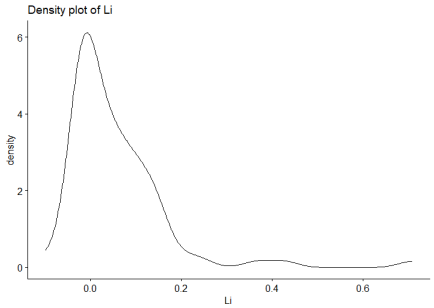

Figure B.51: Density plot of Li.

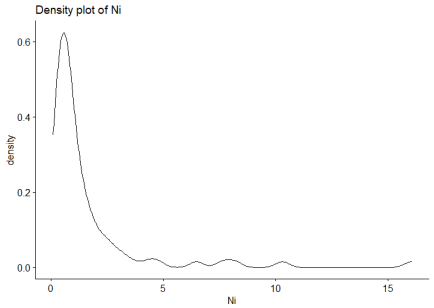

Figure B.55: Density plot of Ni.

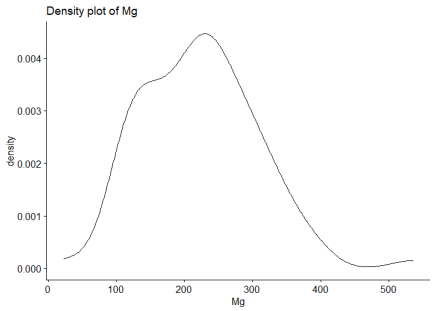

Figure B.52: Density plot of Mg.

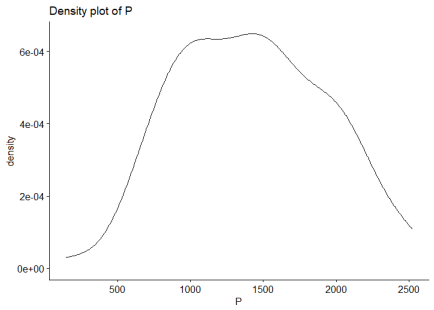

Figure B.56: Density plot of P.

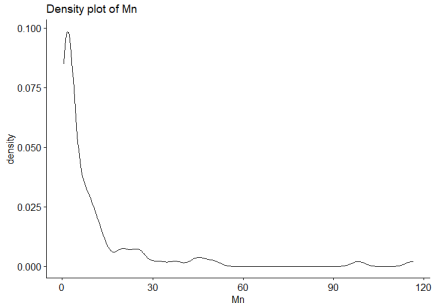

Figure B.53: Density plot of Mn.

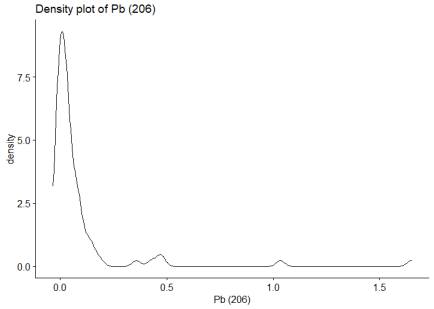

Figure B.57: Density plot of Pb (206).

Institutional Repository - Library & Information Centre - University of Thessaly
19/04/2024 03:53:45 EEST - 18.222.197.243

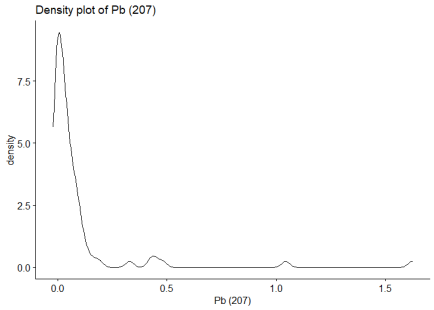

Figure B.58: Density plot of Pb (207).

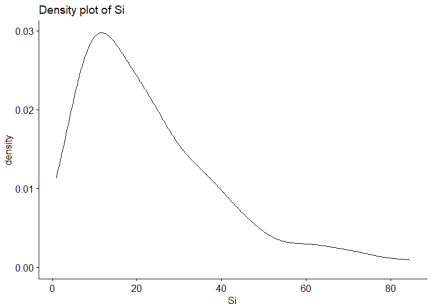

Figure B.62: Density plot of Si.

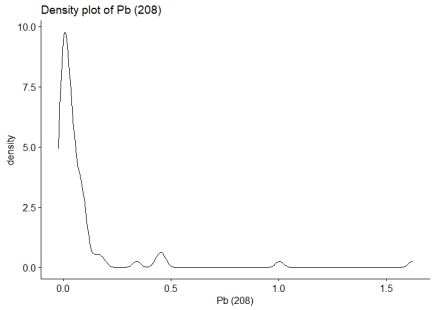

Figure B.59: Density plot of Pb (208).

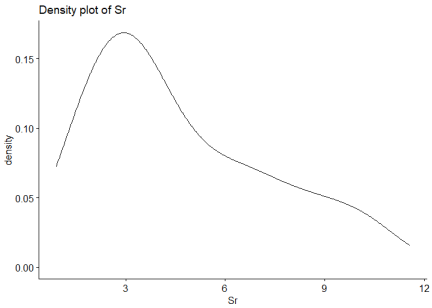

Figure B.63: Density plot of Sr.

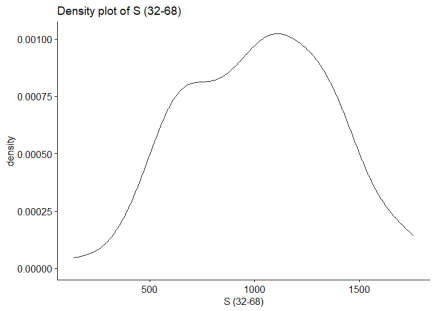

Figure B.60: Density plot of S (32 -> 68).

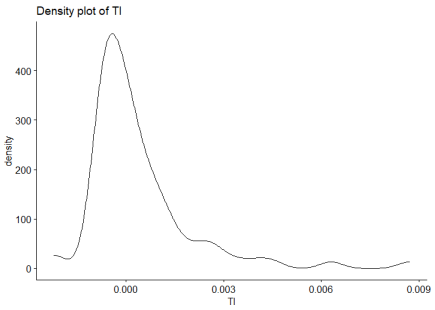

Figure B.64: Density plot of Tl.

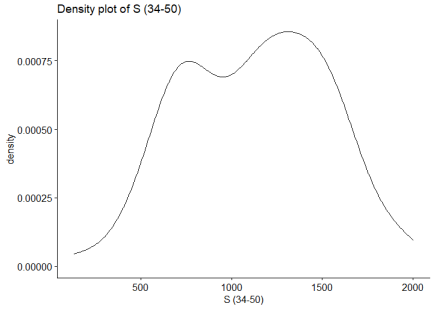

Figure B.61: Density plot of S (34 -> 50).

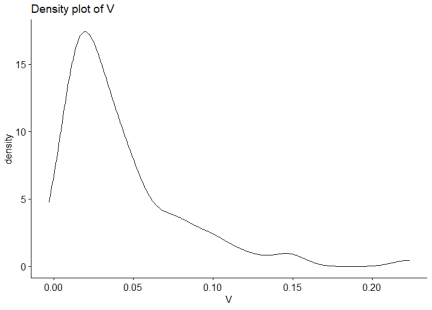

Figure B.65: Density plot of V.

Institutional Repository - Library & Information Centre - University of Thessaly
19/04/2024 03:53:45 EEST - 18.222.197.243

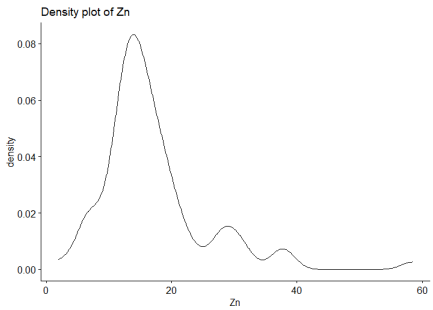

Figure B.66: Density plot of Zn.

Institutional Repository - Library & Information Centre - University of Thessaly
19/04/2024 03:53:45 EEST - 18.222.197.243

B.4 Quantile - Quantile plots

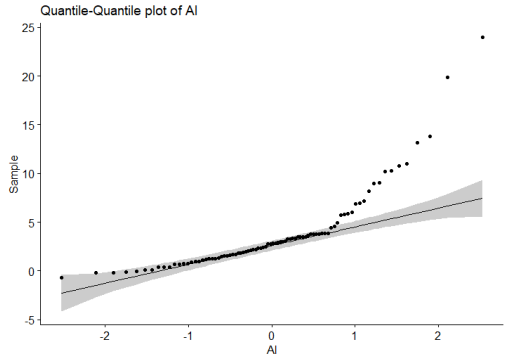

Figure B.67: Quantile - Quantile plot of Al.

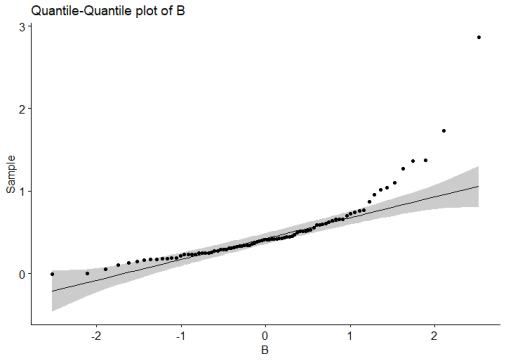

Figure B.70: Quantile - Quantile plot of B.

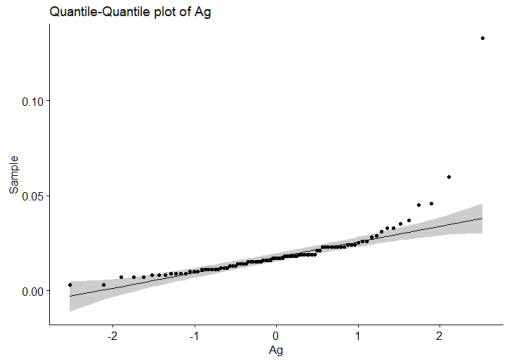

Figure B.68: Quantile - Quantile plot of Ag.

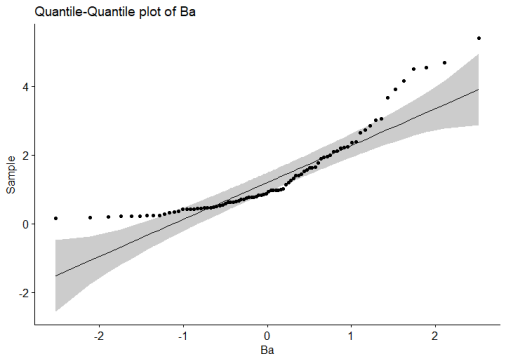

Figure B.71: Quantile - Quantile plot of Ba.

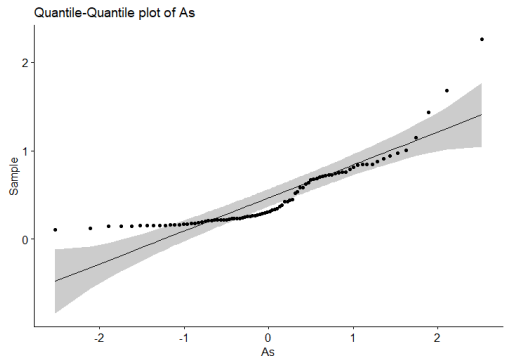

Figure B.69: Quantile - Quantile plot of As.

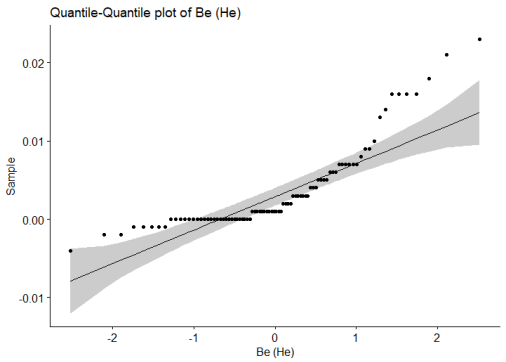

Figure B.72: Quantile - Quantile plot of Be (He).

Institutional Repository - Library & Information Centre - University of Thessaly
19/04/2024 03:53:45 EEST - 18.222.197.243

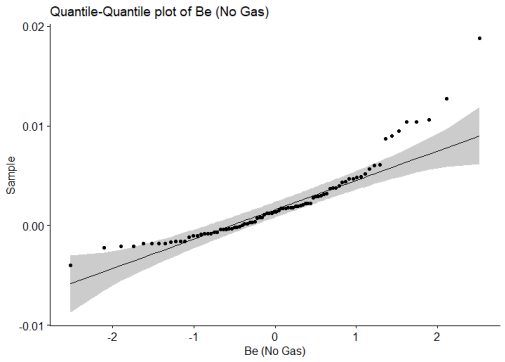

Figure B.73: Quantile - Quantile plot of Be (No Gas).

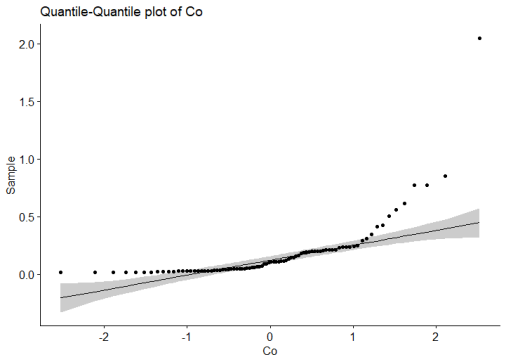

Figure B.76: Quantile - Quantile plot of Co.

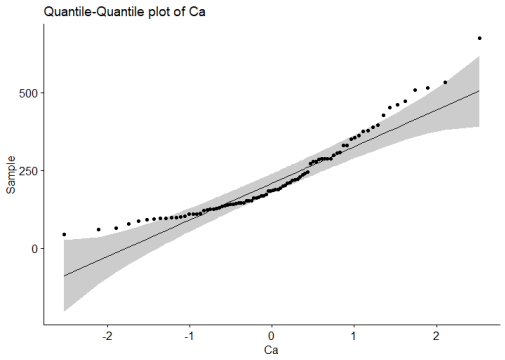

Figure B.74: Quantile - Quantile plot of Ca.

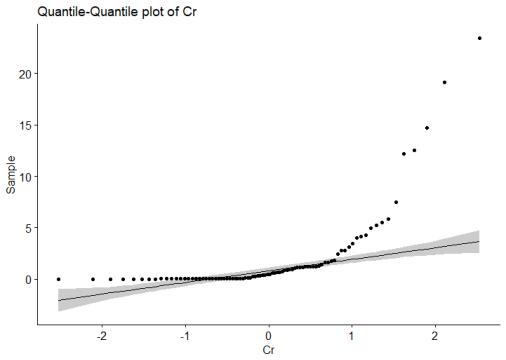

Figure B.77: Quantile - Quantile plot of Cr.

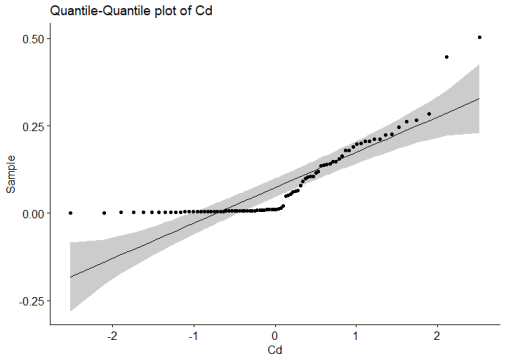

Figure B.75: Quantile - Quantile plot of Cd.

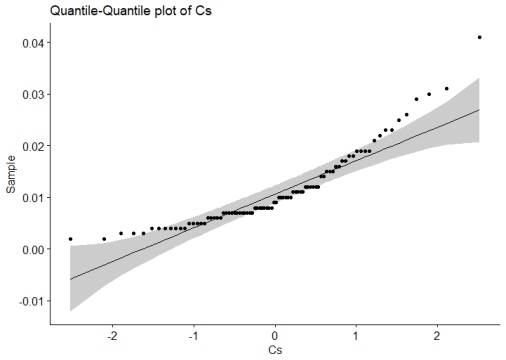

Figure B.78: Quantile - Quantile plot of Cs.

Institutional Repository - Library & Information Centre - University of Thessaly
19/04/2024 03:53:45 EEST - 18.222.197.243

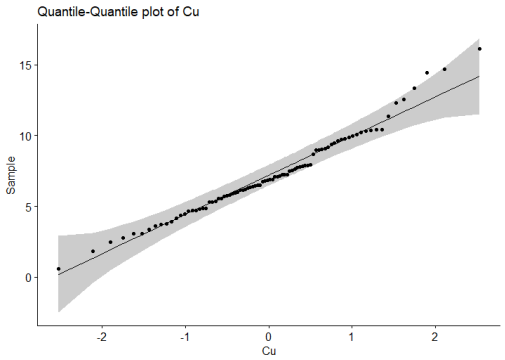

Figure B.79: Quantile - Quantile plot of Cr.

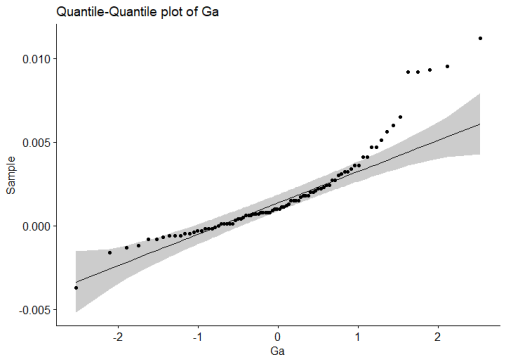

Figure B.82: Quantile - Quantile plot of Ga.

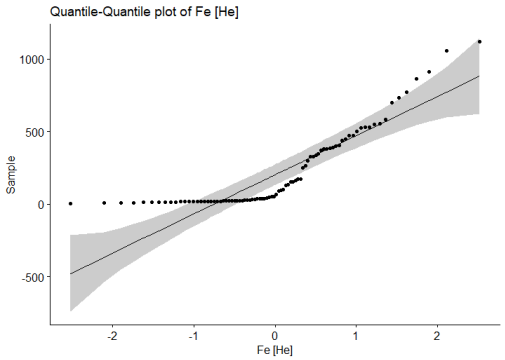

Figure B.80: Quantile - Quantile plot of Fe (He).

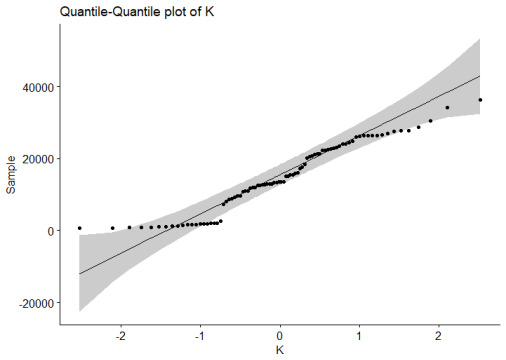

Figure B.83: Quantile - Quantile plot of K.

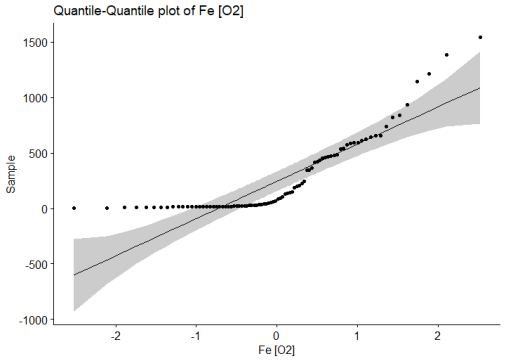

Figure B.81: Quantile - Quantile plot of Fe (O_2).

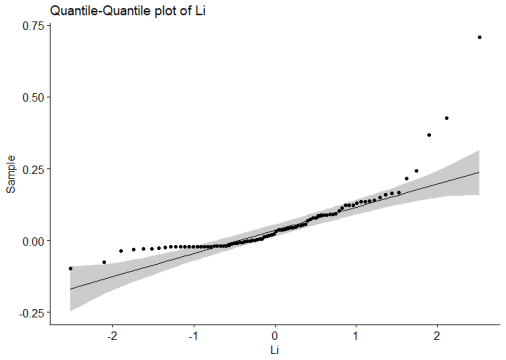

Figure B.84: Quantile - Quantile plot of Li.

Institutional Repository - Library & Information Centre - University of Thessaly
19/04/2024 03:53:45 EEST - 18.222.197.243

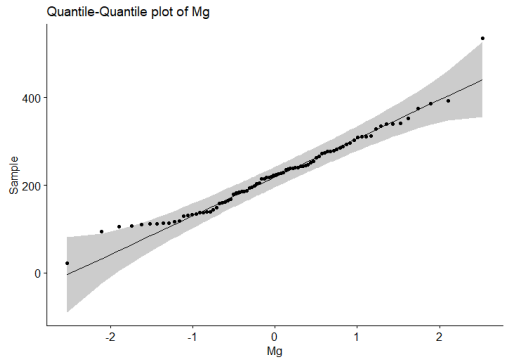

Figure B.85: Quantile - Quantile plot of Mg.

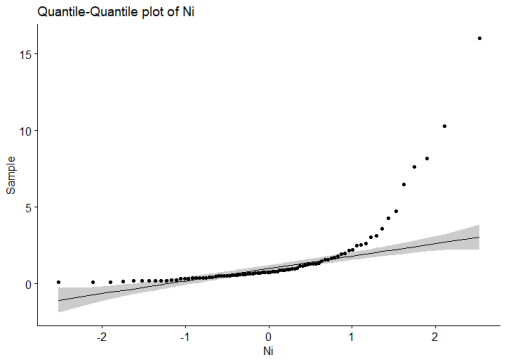

Figure B.88: Quantile - Quantile plot of Ni.

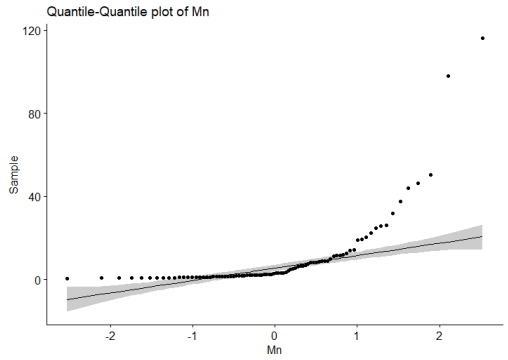

Figure B.86: Quantile - Quantile plot of Mn.

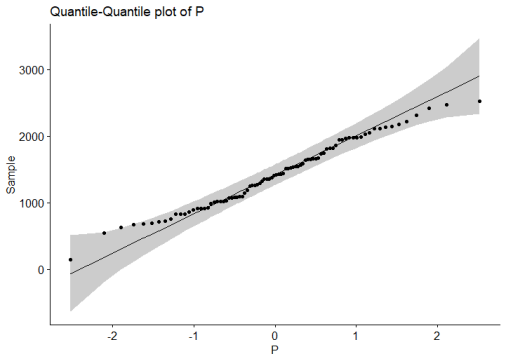

Figure B.89: Quantile - Quantile plot of P.

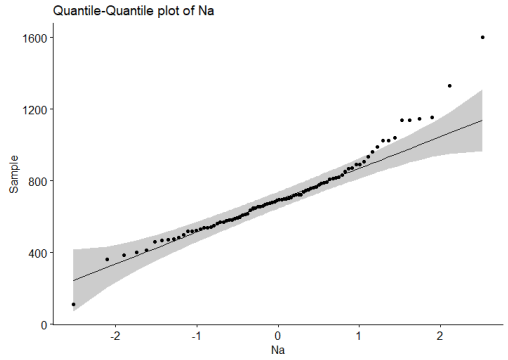

Figure B.87: Quantile - Quantile plot of Na.

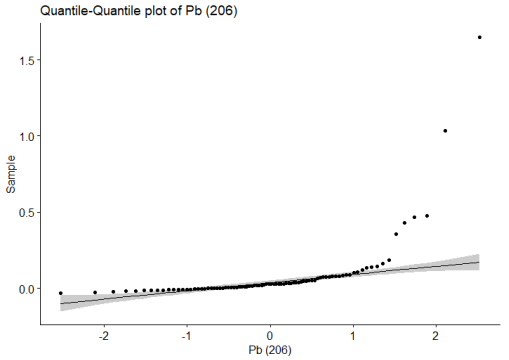

Figure B.90: Quantile - Quantile plot of Pb (206).

Institutional Repository - Library & Information Centre - University of Thessaly
19/04/2024 03:53:45 EEST - 18.222.197.243

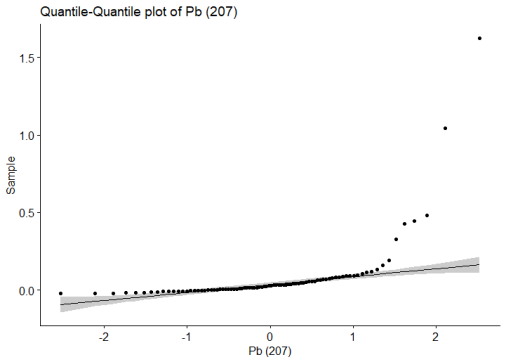

Figure B.91: Quantile - Quantile plot of Pb (207).

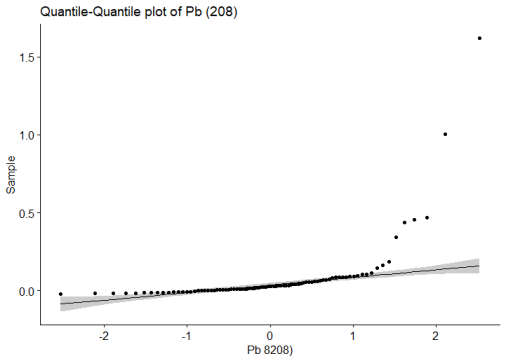

Figure B.92: Quantile - Quantile plot of Pb (208).

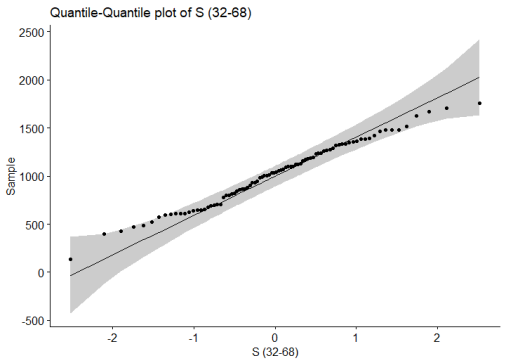

Figure B.93: Quantile - Quantile plot of S (32 -> 68).

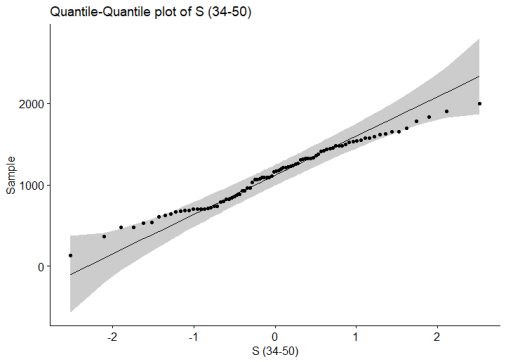

Figure B.94: Quantile - Quantile plot of S (34 -> 50).

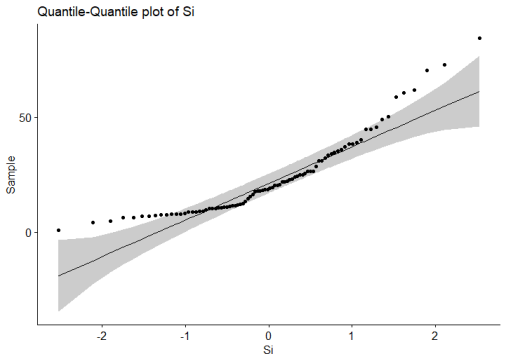

Figure B.95: Quantile - Quantile plot of Si.

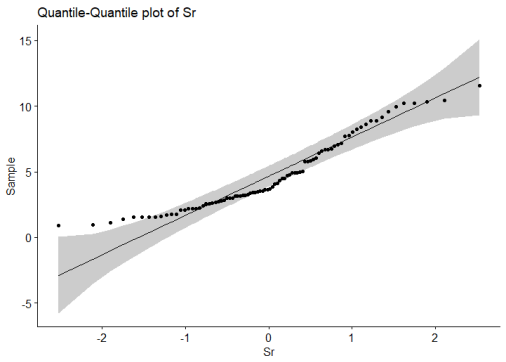

Figure B.96: Quantile - Quantile plot of Sr.

Institutional Repository - Library & Information Centre - University of Thessaly
19/04/2024 03:53:45 EEST - 18.222.197.243

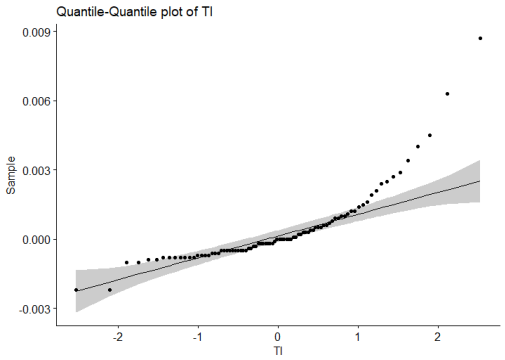

Figure B.97: Quantile - Quantile plot of Tl.

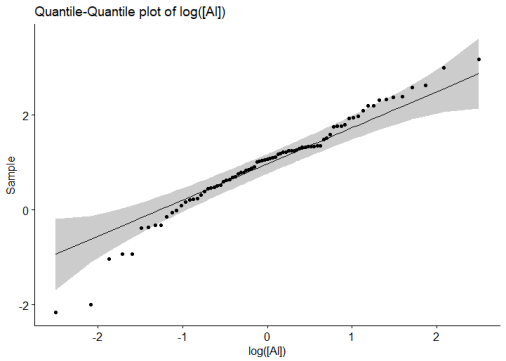

Figure B.100: Quantile - Quantile plot of log[Al].

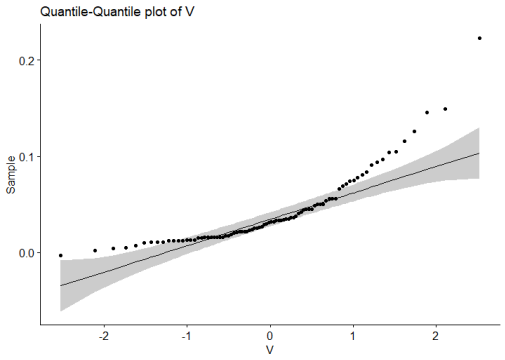

Figure B.98: Quantile - Quantile plot of V.

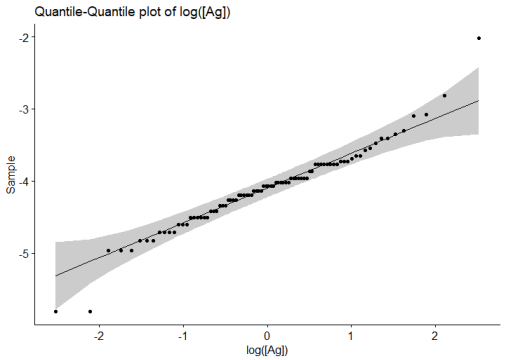

Figure B.101: Quantile - Quantile plot of log[Ag].

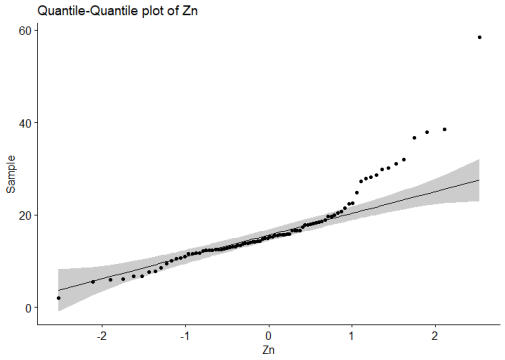

Figure B.99: Quantile - Quantile plot of Zn.

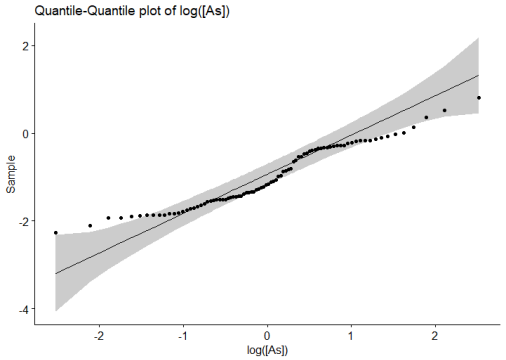

Figure B.102: Quantile - Quantile plot of log[As].

Institutional Repository - Library & Information Centre - University of Thessaly
19/04/2024 03:53:45 EEST - 18.222.197.243

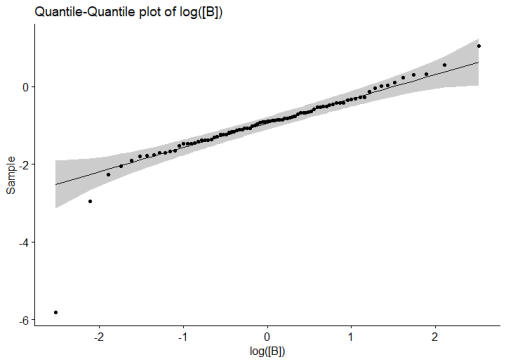

Figure B.103: Quantile - Quantile plot of log[B].

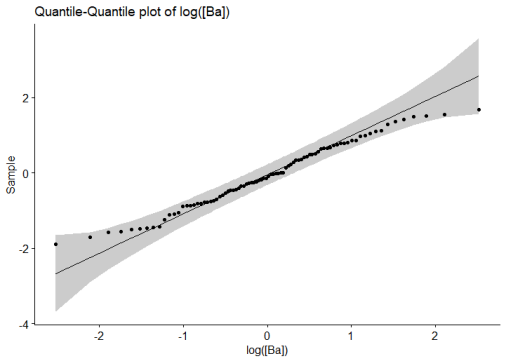

Figure B.104: Quantile - Quantile plot of log[Ba].

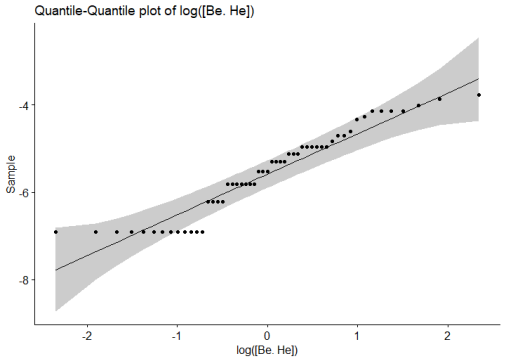

Figure B.105: Quantile - Quantile plot of log[Be. He].

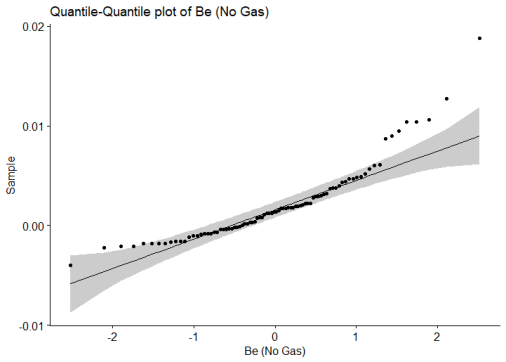

Figure B.106: Quantile - Quantile plot of log[Be. No.Gas].

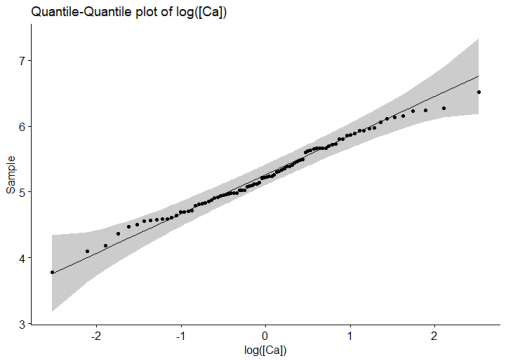

Figure B.107: Quantile - Quantile plot of log[Ca].

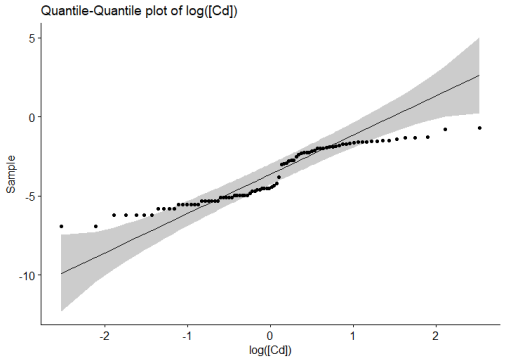

Figure B.108: Quantile - Quantile plot of log[Cd] .

Institutional Repository - Library & Information Centre - University of Thessaly
19/04/2024 03:53:45 EEST - 18.222.197.243

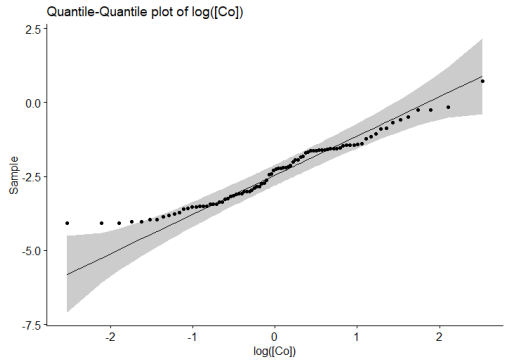

Figure B.109: Quantile - Quantile plot of log[Co].

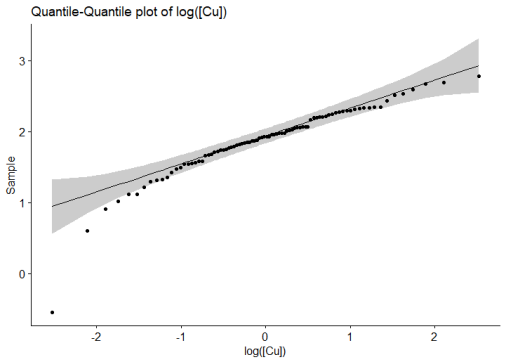

Figure B.112: Quantile - Quantile plot of log[Cr].

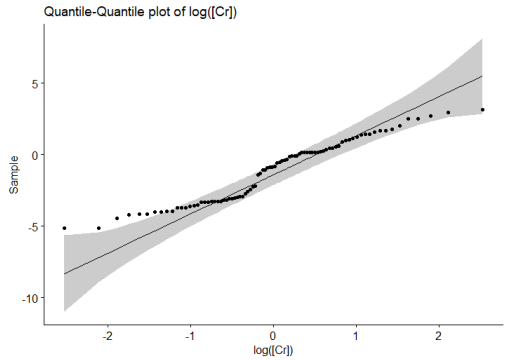

Figure B.110: Quantile - Quantile plot of log[Cr].

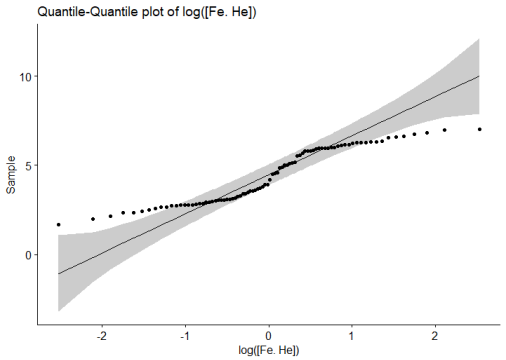

Figure B.113: Quantile - Quantile plot of log[Fe. He].

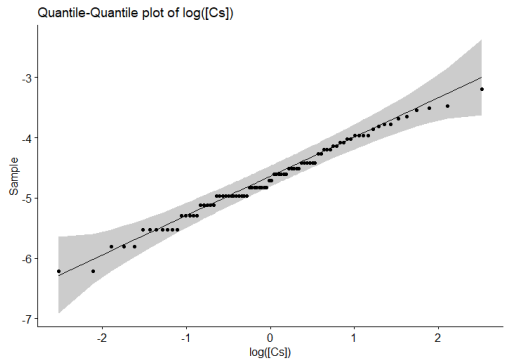

Figure B.111: Quantile - Quantile plot of log[Cs].

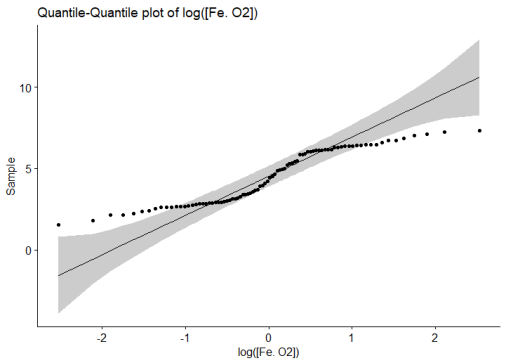

Figure B.114: Quantile - Quantile plot of log[Fe. O_2].

Institutional Repository - Library & Information Centre - University of Thessaly
19/04/2024 03:53:45 EEST - 18.222.197.243

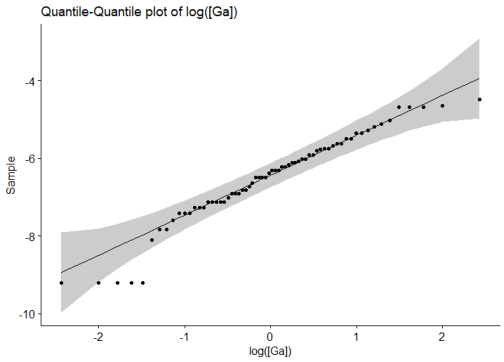

Figure B.115: Quantile - Quantile plot of log[Ga].

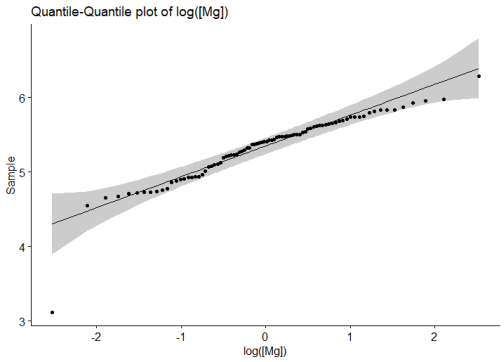

Figure B.118: Quantile - Quantile plot of log[Mg].

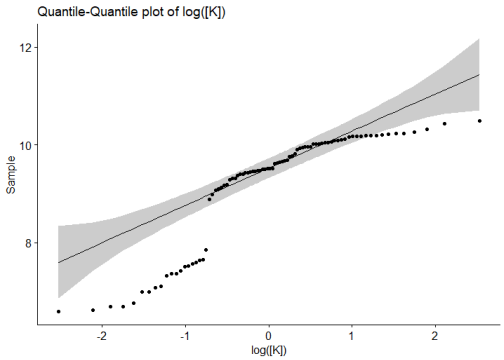

Figure B.116: Quantile - Quantile plot of log[K].

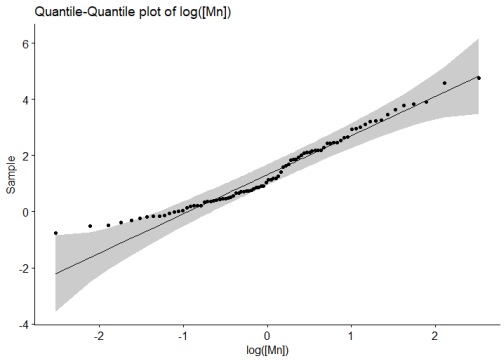

Figure B.119: Quantile - Quantile plot of log[Mn].

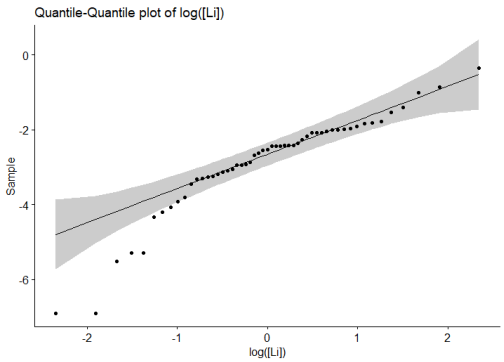

Figure B.117: Quantile - Quantile plot of log[Li].

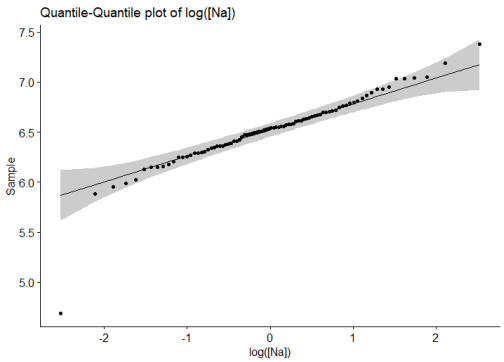

Figure B.120: Quantile - Quantile plot of log[Na].

Institutional Repository - Library & Information Centre - University of Thessaly
19/04/2024 03:53:45 EEST - 18.222.197.243

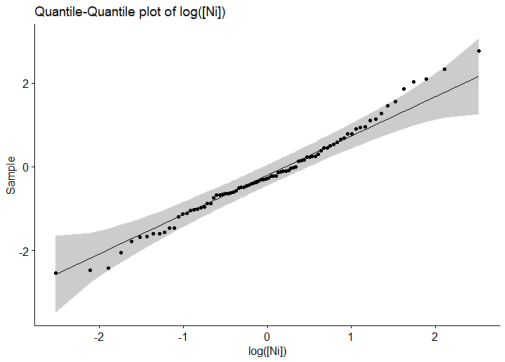

Figure B.121: Quantile - Quantile plot of log[Ni].

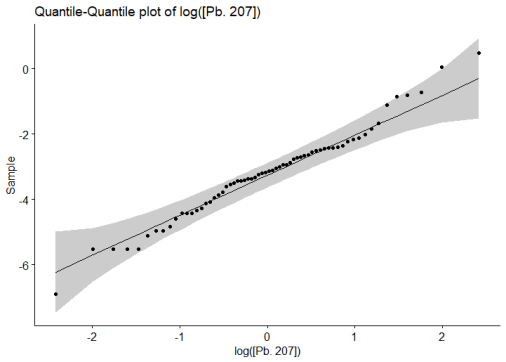

Figure B.124: Quantile - Quantile plot of [Pb.207].

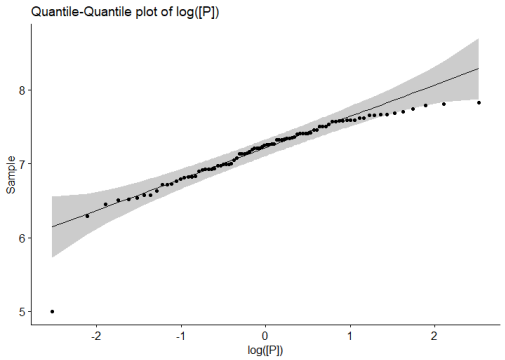

Figure B.122: Quantile - Quantile plot of log[P].

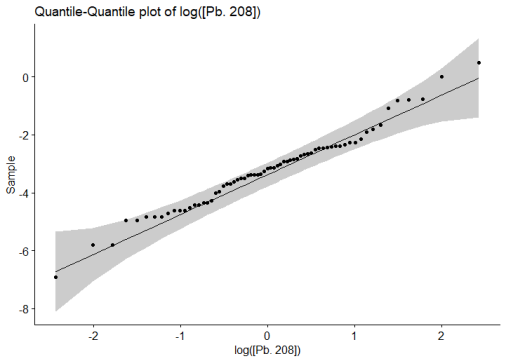

Figure B.125: Quantile - Quantile plot of [Pb.208].

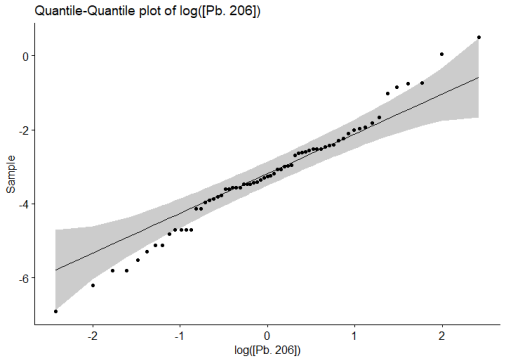

Figure B.123: Quantile - Quantile plot of log[Pb.206].

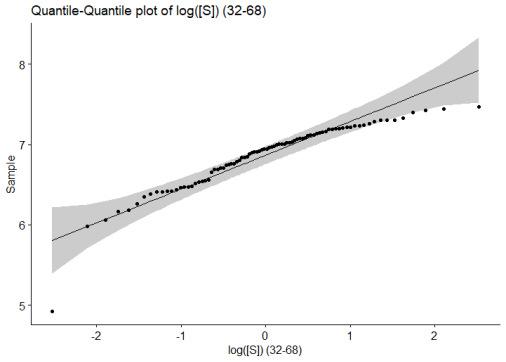

Figure B.126: Quantile - Quantile plot of log[S] (32 -> 68).

Institutional Repository - Library & Information Centre - University of Thessaly
19/04/2024 03:53:45 EEST - 18.222.197.243

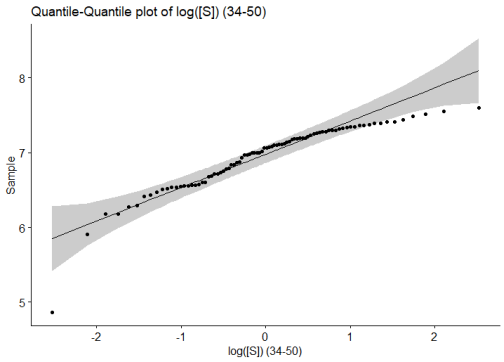

Figure B.127: Quantile - Quantile plot of log [S] (34 -> 50).

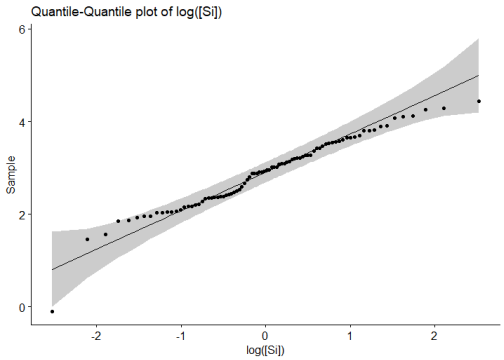

Figure B.128: Quantile - Quantile plot of log[Si].

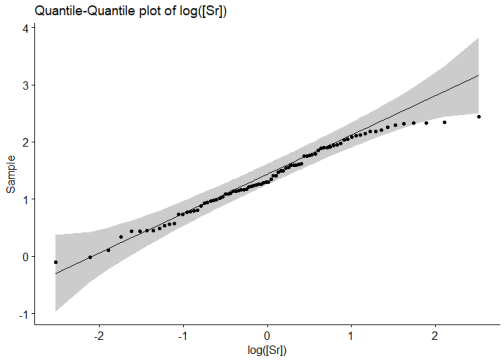

Figure B.129: Quantile - Quantile plot of log[Sr].

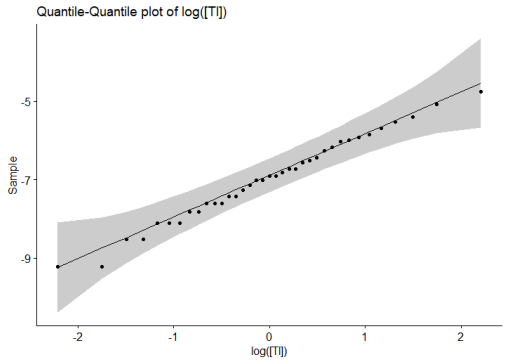

Figure B.130: Quantile - Quantile plot of log[Tl].

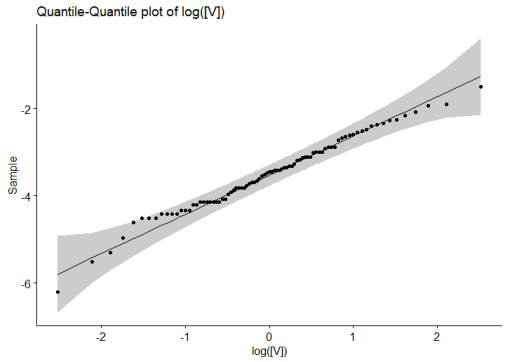

Figure B.131: Quantile - Quantile plot of log[V].

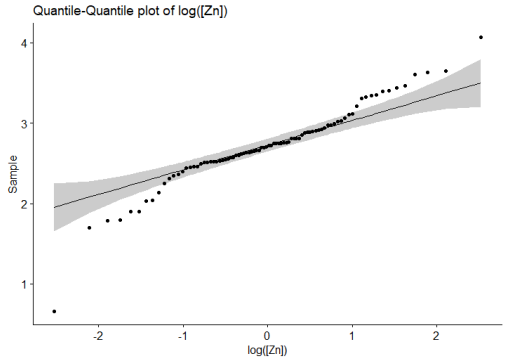

Figure B.132: Quantile - Quantile plot of log[Zn].

Institutional Repository - Library & Information Centre - University of Thessaly
19/04/2024 03:53:45 EEST - 18.222.197.243

Table B.3: Shapiro - Wilk normality test results for the elements detected.

Shapiro - Wilk test	**W**	**P - value**
Hg	0.97025	0.0444
Ag	0.95689	0.005906
Al	0.97182	0.07091
As	0.94489	0.001114
B	0.84051	0.00003916
Ba	0.98184	0.269
Ca	0.98975	0.74
Cd	0.90096	0.006887
Co	0.95968	0.008889
Cr	0.94401	0.0009919
Cs	0.98845	0.6483
Cu	0.9017	0.007421
Fe (He)	0.90517	0.01059
Fe (O_2)	0.90584	0.01136
K	0.81149	4.12e-09
Li	0.89859	0.0002892
Mg	0.90507	0.01049
Mn	0.95285	0.003319
Na	0.89292	0.003103
Ni	0.98562	0.4594
P	0.89602	0.004204
S (32 ->48)	0.899	0.005653
S (34 ->50)	0.89024	0.002396
Si	0.9654	0.02098
Sr	0.97556	0.1021
V	0.98681	0.5435
Zn	0.94262	0.0008259

Institutional Repository - Library & Information Centre - University of Thessaly
19/04/2024 03:53:45 EEST - 18.222.197.243

B.5 Boxplots by tissue

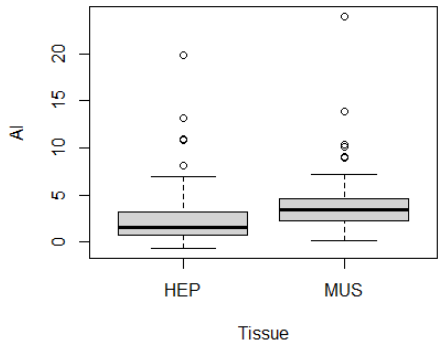

Figure B.133: Boxplot of Al by tissue.

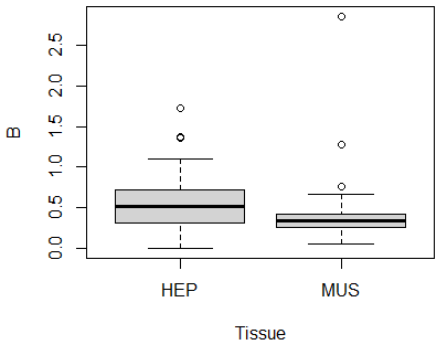

Figure B.136: Boxplot of B by tissue.

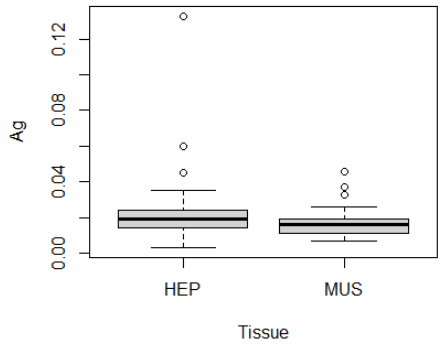

Figure B.134: Boxplot of Ag by tissue.

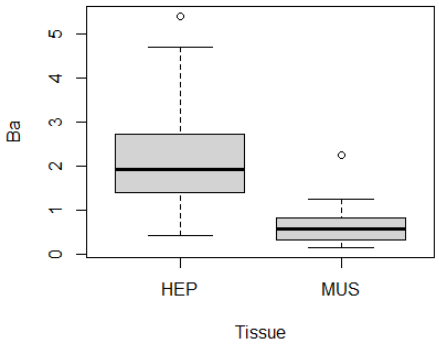

Figure B.137: Boxplot of Ba by tissue.

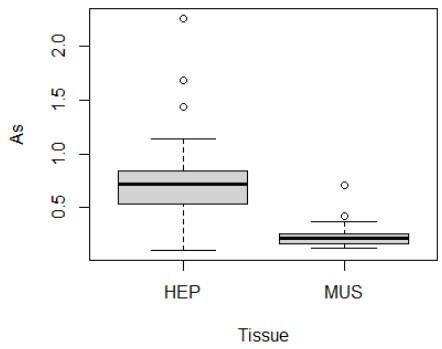

Figure B.135: Boxplot of As by tissue.

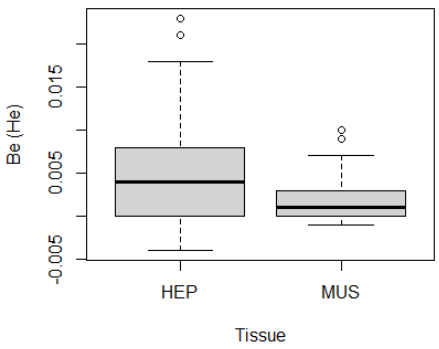

Figure B.138: Boxplot of Be (He) by tissue.

Institutional Repository - Library & Information Centre - University of Thessaly
19/04/2024 03:53:45 EEST - 18.222.197.243

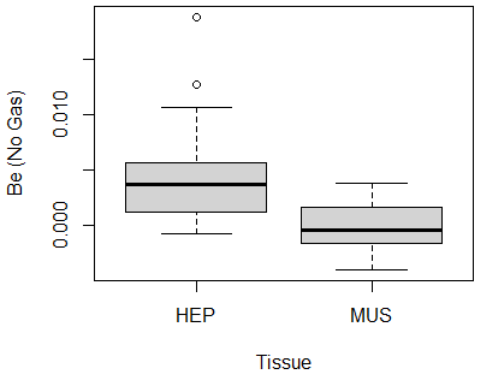

Figure B.139: Boxplot of Be (No Gas) by tissue.

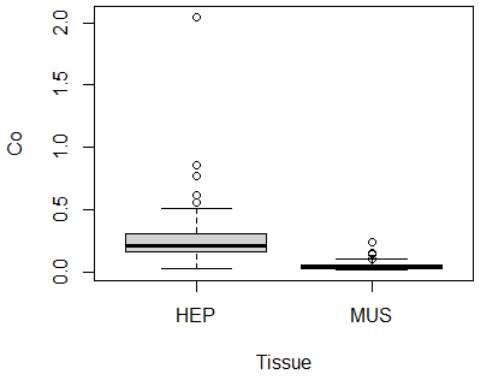

Figure B.142: Boxplot of Co by tissue.

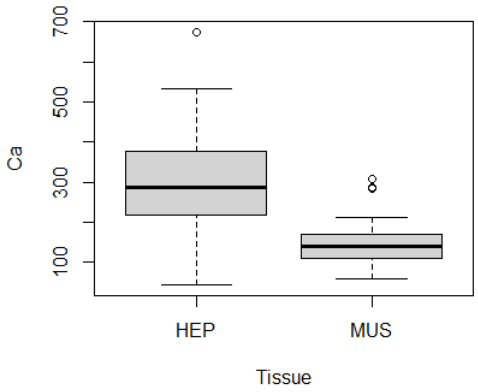

Figure B.140: Boxplot of Ca by tissue.

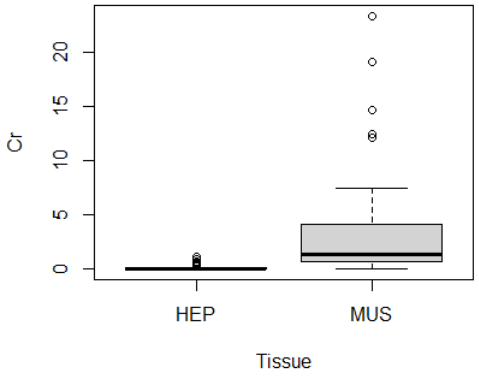

Figure B.143: Boxplot of Cr by tissue.

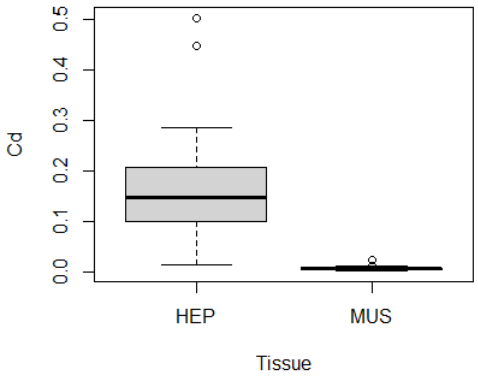

Figure B.141: Boxplot of Cd by tissue.

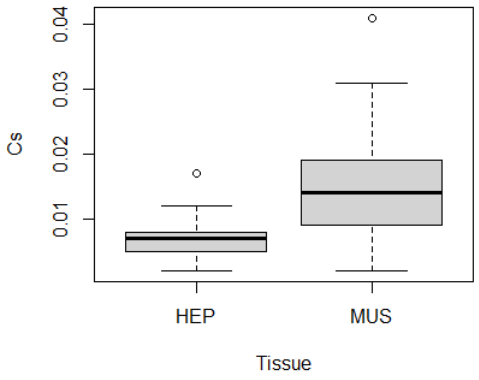

Figure B.144: Boxplot of Cs by tissue.

Institutional Repository - Library & Information Centre - University of Thessaly
19/04/2024 03:53:45 EEST - 18.222.197.243

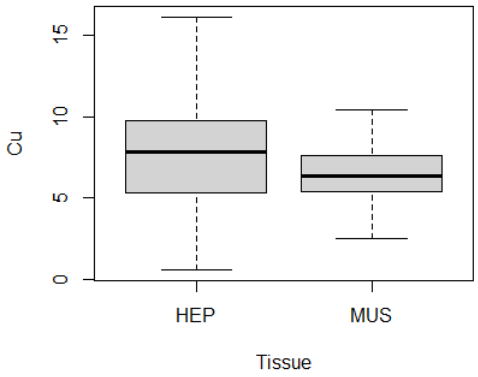

Figure B.145: Boxplot of Cu by tissue.

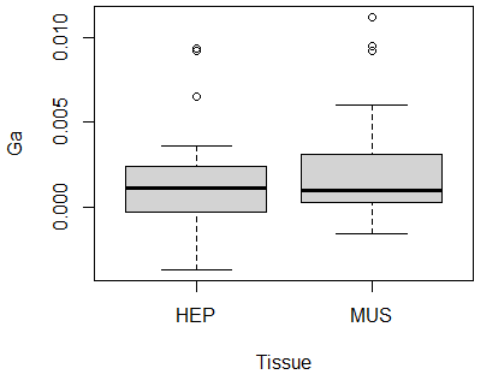

Figure B.148: Boxplot of Ga by tissue.

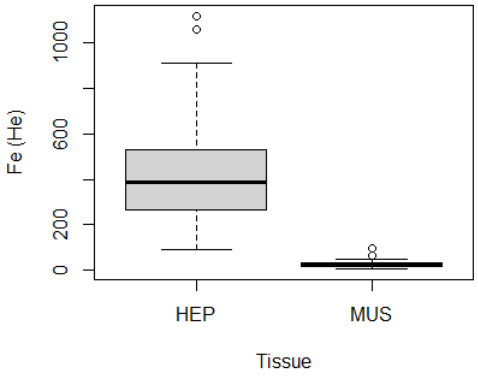

Figure B.146: Boxplot Fe (He) by tissue.

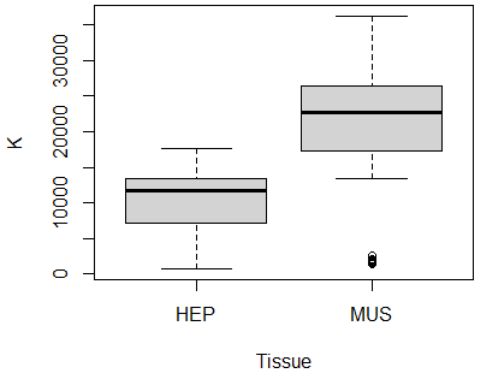

Figure B.149: Boxplot of K by tissue.

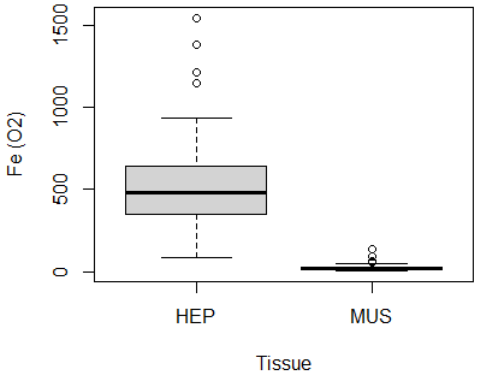

Figure B.147: Boxplot of Fe (O_2) by tissue.

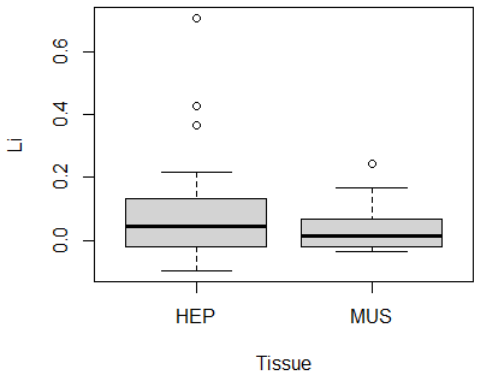

Figure B.150: Boxplot of Li by tissue.

Institutional Repository - Library & Information Centre - University of Thessaly
19/04/2024 03:53:45 EEST - 18.222.197.243

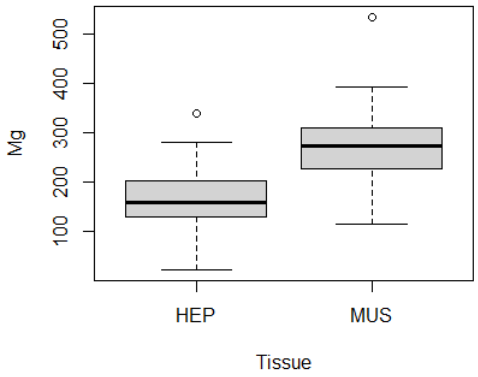

Figure B.151: Boxplot of Mg by tissue.

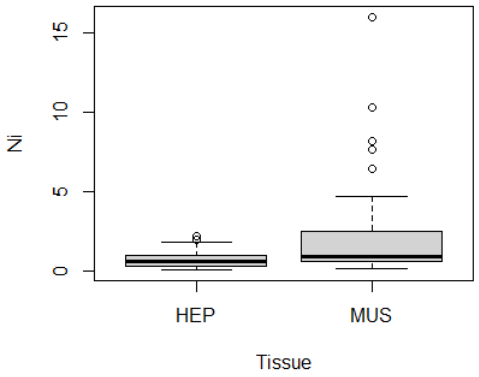

Figure B.154: Boxplot of Ni by tissue.

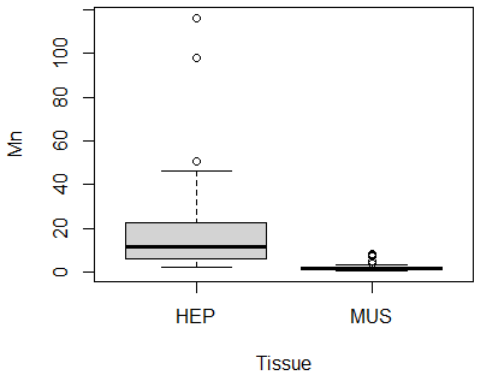

Figure B.152: Boxplot of Mn by tissue.

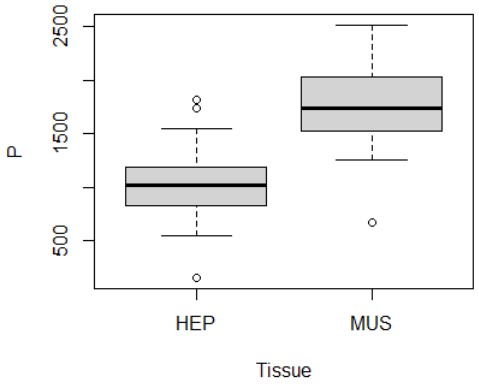

Figure B.155: Boxplot of P by tissue.

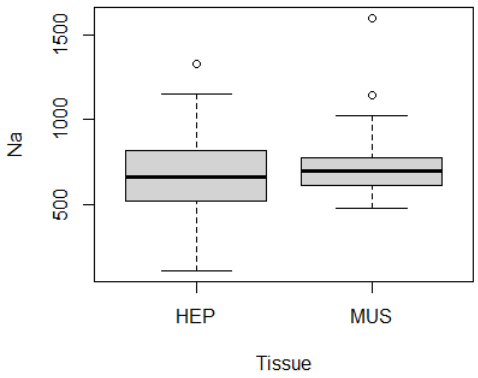

Figure B.153: Boxplot of Na by tissue.

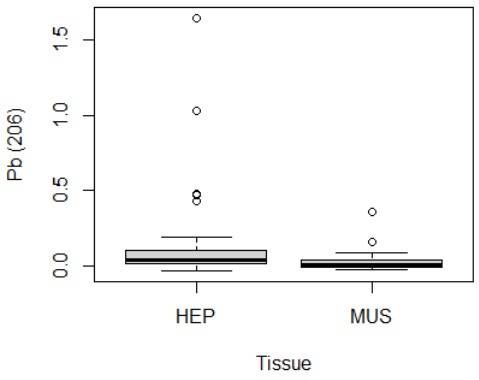

Figure B.156: Boxplot of Pb (206) by tissue.

Institutional Repository - Library & Information Centre - University of Thessaly
19/04/2024 03:53:45 EEST - 18.222.197.243

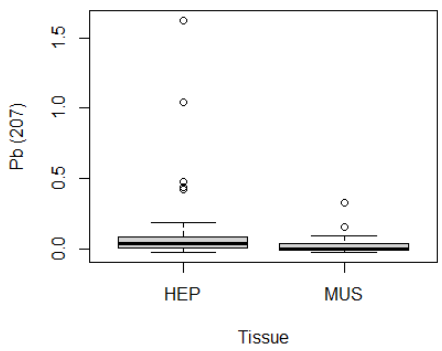

Figure B.157: Boxplot of Pb (207) by tissue.

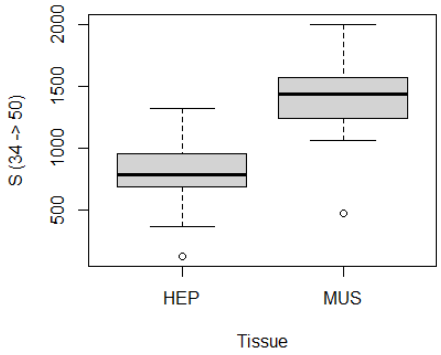

Figure B.160: Boxplot of S (34 -> 50) by tissue.

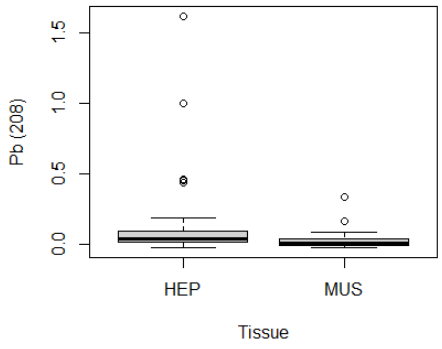

Figure B.158: Boxplot of Pb (208) by tissue.

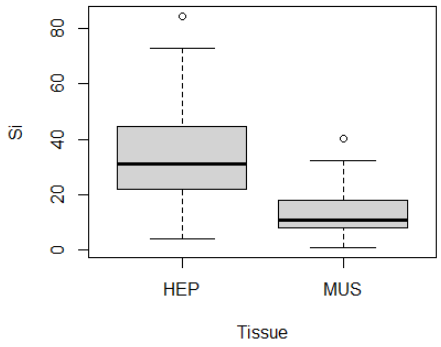

Figure B.161: Boxplot of Si by tissue.

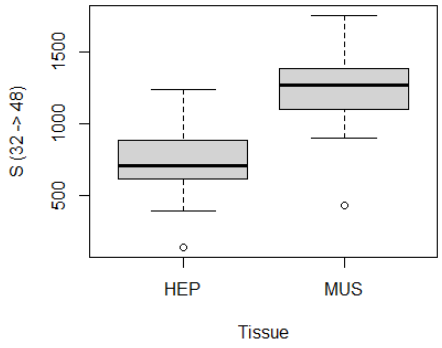

Figure B.159: Boxplot of S(32->68) by tissue.

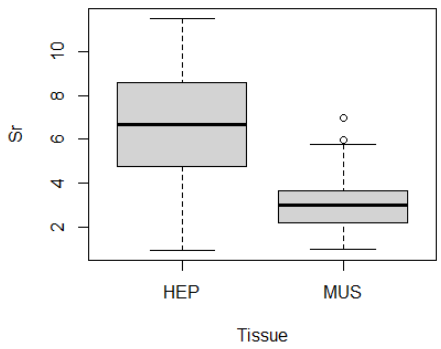

Figure B.162: Boxplot of Sr by tissue.

Institutional Repository - Library & Information Centre - University of Thessaly
19/04/2024 03:53:45 EEST - 18.222.197.243

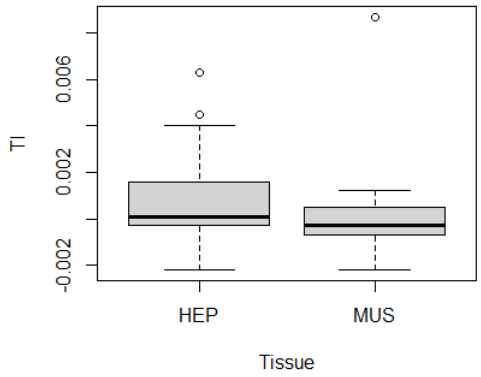

Figure B.163: Boxplot of Tl by tissue.

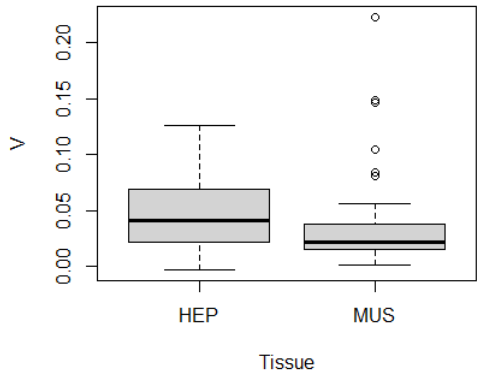

Figure B.164: Boxplot of V by tissue.

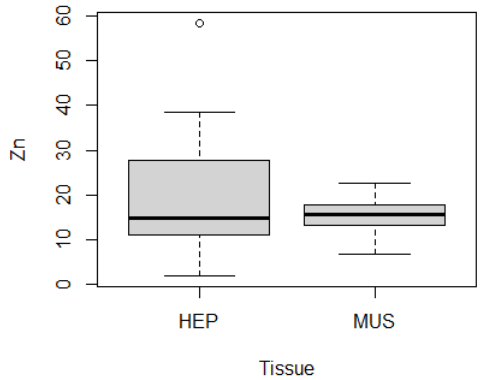

Figure B.165: Boxplot of Zn by tissue.

Institutional Repository - Library & Information Centre - University of Thessaly
19/04/2024 03:53:45 EEST - 18.222.197.243

B.6 Boxplots by sex

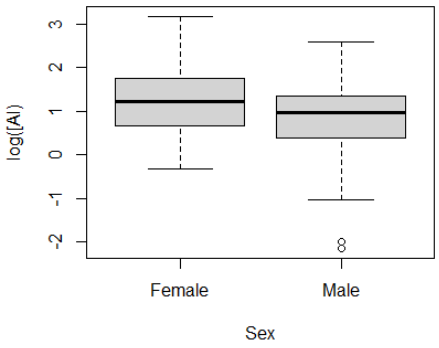

Figure B.166: Boxplot of Al by sex.

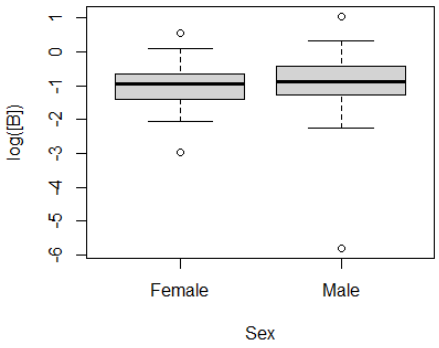

Figure B.169: Boxplot of B by sex.

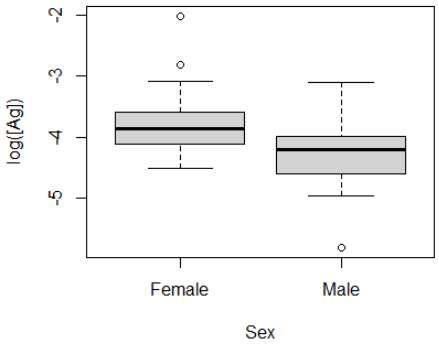

Figure B.167: Boxplot of Ag by sex.

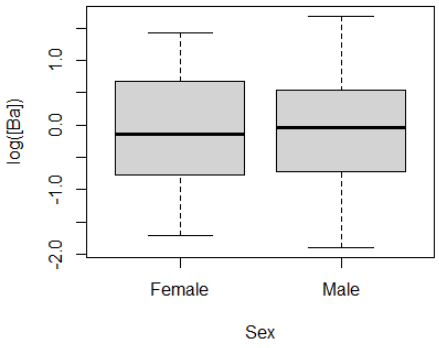

Figure B.170: Boxplot of Ba by sex.

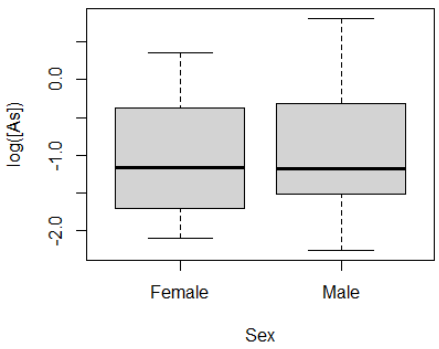

Figure B.168: Boxplot of As by sex.

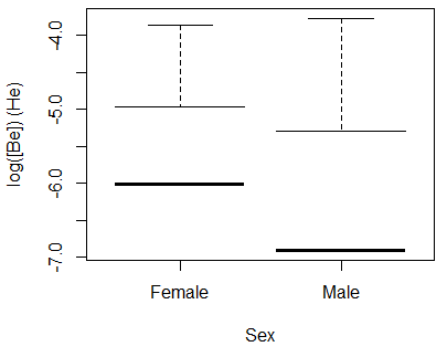

Figure B.171: Boxplot of Be (He) by sex.

Institutional Repository - Library & Information Centre - University of Thessaly
19/04/2024 03:53:45 EEST - 18.222.197.243

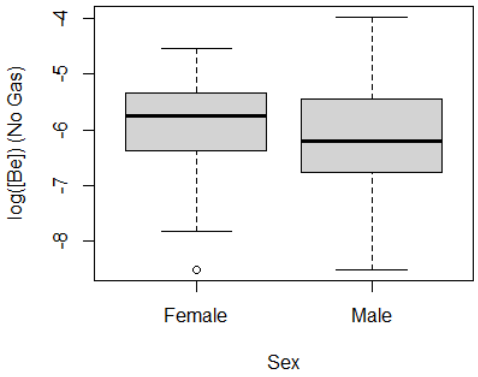

Figure B.172: Boxplot of Be (No Gas) by sex.

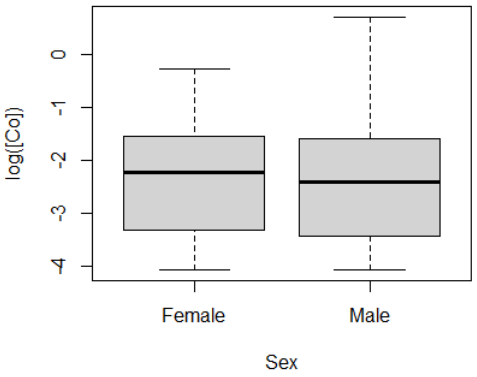

Figure B.175: Boxplot of Co by sex.

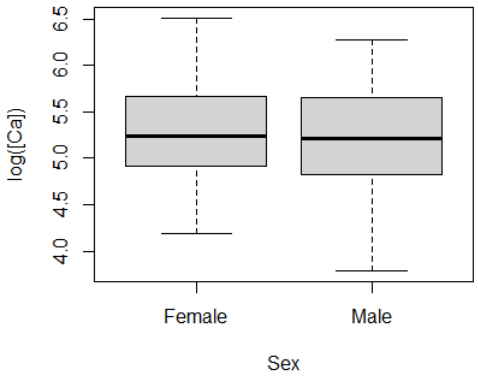

Figure B.173: Boxplot of Ca by sex.

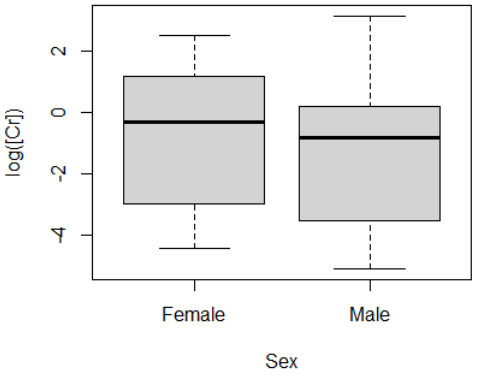

Figure B.176: Boxplot of Cr by sex.

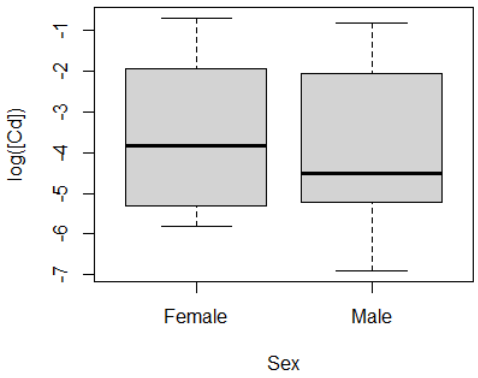

Figure B.174: Boxplot of Cd by sex.

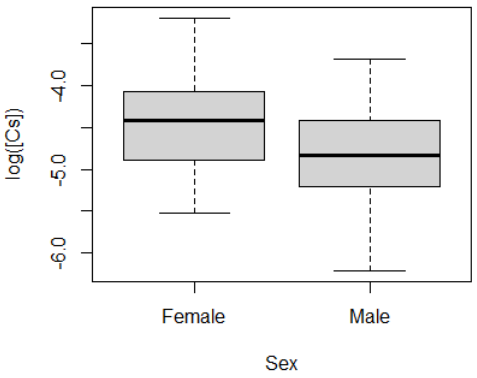

Figure B.177: Boxplot of Cs by sex.

Institutional Repository - Library & Information Centre - University of Thessaly
19/04/2024 03:53:45 EEST - 18.222.197.243

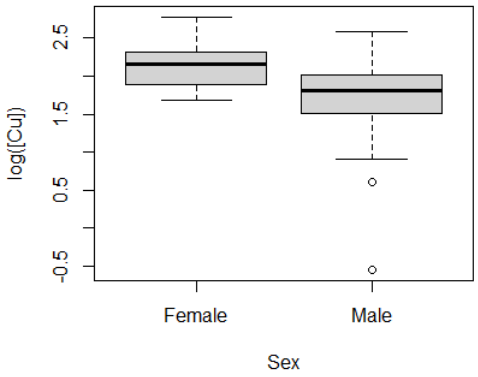

Figure B.178: Boxplot of Cu by sex.

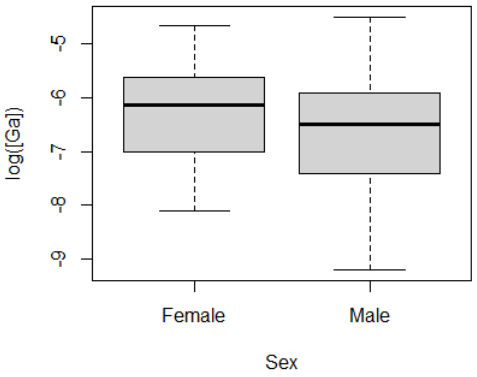

Figure B.181: Boxplot of Ga by sex.

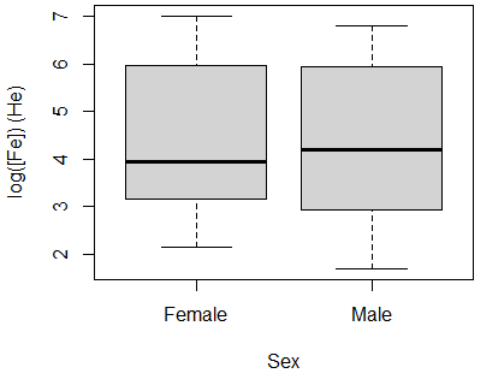

Figure B.179: Boxplot of Fe (He) by sex.

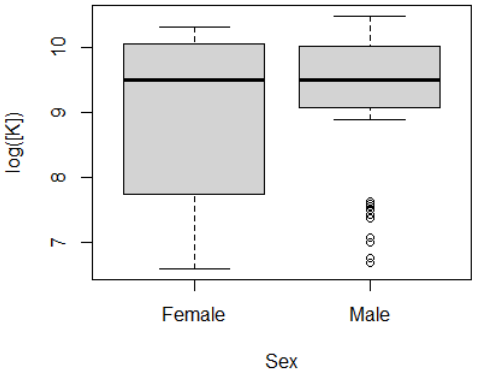

Figure B.182: Boxplot of K by sex.

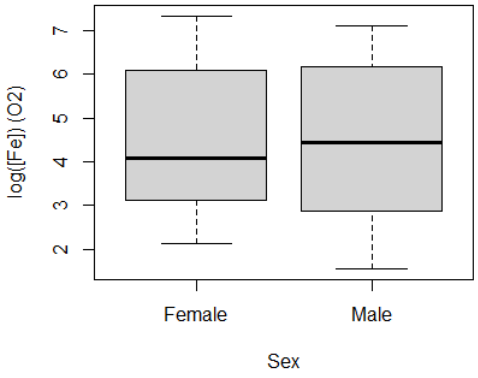

Figure B.180: Boxplot of Fe (O_2) by sex.

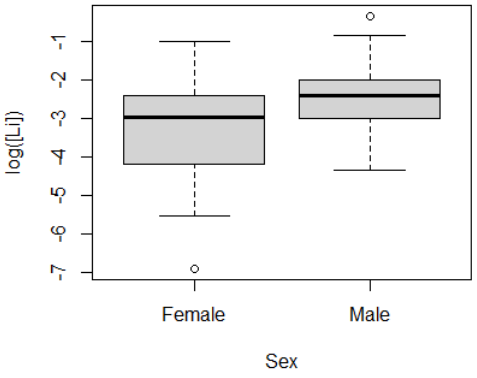

Figure B.183: Boxplot of Li by sex.

Institutional Repository - Library & Information Centre - University of Thessaly
19/04/2024 03:53:45 EEST - 18.222.197.243

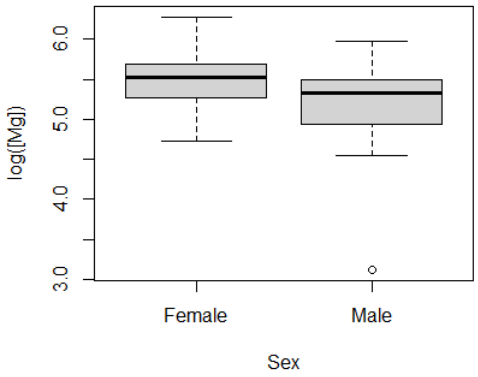

Figure B.184: Boxplot of Mg by sex.

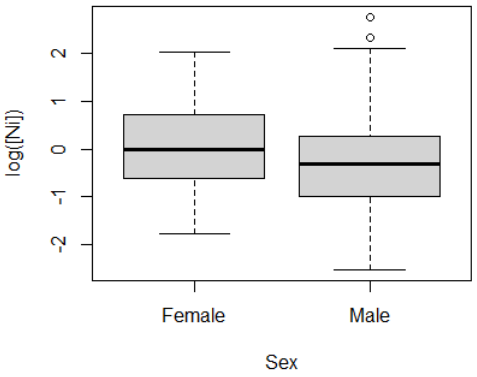

Figure B.187: Boxplot of Ni by sex.

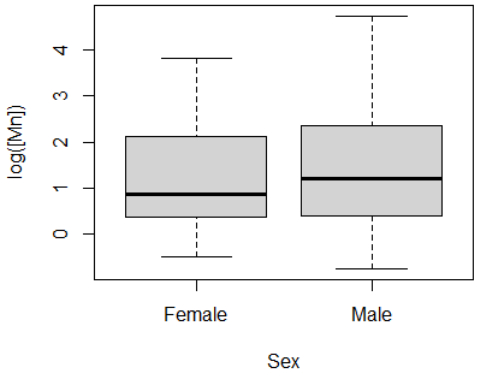

Figure B.185: Boxplot of Mn by sex.

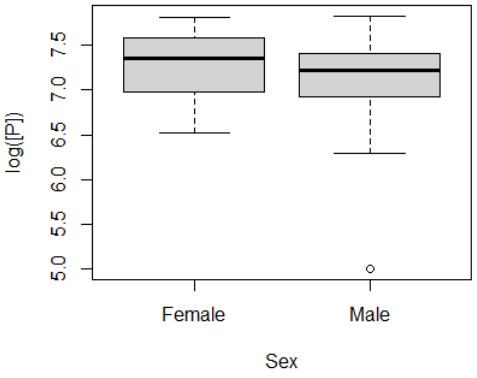

Figure B.188: Boxplot of P by sex.

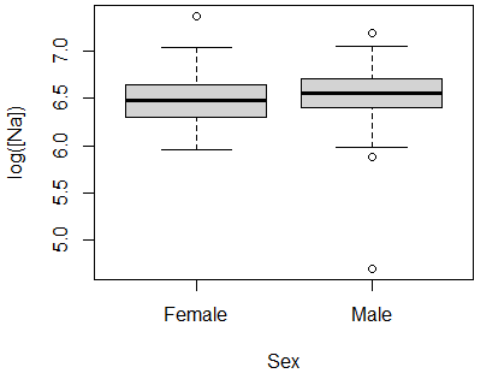

Figure B.186: Boxplot of Na by sex.

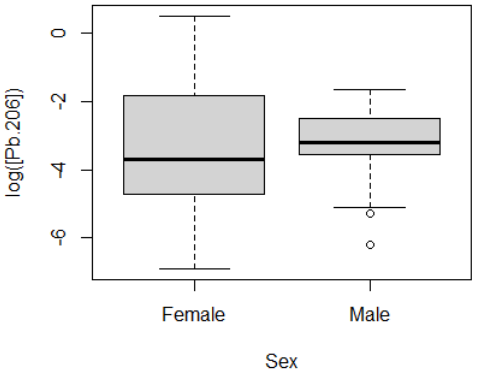

Figure B.189: Boxplot of Pb (206) by sex.

Institutional Repository - Library & Information Centre - University of Thessaly
19/04/2024 03:53:45 EEST - 18.222.197.243

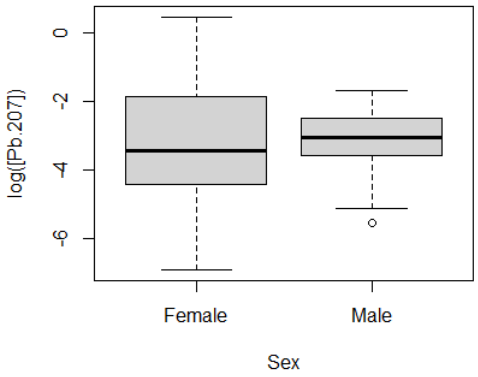

Figure B.190: Boxplot of Pb (207) by sex.

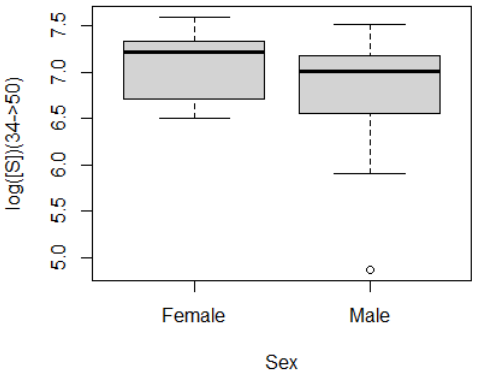

Figure B.193: Boxplot of S(34->50) by sex.

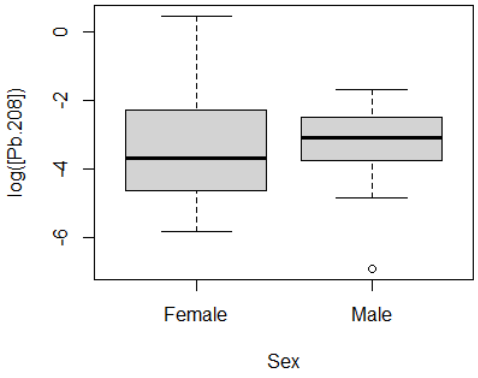

Figure B.191: Boxplot of Pb (208) by sex.

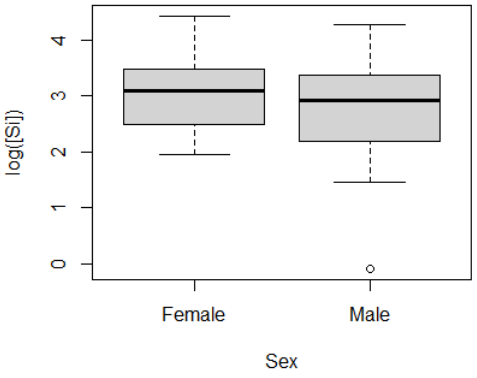

Figure B.194: Boxplot of Si by sex.

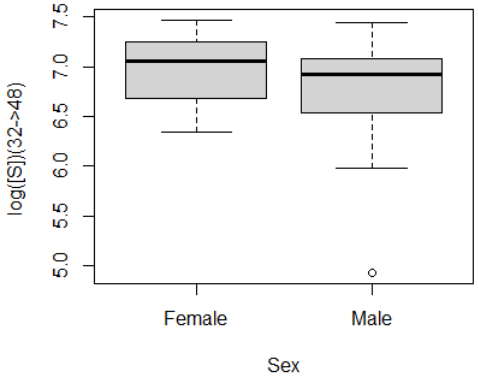

Figure B.192: Boxplot of S(32->68) bysex.

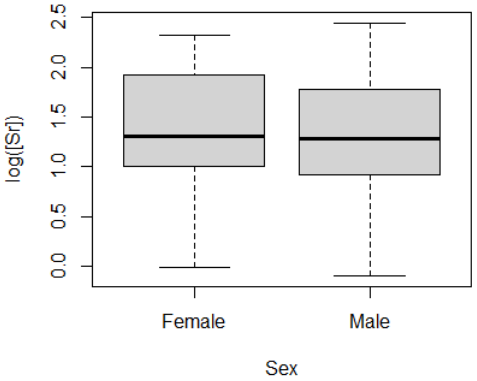

Figure B.195: Boxplot of Sr by sex.

Institutional Repository - Library & Information Centre - University of Thessaly
19/04/2024 03:53:45 EEST - 18.222.197.243

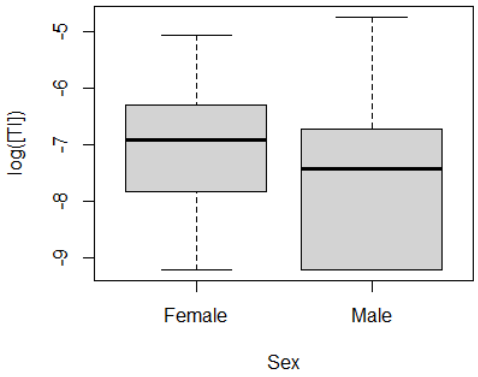

Figure B.196: Boxplot of Tl by sex.

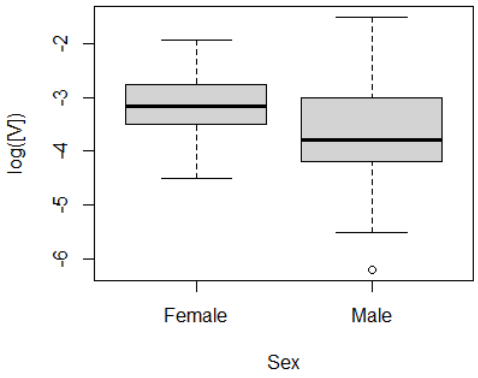

Figure B.197: Boxplot of V by sex.

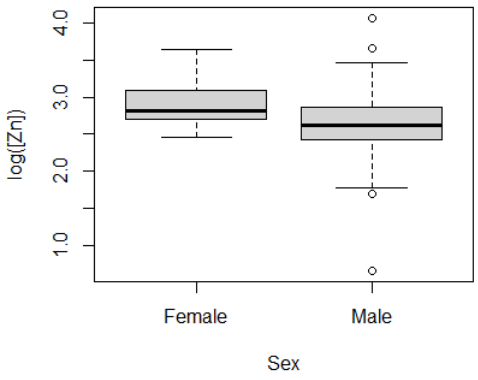

Figure B.198: Boxplot of Zn by sex.

Institutional Repository - Library & Information Centre - University of Thessaly
19/04/2024 03:53:45 EEST - 18.222.197.243

B.7 Correlation tests

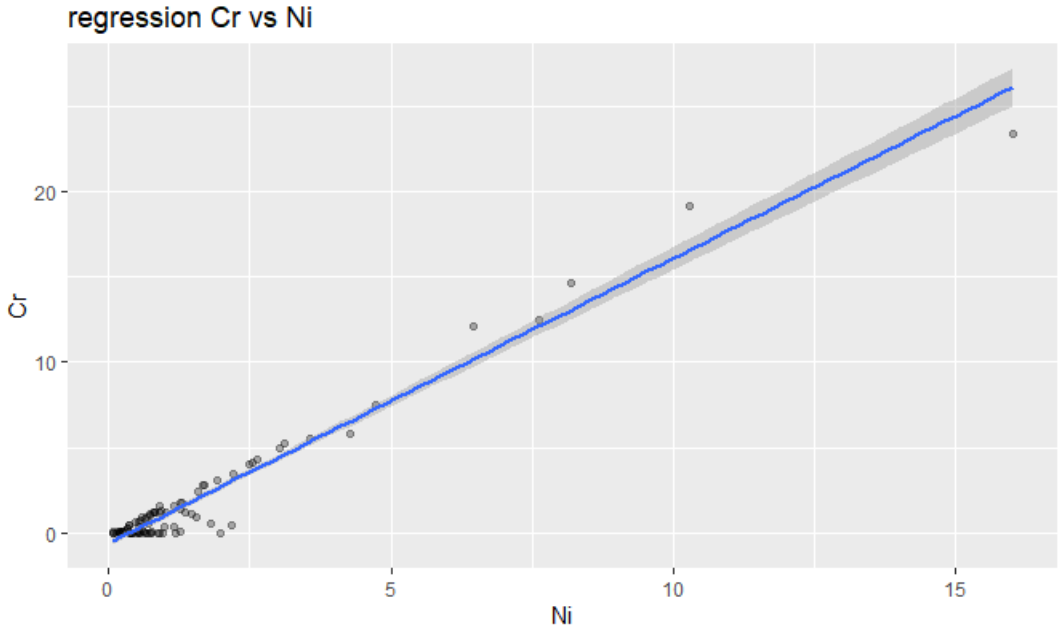

Figure B.199: Correlation test between Cr and Ni.

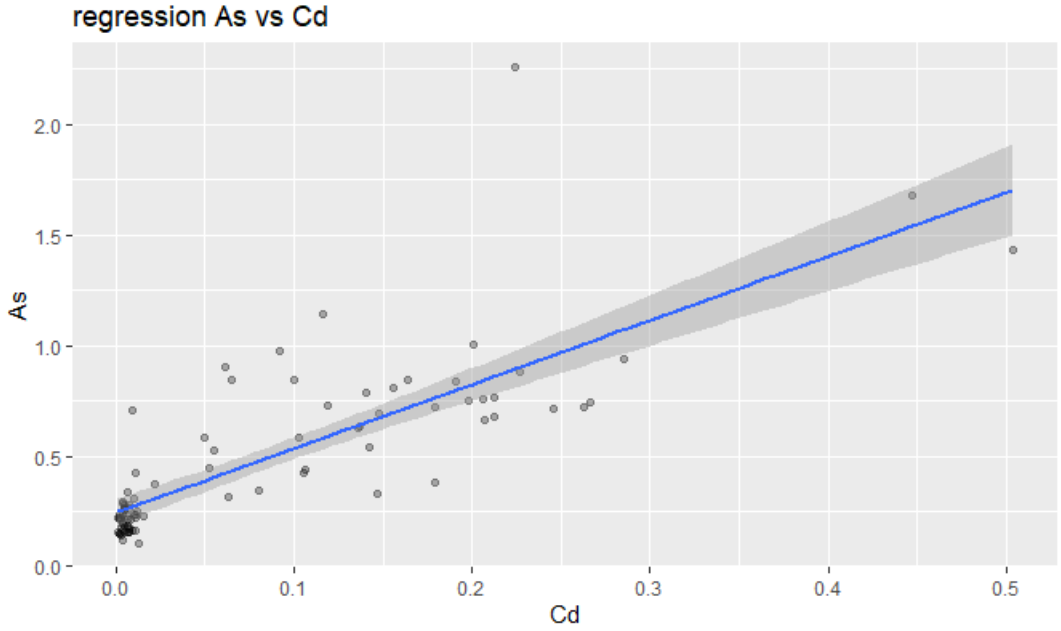

Figure B.200: Correlation test between As and Cd.

Institutional Repository - Library & Information Centre - University of Thessaly
19/04/2024 03:53:45 EEST - 18.222.197.243

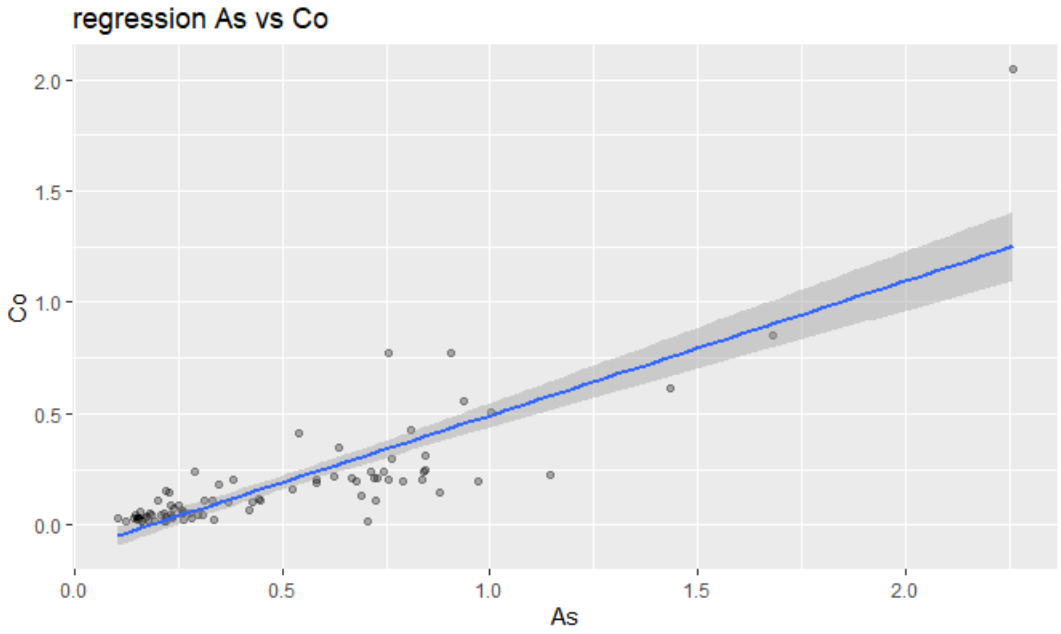

Figure B.201: Correlation test between As and Co.

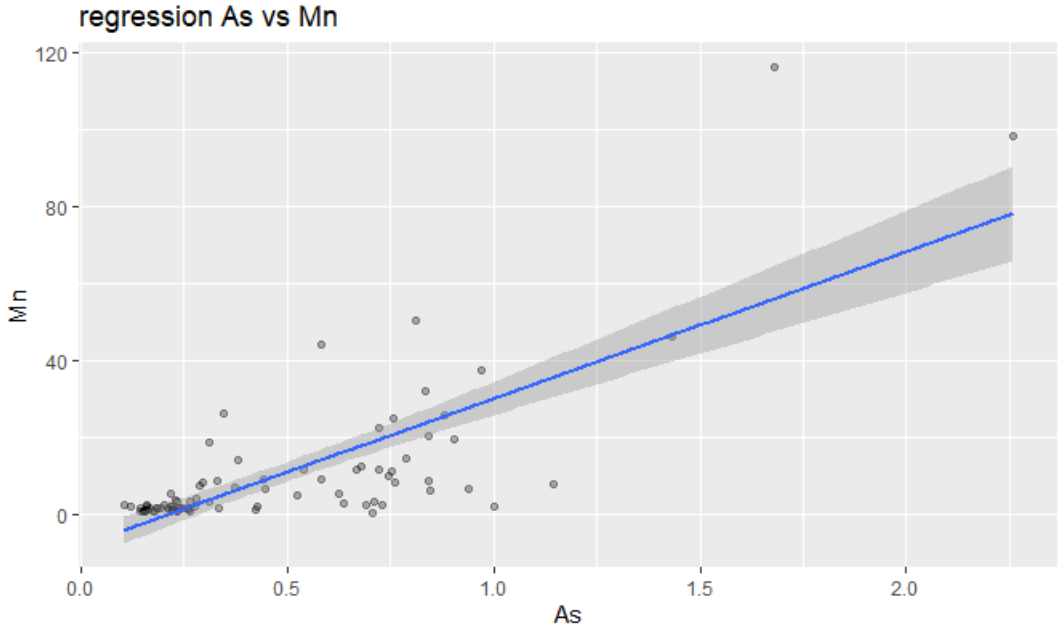

Figure B.202: Correlation test between As and Mn.

Institutional Repository - Library & Information Centre - University of Thessaly
19/04/2024 03:53:45 EEST - 18.222.197.243

Table B.4: Two sample t-test by sex.

	t	df	p value	mean female	mean male
Hg	1,906	84,000	0,060	-2,738	-3,166
Ag	4,354	84,000	0,000	-3,787	-4,287
Al	1,807	79,000	0,075	1,219	0,812
As	-0,413	84,000	0,680	-1,040	-0,974
B	-0,335	83,000	0,738	-0,997	-0,934
Ba	-0,066	84,000	0,947	-0,074	-0,061
Be (He)	6,441	84,000	0,000	0,004	0,000
Ca	0,146	84,000	0,885	5,262	5,244
Cd	0,566	84,000	0,573	-3,597	-3,824
Co	0,558	84,000	0,578	-2,286	-2,426
Cr	1,271	84,000	0,207	-0,752	-1,376
Cs	2,934	84,000	0,004	-4,423	-4,827
Cu	4,127	84,000	0,000	2,141	1,724
Fe (He)	0,474	84,000	0,637	4,515	4,350
Fe (O_2)	0,397	84,000	0,693	4,582	4,432
K	-0,674	84,000	0,502	9,060	9,236
Li	-2,642	51,000	0,011	-3,396	-2,476
Mg	1,950	84,000	0,055	5,446	5,255
Mn	-0,954	84,000	0,343	1,203	1,484
Na	-0,532	84,000	0,596	6,492	6,533
Ni	1,266	84,000	0,209	0,001	-0,301
P	1,686	84,000	0,095	7,284	7,120
S (32 ->48)	1,825	84,000	0,072	6,963	6,799
S (34 ->50)	1,826	84,000	0,071	7,061	6,886
Si	1,588	84,000	0,116	3,059	2,786
Sr	0,444	84,000	0,658	1,407	1,346
V	2,601	83,000	0,011	-3,189	-3,677
Zn	3,001	84,000	0,004	2,919	2,604

Table B.5: Two sample t-test by tissue.

	t	df	p value	mean hepato	mean muscle
Hg	-6,400	84,000	0,000	0,033	0,113
Ag	1,867	84,000	0,065	0,023	0,017
Al	-1,623	84,000	0,108	3,047	4,494
As	8,772	84,000	0,000	0,747	0,230
B	1,814	84,000	0,073	0,577	0,419
Ba	7,703	84,000	0,000	2,144	0,622
Be (He)	3,575	84,000	0,001	0,006	0,002
Ca	7,001	84,000	0,000	302,230	148,864
Cd	10,357	84,000	<2.2e-16	0,161	0,006
Co	5,173	84,000	0,000	0,315	0,051
Cr	-4,208	84,000	0,000	0,200	3,574
Cs	-6,116	84,000	0,000	0,007	0,015
Cu	2,097	84,000	0,039	7,868	6,568
Fe (He)	10,900	84,000	<2.2e-16	435,645	25,012
Fe (O_2)	10,161	84,000	0,000	538,340	26,657
K	-5,470	84,000	0,000	9621,147	19425,988
Li	2,032	84,000	0,045	0,080	0,032
Mg	-7,515	84,000	0,000	166,925	273,937
Mn	4,766	84,000	0,000	19,023	2,018
Na	-0,621	84,000	0,536	697,661	727,802
Ni	-3,153	84,000	0,002	0,727	2,272
P	-9,425	84,000	0,000	1038,484	1766,585
S (32 ->48)	-9,670	84,000	0,000	762,224	1252,642
S (34 ->50)	-10,737	84,000	<2.2e-16	812,882	1410,656
Si	6,839	84,000	0,000	34,036	13,562
Sr	7,307	84,000	0,000	6,450	3,074
V	1,080	84,000	0,283	0,047	0,038
Zn	2,008	84,000	0,048	18,843	15,206

Institutional Repository - Library & Information Centre - University of Thessaly
19/04/2024 03:53:45 EEST - 18.222.197.243

Institutional Repository - Library & Information Centre - University of Thessaly
19/04/2024 03:53:45 EEST - 18.222.197.243

Appendix C

R Codes

```r
library(tidyverse)
library(ggplot2)
library(corrgram)
library(corrplot)
library(qwraps2)
library(dplyr)
library(ggpubr)
library(corrgram)
library(corrplot)
library(lubridate)

#load the data
gmb <-read.csv("Tables_.csv",
sep=";",na.strings=c("","  ","NA"))
gmb<-as_tibble(gmb)
View(gmb) # click on data on environment table
str(gmb)
attach(gmb)



# transform Sex and Tissue in factors

gmb$Sex <- as.factor(gmb$Sex)
levels(gmb$Sex) <- c("F","M")
gmb$Tissue <- as.factor(gmb$Tissue)
levels(gmb$Tissue)<-c("H","M")

# exploratory analysis

hist(log(gmb$Hg), col='cadetblue', xlab = 'log([Hg])', ylab = 'Frequency', ...
    main = 'Histogram of log([Hg])')
hist(log(gmb$Ag), col='cadetblue', xlab = 'log([Ag])', ylab = 'Frequency', ...
    main = 'Histogram of log([Ag])')
hist(log(gmb$Al),col='cadetblue', xlab = 'log([Al])', ylab = 'Frequency', ...
    main = 'Histogram of log([Al])')
hist(log(gmb$As), col='cadetblue', xlab = 'log([As])', ylab = 'Frequency', ...
    main = 'Histogram of log([As])')
hist(log(gmb$B),col='cadetblue', xlab = 'log([B])', ylab = 'Frequency', main ...
    = 'Histogram of log([B])')
hist(log(gmb$Ba), col='cadetblue', xlab = 'log([Ba])', ylab = 'Frequency', ...
    main = 'Histogram of log([Ba])')
```


Institutional Repository - Library & Information Centre - University of Thessaly
19/04/2024 03:53:45 EEST - 18.222.197.243

```
hist(log(gmb$Be..No.Gas.), col='cadetblue', xlab = 'log([Be (No Gas)])', ...
    ylab = 'Frequency', main = 'Histogram of log([Be (No Gas)])')
hist(log(gmb$Be..He.), col='cadetblue', xlab = 'log([Be (He)])', ylab = ...
    'Frequency', main = 'Histogram of log([Be (He)])')
hist(log(gmb$Ca), col='cadetblue', xlab = 'log([Ca])', ylab = 'Frequency', ...
    main = 'Histogram of log([Ca])')
hist(log(gmb$Cd), col='cadetblue', xlab = 'log([Cd])', ylab = 'Frequency', ...
    main = 'Histogram of log([Cd])')
hist(log(gmb$Co), col='cadetblue', xlab = 'log([Co])', ylab = 'Frequency', ...
    main = 'Histogram of log([Co])')
hist(log(gmb$Cr), col='cadetblue', xlab = 'log([Cr])', ylab = 'Frequency', ...
    main = 'Histogram of log([Cr])')
hist(log(gmb$Cs), col='cadetblue', xlab = 'log([Cs])', ylab = 'Frequency', ...
    main = 'Histogram of log([Cs])')
hist(log(gmb$Cu), col='cadetblue', xlab = 'log([Cu])', ylab = 'Frequency', ...
    main = 'Histogram of log([Cu])')
hist(log(gmb$Fe..He.), col='cadetblue', xlab = 'log([Fe (He)])', ylab = ...
    'Frequency', main = 'Histogram of log([Fe (He)])')
hist(log(gmb$Fe..O2.), col='cadetblue', xlab = 'log([Fe (O2)])', ylab = ...
    'Frequency', main = 'Histogram of log([Fe (O2)])')
hist(log(gmb$Ga), col='cadetblue', xlab = 'log([Ga])', ylab = 'Frequency', ...
    main = 'Histogram of log([Ga])')
hist(log(gmb$K), col='cadetblue', xlab = 'log([K])', ylab = 'Frequency', ...
    main = 'Histogram of log([K])')
hist(log(gmb$Li), col='cadetblue', xlab = 'log([Li])', ylab = 'Frequency', ...
    main = 'Histogram of log([Li])')
hist(log(gmb$Mg), col='cadetblue', xlab = 'log([Mg])', ylab = 'Frequency', ...
    main = 'Histogram of log([Mg])')
hist(log(gmb$Mn), col='cadetblue', xlab = 'log([Mn])', ylab = 'Frequency', ...
    main = 'Histogram of log([Mn])')
hist(log(gmb$Na), col='cadetblue', xlab = 'log([Na])', ylab = 'Frequency', ...
    main = 'Histogram of log([Na])')
hist(log(gmb$Ni), col='cadetblue', xlab = 'log([Ni])', ylab = 'Frequency', ...
    main = 'Histogram of log([Ni])')
hist(log(gmb$P), col='cadetblue', xlab = 'log([P])', ylab = 'Frequency', ...
    main = 'Histogram of log([P])')
hist(log(gmb$Pb..He.), col='cadetblue', xlab = 'log([Pb (206)])', ylab = ...
    'Frequency', main = 'Histogram of log([Pb (206)])')
hist(log(gmb$X207Pb), col='cadetblue', xlab = 'log([Pb (207)])', ylab = ...
    'Frequency', main = 'Histogram of log([Pb (207)])')
hist(log(gmb$X208Pb), col='cadetblue', xlab = 'log([Pb (208)])', ylab = ...
    'Frequency', main = 'Histogram of log([Pb (208)])')
hist(log(gmb$X32S), col='cadetblue', xlab = 'log([S (32)])', ylab = ...
    'Frequency', main = 'Histogram of log([S (32)])')
hist(log(gmb$X34S), col='cadetblue', xlab = 'log([S (34)])', ylab = ...
    'Frequency', main = 'Histogram of log([S] (34))')
hist(log(gmb$Si), col='cadetblue', xlab = 'log([Si])', ylab = 'Frequency', ...
    main = 'Histogram of log([Si])')
hist(log(gmb$Sr), col='cadetblue', xlab = 'log([Sr])', ylab = 'Frequency', ...
    main = 'Histogram of log([Sr])')
hist(log(gmb$Tl), col='cadetblue', xlab = 'log([Tl])', ylab = 'Frequency', ...
    main = 'Histogram of log([Tl])')
hist(log(gmb$V), col='cadetblue', xlab = 'log([V])', ylab = 'Frequency', ...
    main = 'Histogram of log([V])')
hist(log(gmb$Zn),col='cadetblue', xlab = 'log([Zn])', ylab = 'Frequency', ...
    main = 'Histogram of log([Zn])')

# bartlett test gender

bartlett.test(Hg ¬ Sex, data=gmb)
bartlett.test(Ag ¬ Sex, data=gmb)
```


Institutional Repository - Library & Information Centre - University of Thessaly
19/04/2024 03:53:45 EEST - 18.222.197.243

```
bartlett.test(Al ~ Sex, data=gmb)
bartlett.test(As ~ Sex, data=gmb)
bartlett.test(B ~ Sex, data=gmb)
bartlett.test(Ba ~ Sex, data=gmb)
bartlett.test(Be..No.Gas. ~ Sex, data=gmb)
bartlett.test(Be..He. ~ Sex, data=gmb)
bartlett.test(Ca ~ Sex, data=gmb)
bartlett.test(Cd ~ Sex, data=gmb)
bartlett.test(Co ~ Sex, data=gmb)
bartlett.test(Cr ~ Sex, data=gmb)
bartlett.test(Cs ~ Sex, data=gmb)
bartlett.test(Cu ~ Sex, data=gmb)
bartlett.test(Fe..He. ~ Sex, data=gmb)
bartlett.test(Fe..O2. ~ Sex, data=gmb)
bartlett.test(Ga ~ Sex, data=gmb)
bartlett.test(K ~ Sex, data=gmb)
bartlett.test(Li ~ Sex, data=gmb)
bartlett.test(Mg ~ Sex, data=gmb)
bartlett.test(Mn ~ Sex, data=gmb)
bartlett.test(Na ~ Sex, data=gmb)
bartlett.test(Ni ~ Sex, data=gmb)
bartlett.test(P ~ Sex, data=gmb)
bartlett.test(Pb..He. ~ Sex, data=gmb)
bartlett.test(X207Pb ~ Sex, data=gmb)
bartlett.test(X208Pb ~ Sex, data=gmb)
bartlett.test(X32S ~ Sex, data=gmb)
bartlett.test(X34S ~ Sex, data=gmb)
bartlett.test(Si ~ Sex, data=gmb)
bartlett.test(Sr ~ Sex, data=gmb)
bartlett.test(Tl ~ Sex, data=gmb)
bartlett.test(V ~ Sex, data=gmb)
bartlett.test(Zn ~ Sex, data=gmb)


# test for normality

ggdensity(gmb$Hg,
main = "Density plot of Hg",
xlab = "Hg")
ggqqplot(gmb$Hg, main = "Quantile-Quantile plot of Hg",
xlab = "Hg")
ggqqplot(log(gmb$Hg),
main = "Quantile-Quantile plot of log([Hg])",
xlab = "log(gmb$Hg)")
shapiro.test(log(gmb$Hg))



ggdensity(gmb$Ag,
main = "Density plot of Ag",
xlab = "Ag")
ggqqplot(gmb$Ag,
main = "Quantile-Quantile plot of Ag",
xlab = "Ag")
ggqqplot(log(gmb$Ag),
main = "Quantile-Quantile plot of log([Ag])",
xlab = "log([Ag])")
shapiro.test(log(gmb$Ag))

ggdensity(gmb$Al,
main = "Density plot of Al",
```


Institutional Repository - Library & Information Centre - University of Thessaly
19/04/2024 03:53:45 EEST - 18.222.197.243

```
xlab = "Al")
ggqqplot(gmb$Al,
main = "Quantile-Quantile plot of Al",
xlab = "Al")
ggqqplot(log(gmb$Al),
main = "Quantile-Quantile plot of log([Al])",
xlab = "log([Al])")
shapiro.test(log(gmb$Al))


ggdensity(gmb$As,
main = "Density plot of As",
xlab = "As")
ggqqplot(gmb$As,
main = "Quantile-Quantile plot of As",
xlab = "As")
ggqqplot(log(gmb$As),
main = "Quantile-Quantile plot of log([As])",
xlab = "log([As])")
shapiro.test(log(gmb$As))


ggdensity(gmb$B,
main = "Density plot of B",
xlab = "B")
ggqqplot(gmb$B,
main = "Quantile-Quantile plot of B",
xlab = "B")
ggqqplot(log(gmb$B),
main = "Quantile-Quantile plot of log([B])",
xlab = "log([B])")
shapiro.test(log(gmb$B))


ggdensity(gmb$Ba,
main = "Density plot of Ba",
xlab = "Ba")
ggqqplot(gmb$Ba,
main = "Quantile-Quantile plot of Ba",
xlab = "Ba")
ggqqplot(log(gmb$Ba),
main = "Quantile-Quantile plot of log([Ba])",
xlab = "log([Ba])")
shapiro.test(log(gmb$Ba))


ggdensity(gmb$Be..No.Gas.,
main = "Density plot of Be (No Gas)",
xlab = "Be (No Gas)")
ggqqplot(gmb$Be..No.Gas.,
main = "Quantile-Quantile plot of Be (No Gas)",
xlab = "Be (No Gas)")
ggqqplot(log(gmb$Be..No.Gas.),
main = "Quantile-Quantile plot of log([Be. No Gas])",
xlab = "log([Be. No Gas])")
shapiro.test(log(gmb$Be..No.Gas.))


ggdensity(gmb$Be..He.,
main = "Density plot of Be (He)",
xlab = "Be (He)")
```


Institutional Repository - Library & Information Centre - University of Thessaly
19/04/2024 03:53:45 EEST - 18.222.197.243

```
ggqqplot(gmb$Be..He.,
main = "Quantile-Quantile plot of Be (He)",
xlab = "Be (He)")
ggqqplot(log(gmb$Be..He.),
main = "Quantile-Quantile plot of log([Be. He])",
xlab = "log([Be. He])")
shapiro.test(log(gmb$Be..He.))


ggdensity(gmb$Ca,
main = "Density plot of Ca",
xlab = "Ca")
ggqqplot(gmb$Ca,
main = "Quantile-Quantile plot of Ca",
xlab = "Ca")
ggqqplot(log(gmb$Ca),
main = "Quantile-Quantile plot of log([Ca])",
xlab = "log([Ca])")
shapiro.test(log(gmb$Ca))


ggdensity(gmb$Cd,
main = "Density plot of Cd",
xlab = "Cd")
ggqqplot(gmb$Cd,
main = "Quantile-Quantile plot of Cd",
xlab = "Cd")
ggqqplot(log(gmb$Cd),
main = "Quantile-Quantile plot of log([Cd])",
xlab = "log([Cd])")
shapiro.test(log(gmb$Cd))


ggdensity(gmb$Co,
main = "Density plot of Co",
xlab = "Co")
ggqqplot(gmb$Co,
main = "Quantile-Quantile plot of Co",
xlab = "Co")
ggqqplot(log(gmb$Co),
main = "Quantile-Quantile plot of log([Co])",
xlab = "log([Co])")
shapiro.test(log(gmb$Co))


ggdensity(gmb$Cr,
main = "Density plot of Cr",
xlab = "Cr")
ggqqplot(gmb$Cr,
main = "Quantile-Quantile plot of Cr",
xlab = "Cr")
ggqqplot(log(gmb$Cr),
main = "Quantile-Quantile plot of log([Cr])",
xlab = "log([Cr])")
shapiro.test(log(gmb$Cr))


ggdensity(gmb$Cs,
main = "Density plot of Cs",
xlab = "Cs")
ggqqplot(gmb$Cs,
```


Institutional Repository - Library & Information Centre - University of Thessaly
19/04/2024 03:53:45 EEST - 18.222.197.243

```
main = "Quantile-Quantile plot of Cs",
xlab = "Cs")
ggqqplot(log(gmb$Cs),
main = "Quantile-Quantile plot of log([Cs])",
xlab = "log([Cs])")
shapiro.test(log(gmb$Cs))


ggdensity(gmb$Cu,
main = "Density plot of Cu",
xlab = "Cu")
ggqqplot(gmb$Cu,
main = "Quantile-Quantile plot of Cu",
xlab = "Cu")
ggqqplot(log(gmb$Cu),
main = "Quantile-Quantile plot of log([Cu])",
xlab = "log([Cu])")
shapiro.test(log(gmb$Cu))


ggdensity(gmb$Fe..He.,
main = "Density plot of Fe [He]",
xlab = "Fe [He]")
ggqqplot(gmb$Fe..He.,
main = "Quantile-Quantile plot of Fe [He]",
xlab = "Fe [He]")
ggqqplot(log(gmb$Fe..He.),
main = "Quantile-Quantile plot of log([Fe. He])",
xlab = "log([Fe. He])")
shapiro.test(log(gmb$Fe..He.))


ggdensity(gmb$Fe..O2.,
main = "Density plot of Fe [O2]",
xlab = "Fe [O2]")
ggqqplot(gmb$Fe..O2.,
main = "Quantile-Quantile plot of Fe [O2]",
xlab = "Fe [O2]")
ggqqplot(log(gmb$Fe..O2.),
main = "Quantile-Quantile plot of log([Fe. O2])",
xlab = "log([Fe. O2])")
shapiro.test(log(gmb$Fe..O2.))


ggdensity(gmb$Ga,
main = "Density plot of Ga",
xlab = "Ga")
ggqqplot(gmb$Ga,
main = "Quantile-Quantile plot of Ga",
xlab = "Ga")
ggqqplot(log(gmb$Ga),
main = "Quantile-Quantile plot of log([Ga])",
xlab = "log([Ga])")
shapiro.test(log(gmb$Ga))


ggdensity(gmb$K,
main = "Density plot of K",
xlab = "K")
ggqqplot(gmb$K,
main = "Quantile-Quantile plot of K",
```


Institutional Repository - Library & Information Centre - University of Thessaly
19/04/2024 03:53:45 EEST - 18.222.197.243

```
xlab = "K")
ggqqplot(log(gmb$K),
main = "Quantile-Quantile plot of log([K])",
xlab = "log([K])")
shapiro.test(log(gmb$K))


ggdensity(gmb$Li,
main = "Density plot of Li",
xlab = "Li")
ggqqplot(gmb$Li,
main = "Quantile-Quantile plot of Li",
xlab = "Li")
ggqqplot(log(gmb$Li),
main = "Quantile-Quantile plot of log([Li])",
xlab = "log([Li])")
shapiro.test(log(gmb$Li))


ggdensity(gmb$Mg,
main = "Density plot of Mg",
xlab = "Mg")
ggqqplot(gmb$Mg,
main = "Quantile-Quantile plot of Mg",
xlab = "Mg")
ggqqplot(log(gmb$Mg),
main = "Quantile-Quantile plot of log([Mg])",
xlab = "log([Mg])")
shapiro.test(log(gmb$Mg))


ggdensity(gmb$Mn,
main = "Density plot of Mn",
xlab = "Mn")
ggqqplot(gmb$Mn,
main = "Quantile-Quantile plot of Mn",
xlab = "Mn")
ggqqplot(log(gmb$Mn),
main = "Quantile-Quantile plot of log([Mn])",
xlab = "log([Mn])")
shapiro.test(log(gmb$Mn))


ggdensity(gmb$Na,
main = "Density plot of Na",
xlab = "Na")
ggqqplot(gmb$Na,
main = "Quantile-Quantile plot of Na",
xlab = "Na")
ggqqplot(log(gmb$Na),
main = "Quantile-Quantile plot of log([Na])",
xlab = "log([Na])")
shapiro.test(log(gmb$Na))


ggdensity(gmb$Ni,
main = "Density plot of Ni",
xlab = "Ni")
ggqqplot(gmb$Ni,
main = "Quantile-Quantile plot of Ni",
xlab = "Ni")
```


Institutional Repository - Library & Information Centre - University of Thessaly
19/04/2024 03:53:45 EEST - 18.222.197.243

```
ggqqplot(log(gmb$Ni),
main = "Quantile-Quantile plot of log([Ni])",
xlab = "log([Ni])")
shapiro.test(log(gmb$Ni))


ggdensity(gmb$P,
main = "Density plot of P",
xlab = "P")
ggqqplot(gmb$P,
main = "Quantile-Quantile plot of P",
xlab = "P")
ggqqplot(log(gmb$P),
main = "Quantile-Quantile plot of log([P])",
xlab = "log([P])")
shapiro.test(log(gmb$P))


ggdensity(gmb$Pb..He.,
main = "Density plot of Pb (206)",
xlab = "Pb (206)")
ggqqplot(gmb$Pb..He.,
main = "Quantile-Quantile plot of Pb (206)",
xlab = "Pb (206)")
ggqqplot(log(gmb$Pb..He.),
main = "Quantile-Quantile plot of log([Pb. 206])",
xlab = "log([Pb. 206])")
shapiro.test(log(gmb$Pb..He.))


ggdensity(gmb$X207Pb,
main = "Density plot of Pb (207)",
xlab = "Pb (207)")
ggqqplot(gmb$X207Pb,
main = "Quantile-Quantile plot of Pb (207)",
xlab = "Pb (207)")
ggqqplot(log(gmb$X207Pb),
main = "Quantile-Quantile plot of log([Pb. 207])",
xlab = "log([Pb. 207])")
shapiro.test(log(gmb$X207Pb))


ggdensity(gmb$X208Pb,
main = "Density plot of Pb (208)",
xlab = "Pb (208)")
ggqqplot(gmb$X208Pb,
main = "Quantile-Quantile plot of Pb (208)",
xlab = "Pb 8208)")
ggqqplot(log(gmb$X208Pb),
main = "Quantile-Quantile plot of log([Pb. 208])",
xlab = "log([Pb. 208])")
shapiro.test(log(gmb$X208Pb))


ggdensity(gmb$X32S,
main = "Density plot of S (32-68)",
xlab = "S (32-68)")
ggqqplot(gmb$X32S,
main = "Quantile-Quantile plot of S (32-68)",
xlab = "S (32-68)")
ggqqplot(log(gmb$X32S),
```


Institutional Repository - Library & Information Centre - University of Thessaly
19/04/2024 03:53:45 EEST - 18.222.197.243

```
436 main = "Quantile-Quantile plot of log([S]) (32-68)",
437 xlab = "log([S]) (32-68)")
438 shapiro.test(log(gmb$X32S))
439
440
441 ggdensity(gmb$X34S,
442 main = "Density plot of S (34-50)",
443 xlab = "S (34-50)")
444 ggqqplot(gmb$X34S,
445 main = "Quantile-Quantile plot of S (34-50)",
446 xlab = "S (34-50)")
447 ggqqplot(log(gmb$X34S),
448 main = "Quantile-Quantile plot of log([S]) (34-50)",
449 xlab = "log([S]) (34-50)")
450 shapiro.test(log(gmb$X34S))
451
452
453 ggdensity(gmb$Si,
454 main = "Density plot of Si",
455 xlab = "Si")
456 ggqqplot(gmb$Si,
457 main = "Quantile-Quantile plot of Si",
458 xlab = "Si")
459 ggqqplot(log(gmb$Si),
460 main = "Quantile-Quantile plot of log([Si])",
461 xlab = "log([Si])")
462 shapiro.test(log(gmb$Si))
463
464
465 ggdensity(gmb$Sr,
466 main = "Density plot of Sr",
467 xlab = "Sr")
468 ggqqplot(gmb$Sr,
469 main = "Quantile-Quantile plot of Sr",
470 xlab = "Sr")
471 ggqqplot(log(gmb$Sr),
472 main = "Quantile-Quantile plot of log([Sr])",
473 xlab = "log([Sr])")
474 shapiro.test(log(gmb$Sr))
475
476
477 ggdensity(gmb$Tl,
478 main = "Density plot of Tl",
479 xlab = "Tl")
480 ggqqplot(gmb$Tl,
481 main = "Quantile-Quantile plot of Tl",
482 xlab = "Tl")
483 ggqqplot(log(gmb$Tl),
484 main = "Quantile-Quantile plot of log([Tl])",
485 xlab = "log([Tl])")
486 shapiro.test(log(gmb$Tl))
487
488
489 ggdensity(gmb$V,
490 main = "Density plot of V",
491 xlab = "V")
492 ggqqplot(gmb$V,
493 main = "Quantile-Quantile plot of V",
494 xlab = "V")
495 ggqqplot(log(gmb$V),
496 main = "Quantile-Quantile plot of log([V])",
```


Institutional Repository - Library & Information Centre - University of Thessaly
19/04/2024 03:53:45 EEST - 18.222.197.243

```
xlab = "log([V])")
shapiro.test(log(gmb$V))


ggdensity(gmb$Zn,
main = "Density plot of Zn",
xlab = "Zn")
ggqqplot(gmb$Zn,
main = "Quantile-Quantile plot of Zn",
xlab = "Zn")
ggqqplot(log(gmb$Zn),
main = "Quantile-Quantile plot of log([Zn])",
xlab = "log([Zn])")
shapiro.test(log(gmb$Zn))




# bartlett test tissue

bartlett.test(Hg ¬ Tissue, data=gmb)
boxplot(Hg ¬ Tissue,
data = gmb,
names=c("HEP","MUS"),
ylab="Hg")

bartlett.test(Ag ¬ Tissue, data=gmb)
boxplot(Ag ¬ Tissue,
data = gmb,
names=c("HEP","MUS"),
ylab="Ag")

bartlett.test(Al ¬ Tissue, data=gmb)
boxplot(Al ¬ Tissue,
data = gmb,
names=c("HEP","MUS"),
ylab="Al")

bartlett.test(As ¬ Tissue, data=gmb)
boxplot(As ¬ Tissue,
data = gmb,
names=c("HEP","MUS"),
ylab="As")

bartlett.test(B ¬ Tissue, data=gmb)
boxplot(B ¬ Tissue,
data = gmb,
names=c("HEP","MUS"),
ylab="B")

bartlett.test(Ba ¬ Tissue, data=gmb)
boxplot(Ba ¬ Tissue,
data = gmb,
names=c("HEP","MUS"),
ylab="Ba")

bartlett.test(Be..No.Gas. ¬ Tissue, data=gmb)
boxplot(Be..No.Gas.¬ Tissue,
data = gmb,
names=c("HEP","MUS"),
ylab="Be (No Gas)")
```


Institutional Repository - Library & Information Centre - University of Thessaly
19/04/2024 03:53:45 EEST - 18.222.197.243

```
558
559 bartlett.test(Be..He. ¬ Tissue, data=gmb)
560 boxplot(Be..He. ¬ Tissue,
561 data = gmb,
562 names=c("HEP","MUS"),
563 ylab="Be (He)")
564
565 bartlett.test(Ca ¬ Tissue, data=gmb)
566 boxplot(Ca ¬ Tissue,
567 data = gmb,
568 names=c("HEP","MUS"),
569 ylab="Ca")
570
571 bartlett.test(Cd ¬ Tissue, data=gmb)
572 boxplot(Cd ¬ Tissue,
573 data = gmb,
574 names=c("HEP","MUS"),
575 ylab="Cd")
576
577 bartlett.test(Co ¬ Tissue, data=gmb)
578 boxplot(Co ¬ Tissue,
579 data = gmb,
580 names=c("HEP","MUS"),
581 ylab="Co")
582
583 bartlett.test(Cr ¬ Tissue, data=gmb)
584 boxplot(Cr ¬ Tissue,
585 data = gmb,
586 names=c("HEP","MUS"),
587 ylab="Cr")
588
589 bartlett.test(Cs ¬ Tissue, data=gmb)
590 boxplot(Cs ¬ Tissue,
591 data = gmb,
592 names=c("HEP","MUS"),
593 ylab="Cs")
594
595 bartlett.test(Cu ¬ Tissue, data=gmb)
596 boxplot(Cu ¬ Tissue,
597 data = gmb,
598 names=c("HEP","MUS"),
599 ylab="Cu")
600
601 bartlett.test(Fe..He. ¬ Tissue, data=gmb)
602 boxplot(Fe..He. ¬ Tissue,
603 data = gmb,
604 names=c("HEP","MUS"),
605 ylab="Fe (He)")
606
607 bartlett.test(Fe..O2. ¬ Tissue, data=gmb)
608 boxplot(Fe..O2. ¬ Tissue,
609 data = gmb,
610 names=c("HEP","MUS"),
611 ylab="Fe (O2)")
612
613 bartlett.test(Ga ¬ Tissue, data=gmb)
614 boxplot(Ga ¬ Tissue,
615 data = gmb,
616 names=c("HEP","MUS"),
617 ylab="Ga")
618
```


Institutional Repository - Library & Information Centre - University of Thessaly
19/04/2024 03:53:45 EEST - 18.222.197.243

```
bartlett.test(K ¬ Tissue, data=gmb)
boxplot(K ¬ Tissue,
data = gmb,
names=c("HEP","MUS"),
ylab="K")

bartlett.test(Li ¬ Tissue, data=gmb)
boxplot(Li ¬ Tissue,
data = gmb,
names=c("HEP","MUS"),
ylab="Li")

bartlett.test(Mg ¬ Tissue, data=gmb)
boxplot(Mg ¬ Tissue,
data = gmb,
names=c("HEP","MUS"),
ylab="Mg")

bartlett.test(Mn ¬ Tissue, data=gmb)
boxplot(Mn ¬ Tissue,
data = gmb,
names=c("HEP","MUS"),
ylab="Mn")

bartlett.test(Na ¬ Tissue, data=gmb)
boxplot(Na ¬ Tissue,
data = gmb,
names=c("HEP","MUS"),
ylab="Na")

bartlett.test(Ni ¬ Tissue, data=gmb)
boxplot(Ni ¬ Tissue,
data = gmb,
names=c("HEP","MUS"),
ylab="Ni")

bartlett.test(P ¬ Tissue, data=gmb)
boxplot(P ¬ Tissue,
data = gmb,
names=c("HEP","MUS"),
ylab="P")

bartlett.test(Pb..He. ¬ Tissue, data=gmb)
boxplot(Pb..He. ¬ Tissue,
data = gmb,
names=c("HEP","MUS"),
ylab="Pb (206)")

bartlett.test(X207Pb ¬ Tissue, data=gmb)
boxplot(X207Pb ¬ Tissue,
data = gmb,
names=c("HEP","MUS"),
ylab="Pb (207)")

bartlett.test(X208Pb ¬ Tissue, data=gmb)
boxplot(X208Pb ¬ Tissue,
data = gmb,
names=c("HEP","MUS"),
ylab="Pb (208)")

bartlett.test(X32S ¬ Tissue, data=gmb)
```


Institutional Repository - Library & Information Centre - University of Thessaly
19/04/2024 03:53:45 EEST - 18.222.197.243

```
boxplot(X32S ¬ Tissue,
data = gmb,
names=c("HEP","MUS"),
ylab="S (32 -> 48)")

bartlett.test(X34S ¬ Tissue, data=gmb)
boxplot(X34S ¬ Tissue,
data = gmb,
names=c("HEP","MUS"),
ylab="S (34 -> 50)")

bartlett.test(Si ¬ Tissue, data=gmb)
boxplot(Si ¬ Tissue,
data = gmb,
names=c("HEP","MUS"),
ylab="Si")

bartlett.test(Sr ¬ Tissue, data=gmb)
boxplot(Sr ¬ Tissue,
data = gmb,
names=c("HEP","MUS"),
ylab="Sr")

bartlett.test(Tl ¬ Tissue, data=gmb)
boxplot(Tl ¬ Tissue,
data = gmb,
names=c("HEP","MUS"),
ylab="Tl")

bartlett.test(V ¬ Tissue, data=gmb)
boxplot(V ¬ Tissue,
data = gmb,
names=c("HEP","MUS"),
ylab="V")

bartlett.test(Zn ¬ Tissue, data=gmb)
boxplot(Zn ¬ Tissue,
data = gmb,
names=c("HEP","MUS"),
ylab="Zn")


# bartlett test sex

bartlett.test(Hg ¬ Tissue, data=gmb)
boxplot(log(Hg) ¬ Sex,
data = gmb,
names=c("Female","Male"),
ylab="log([Hg])")

bartlett.test(Ag ¬ Sex, data=gmb)
boxplot(log(Ag) ¬ Sex,
data = gmb,
names=c("Female","Male"),
ylab="log([Ag])")

bartlett.test(Al ¬ Sex, data=gmb)
boxplot(log(Al) ¬ Sex,
data = gmb,
names=c("Female","Male"),
ylab="log([Al)")
```


Institutional Repository - Library & Information Centre - University of Thessaly
19/04/2024 03:53:45 EEST - 18.222.197.243

```
741
742 bartlett.test(As ¬ Sex, data=gmb)
743 boxplot(log(As) ¬ Sex,
744 data = gmb,
745 names=c("Female","Male"),
746 ylab="log([As])")
747
748 bartlett.test(B ¬ Sex, data=gmb)
749 boxplot(log(B) ¬ Sex,
750 data = gmb,
751 names=c("Female","Male"),
752 ylab="log([B])")
753
754 bartlett.test(Ba ¬ Sex, data=gmb)
755 boxplot(log(Ba) ¬ Sex,
756 data = gmb,
757 names=c("Female","Male"),
758 ylab="log([Ba])")
759
760 bartlett.test(Be..No.Gas. ¬ Sex, data=gmb)
761 boxplot(log(Be..No.Gas.) ¬ Sex,
762 data = gmb,
763 names=c("Female","Male"),
764 ylab="log([Be]) (No Gas)")
765
766 bartlett.test(Be..He. ¬ Sex, data=gmb)
767 boxplot(log(Be..He.) ¬ Sex,
768 data = gmb,
769 names=c("Female","Male"),
770 ylab="log([Be]) (He)")
771
772 bartlett.test(Ca ¬ Sex, data=gmb)
773 boxplot(log(Ca) ¬ Sex,
774 data = gmb,
775 names=c("Female","Male"),
776 ylab="log([Ca])")
777
778 bartlett.test(Cd ¬ Sex, data=gmb)
779 boxplot(log(Cd) ¬ Sex,
780 data = gmb,
781 names=c("Female","Male"),
782 ylab="log([Cd])")
783
784 bartlett.test(Co ¬ Sex, data=gmb)
785 boxplot(log(Co) ¬ Sex,
786 data = gmb,
787 names=c("Female","Male"),
788 ylab="log([Co])")
789
790 bartlett.test(Cr ¬ Sex, data=gmb)
791 boxplot(log(Cr) ¬ Sex,
792 data = gmb,
793 names=c("Female","Male"),
794 ylab="log([Cr])")
795
796 bartlett.test(Cs ¬ Sex, data=gmb)
797 boxplot(log(Cs) ¬ Sex,
798 data = gmb,
799 names=c("Female","Male"),
800 ylab="log([Cs])")
801
```


Institutional Repository - Library & Information Centre - University of Thessaly
19/04/2024 03:53:45 EEST - 18.222.197.243

```
bartlett.test(Cu ¬ Sex, data=gmb)
boxplot(log(Cu) ¬ Sex,
data = gmb,
names=c("Female","Male"),
ylab="log([Cu])")

bartlett.test(Fe..He. ¬ Sex, data=gmb)
boxplot(log(Fe..He.) ¬ Sex,
data = gmb,
names=c("Female","Male"),
ylab="log([Fe]) (He)")

bartlett.test(Fe..O2. ¬ Sex, data=gmb)
boxplot(log(Fe..O2.) ¬ Sex,
data = gmb,
names=c("Female","Male"),
ylab="log([Fe]) (O2)")

bartlett.test(Ga ¬ Sex, data=gmb)
boxplot(log(Ga) ¬ Sex,
data = gmb,
names=c("Female","Male"),
ylab="log([Ga])")

bartlett.test(K ¬ Sex, data=gmb)
boxplot(log(K) ¬ Sex,
data = gmb,
names=c("Female","Male"),
ylab="log([K])")

bartlett.test(Li ¬ Sex, data=gmb)
boxplot(log(Li) ¬ Sex,
data = gmb,
names=c("Female","Male"),
ylab="log([Li])")

bartlett.test(Mg ¬ Sex, data=gmb)
boxplot(log(Mg) ¬ Sex,
data = gmb,
names=c("Female","Male"),
ylab="log([Mg])")

bartlett.test(Mn ¬ Sex, data=gmb)
boxplot(log(Mn) ¬ Sex,
data = gmb,
names=c("Female","Male"),
ylab="log([Mn])")

bartlett.test(Na ¬ Sex, data=gmb)
boxplot(log(Na) ¬ Sex,
data = gmb,
names=c("Female","Male"),
ylab="log([Na])")

bartlett.test(Ni ¬ Sex, data=gmb)
boxplot(log(Ni) ¬ Sex,
data = gmb,
names=c("Female","Male"),
ylab="log([Ni])")

bartlett.test(P ¬ Sex, data=gmb)
```


Institutional Repository - Library & Information Centre - University of Thessaly
19/04/2024 03:53:45 EEST - 18.222.197.243

```
boxplot(log(P) ~ Sex,
data = gmb,
names=c("Female","Male"),
ylab="log([P])")

bartlett.test(Pb..He. ~ Sex, data=gmb)
boxplot(log(Pb..He.) ~ Sex,
data = gmb,
names=c("Female","Male"),
ylab="log([Pb.206])")

bartlett.test(X207Pb ~ Sex, data=gmb)
boxplot(log(X207Pb) ~ Sex,
data = gmb,
names=c("Female","Male"),
ylab="log([Pb.207])")

bartlett.test(X208Pb ~ Sex, data=gmb)
boxplot(log(X208Pb) ~ Sex,
data = gmb,
names=c("Female","Male"),
ylab="log([Pb.208])")

bartlett.test(X32S ~ Sex, data=gmb)
boxplot(log(X32S) ~ Sex,
data = gmb,
names=c("Female","Male"),
ylab="log([S])(32->48) ")

bartlett.test(X34S ~ Sex, data=gmb)
boxplot(log(X34S) ~ Sex,
data = gmb,
names=c("Female","Male"),
ylab="log([S])(34->50)")

bartlett.test(Si ~ Sex, data=gmb)
boxplot(log(Si) ~ Sex,
data = gmb,
names=c("Female","Male"),
ylab="log([Si])")

bartlett.test(Sr ~ Sex, data=gmb)
boxplot(log(Sr) ~ Sex,
data = gmb,
names=c("Female","Male"),
ylab="log([Sr])")

bartlett.test(Tl ~ Sex, data=gmb)
boxplot(log(Tl) ~ Sex,
data = gmb,
names=c("Female","Male"),
ylab="log([Tl])")

bartlett.test(V ~ Sex, data=gmb)
boxplot(log(V) ~ Sex,
data = gmb,
names=c("Female","Male"),
ylab="log([V])")

bartlett.test(Zn ~ Sex, data=gmb)
boxplot(log(Zn) ~ Sex,
```


Institutional Repository - Library & Information Centre - University of Thessaly
19/04/2024 03:53:45 EEST - 18.222.197.243

```
924 data = gmb,
925 names=c("Female","Male"),
926 ylab="log([Zn])")
927
928
929
930 # t test
931
932 t.test(log(Hg) ¬ Sex, data=gmb,
933 var.equal=TRUE,
934 conf.level=0.95)
935
936 t.test(Hg ¬ Tissue, data=gmb,
937 var.equal=TRUE,
938 conf.level=0.95)
939
940 t.test(log(Ag) ¬ Sex, data=gmb,
941 var.equal=TRUE,
942 conf.level=0.95)
943
944 t.test(Ag ¬ Tissue, data=gmb,
945 var.equal=TRUE,
946 conf.level=0.95)
947
948 t.test(log(Al) ¬ Sex, data=gmb,
949 var.equal=TRUE,
950 conf.level=0.95)
951
952 t.test(Al ¬ Tissue, data=gmb,
953 var.equal=TRUE,
954 conf.level=0.95)
955
956 t.test(log(As) ¬ Sex, data=gmb,
957 var.equal=TRUE,
958 conf.level=0.95)
959
960 t.test(As ¬ Tissue, data=gmb,
961 var.equal=TRUE,
962 conf.level=0.95)
963
964 t.test(log(B) ¬ Sex, data=gmb,
965 var.equal=TRUE,
966 conf.level=0.95)
967
968 t.test(B ¬ Tissue, data=gmb,
969 var.equal=TRUE,
970 conf.level=0.95)
971
972 t.test(log(Ba) ¬ Sex, data=gmb,
973 var.equal=TRUE,
974 conf.level=0.95)
975
976 t.test(Ba ¬ Tissue, data=gmb,
977 var.equal=TRUE,
978 conf.level=0.95)
979
980 t.test(log(Be..He.) ¬ Sex, data=gmb,
981 var.equal=TRUE,
982 conf.level=0.95)
983
984 t.test(Be..He. ¬ Tissue, data=gmb,
```


Institutional Repository - Library & Information Centre - University of Thessaly
19/04/2024 03:53:45 EEST - 18.222.197.243

```
var.equal=TRUE,
conf.level=0.95)

t.test(log(Be..No.Gas) ¬ Sex, data=gmb,
var.equal=TRUE,
conf.level=0.95)

t.test(Be..No.Gas.¬ Tissue, data=gmb,
var.equal=TRUE,
conf.level=0.95)

t.test(log(Ca) ¬ Sex, data=gmb,
var.equal=TRUE,
conf.level=0.95)

t.test(Ca ¬ Tissue, data=gmb,
var.equal=TRUE,
conf.level=0.95)

t.test(log(Cd) ¬ Sex, data=gmb,
var.equal=TRUE,
conf.level=0.95)

t.test(Cd ¬ Tissue, data=gmb,
var.equal=TRUE,
conf.level=0.95)

t.test(log(Co) ¬ Sex, data=gmb,
var.equal=TRUE,
conf.level=0.95)

t.test(Co ¬ Tissue, data=gmb,
var.equal=TRUE,
conf.level=0.95)

t.test(log(Cr) ¬ Sex, data=gmb,
var.equal=TRUE,
conf.level=0.95)

t.test(Cr ¬ Tissue, data=gmb,
var.equal=TRUE,
conf.level=0.95)

t.test(log(Cs) ¬ Sex, data=gmb,
var.equal=TRUE,
conf.level=0.95)

t.test(Cs ¬ Tissue, data=gmb,
var.equal=TRUE,
conf.level=0.95)

t.test(log(Cu) ¬ Sex, data=gmb,
var.equal=TRUE,
conf.level=0.95)

t.test(Cu ¬ Tissue, data=gmb,
var.equal=TRUE,
conf.level=0.95)

t.test(log(Fe..He.) ¬ Sex, data=gmb,
var.equal=TRUE,
```


Institutional Repository - Library & Information Centre - University of Thessaly
19/04/2024 03:53:45 EEST - 18.222.197.243

```
conf.level=0.95)

t.test(Fe..He. ~ Tissue, data=gmb,
var.equal=TRUE,
conf.level=0.95)

t.test(log(Fe..O2.) ~ Sex, data=gmb,
var.equal=TRUE,
conf.level=0.95)

t.test(Fe..O2. ~ Tissue, data=gmb,
var.equal=TRUE,
conf.level=0.95)

t.test(na.exclude(log(Ga) ~ Sex), data=gmb,
var.equal=TRUE,
conf.level=0.95)

t.test(Ga ~ Tissue, data=gmb,
var.equal=TRUE,
conf.level=0.95)

t.test(log(K) ~ Sex, data=gmb,
var.equal=TRUE,
conf.level=0.95)

t.test(K ~ Tissue, data=gmb,
var.equal=TRUE,
conf.level=0.95)

t.test(log(Li) ~ Sex, data=gmb,
var.equal=TRUE,
conf.level=0.95)

t.test(Li ~ Tissue, data=gmb,
var.equal=TRUE,
conf.level=0.95)

t.test(log(Mg) ~ Sex, data=gmb,
var.equal=TRUE,
conf.level=0.95)

t.test(Mg ~ Tissue, data=gmb,
var.equal=TRUE,
conf.level=0.95)

t.test(log(Mn) ~ Sex, data=gmb,
var.equal=TRUE,
conf.level=0.95)

t.test(Mn ~ Tissue, data=gmb,
var.equal=TRUE,
conf.level=0.95)

t.test(log(Na) ~ Sex, data=gmb,
var.equal=TRUE,
conf.level=0.95)

t.test(Na ~ Tissue, data=gmb,
var.equal=TRUE,
conf.level=0.95)
```


Institutional Repository - Library & Information Centre - University of Thessaly
19/04/2024 03:53:45 EEST - 18.222.197.243

```
1107
1108 t.test(log(Ni) ¬ Sex, data=gmb,
1109 var.equal=TRUE,
1110 conf.level=0.95)
1111
1112 t.test(Ni ¬ Tissue, data=gmb,
1113 var.equal=TRUE,
1114 conf.level=0.95)
1115
1116 t.test(log(P) ¬ Sex, data=gmb,
1117 var.equal=TRUE,
1118 conf.level=0.95)
1119
1120 t.test(P ¬ Tissue, data=gmb,
1121 var.equal=TRUE,
1122 conf.level=0.95)
1123
1124 t.test(log(Pb..He) ¬ Sex, data=gmb,
1125 var.equal=TRUE,
1126 conf.level=0.95)
1127
1128 t.test(Pb..He ¬ Tissue, data=gmb,
1129 var.equal=TRUE,
1130 conf.level=0.95)
1131
1132 t.test(log(Si) ¬ Sex, data=gmb,
1133 var.equal=TRUE,
1134 conf.level=0.95)
1135
1136 t.test(Si ¬ Tissue, data=gmb,
1137 var.equal=TRUE,
1138 conf.level=0.95)
1139
1140 t.test(log(Sr) ¬ Sex, data=gmb,
1141 var.equal=TRUE,
1142 conf.level=0.95)
1143
1144 t.test(Sr ¬ Tissue, data=gmb,
1145 var.equal=TRUE,
1146 conf.level=0.95)
1147
1148 t.test(log(Tl) ¬ Sex, data=gmb,
1149 var.equal=TRUE,
1150 conf.level=0.95)
1151
1152 t.test(Tl ¬ Tissue, data=gmb,
1153 var.equal=TRUE,
1154 conf.level=0.95)
1155
1156 t.test(log(V) ¬ Sex, data=gmb,
1157 var.equal=TRUE,
1158 conf.level=0.95)
1159
1160 t.test(V ¬ Tissue, data=gmb,
1161 var.equal=TRUE,
1162 conf.level=0.95)
1163
1164 t.test(log(X207Pb) ¬ Sex, data=gmb,
1165 var.equal=TRUE,
1166 conf.level=0.95)
1167
```


Institutional Repository - Library & Information Centre - University of Thessaly
19/04/2024 03:53:45 EEST - 18.222.197.243

```
t.test(X207Pb ¬ Tissue, data=gmb,
var.equal=TRUE,
conf.level=0.95)

t.test(log(X208Pb) ¬ Sex, data=gmb,
var.equal=TRUE,
conf.level=0.95)

t.test(X208Pb ¬ Tissue, data=gmb,
var.equal=TRUE,
conf.level=0.95)

t.test(log(X32S) ¬ Sex, data=gmb,
var.equal=TRUE,
conf.level=0.95)

t.test(X32S ¬ Tissue, data=gmb,
var.equal=TRUE,
conf.level=0.95)

t.test(log(X34S) ¬ Sex, data=gmb,
var.equal=TRUE,
conf.level=0.95)

t.test(X34S ¬ Tissue, data=gmb,
var.equal=TRUE,
conf.level=0.95)

t.test(log(Zn) ¬ Sex, data=gmb,
var.equal=TRUE,
conf.level=0.95)


t.test(Zn ¬ Tissue, data=gmb,
var.equal=TRUE,
conf.level=0.95)



# correlations
num.cols<-sapply(gmb,is.numeric)
cor.data <-cor(gmb[,num.cols],use="complete.obs")
corrplot(cor.data)

cor.test(gmb$Cr, gmb$Ni)
ggplot(gmb, aes(x = Ni, y = Cr)) +
geom_point(alpha = 0.3) +
geom_smooth(method = "lm")+ xlab("Ni")+ ylab("Cr")+ ggtitle("regression Cr ...
    vs Ni")


cor.test(gmb$Cd , gmb$As)
ggplot(gmb, aes(x = Cd, y = As)) +
geom_point(alpha = 0.3) +
geom_smooth(method = "lm")+ xlab("Cd")+ ylab("As")+ ggtitle("regression As ...
    vs Cd")

cor.test(gmb$As, gmb$Co)
ggplot(gmb, aes(x = As, y = Co)) +
geom_point(alpha = 0.3) +
```


Institutional Repository - Library & Information Centre - University of Thessaly
19/04/2024 03:53:45 EEST - 18.222.197.243

```
1226 geom_smooth(method = "lm")+ xlab("As")+ ylab("Co")+ ggtitle("regression As ...
       vs Co")
1227
1228 cor.test(gmb$As, gmb$Mn)
1229 ggplot(gmb, aes(x = As, y = Mn)) +
1230 geom_point(alpha = 0.3) +
1231 geom_smooth(method = "lm")+ xlab("As")+ ylab("Mn")+ ggtitle("regression As ...
       vs Mn")
```


Institutional Repository - Library & Information Centre - University of Thessaly
19/04/2024 03:53:45 EEST - 18.222.197.243